ENDOCYTIC RECYCLING PATHWAYS IN *Aspergillus nidulans*

A Dissertation

by

ZACHARY S. SCHULTZHAUS

Submitted to the Office of Graduate and Professional Studies of
Texas A&M University
in partial fulfillment of the requirements for the degree of

DOCTOR OF PHILOSOPHY

Chair of Committee,	Brian D. Shaw
Committee Members,	Daniel J. Ebbole
	Beiyan Nan
	Herman B. Scholthof
Head of Department,	Leland S. Pierson III

May 2017

Major Subject: Plant Pathology

ABSTRACT

Fungi, which dominate many ecosystems as major decomposers and pathogens, generally colonize through the formation of long, tubular cells called hyphae. Understanding hyphal growth has been of interest to cell biologists for a century, and holds the potential to provide insights for many eukaryotic systems. Hyphal growth and shape are intimately connected with membrane trafficking, which is divided into exocytosis (membrane fusion) and endocytosis (membrane fission). Both of these processes are, in turn, essential for hyphal growth. However, endocytosis works to remove membrane, and why it should be important for cell expansion is not known. Here, using genetic manipulation combined with live cell imaging, the role of endocytosis in hyphal growth was scrutinized in the fungus *Aspergillus nidulans*. First, I examined the localization and function of the canonical endocytic coat protein, clathrin, and discovered that it is involved in budding at the Golgi apparatus, but does not appear to play a significant role in endocytosis. Second, I looked for proteins that may traffic through an endocytic recycling pathway within the hyphal tip, which resulted in identification and characterization of the phospholipid flippases DnfA-D in *A. nidulans*. These proteins regulate phospholipid asymmetry in the plasma membrane and the endocytic pathway, and are predicted to be involved in linking endocytosis and exocytosis. I discovered that DnfA and DnfB are stratified within the hyphal tip, likely on different vesicles, and require endocytosis for their steady-state localization. Loss of either DnfA or DnfB function has a minor effect on hyphal shape and growth, but loss of

both is lethal. Additionally, the phospholipid phosphatidylserine is normally concentrated strictly on the outside of secretory vesicles, but the localization of this phospholipid, as well as several secretory proteins, was disrupted and diffused through the cytoplasm in the absence of DnfA. These results highlight the importance of endocytic recycling in the maintenance of polarized hyphal growth, as well the complexity of the homeostatic mechanisms at work in an actively expanding hyphal cell, which involve proteins and a variety of lipids for normal function.

DEDICATION

This dissertation and the work completed toward the fulfillment of the requirements for a Doctorate of Philosophy in Plant Pathology and Microbiology are dedicated to Dr. Aristotel Pappelis, Professor Emeritus of Plant Biology at the University of Southern Illinois.

ACKNOWLEDGEMENTS

I would like to again acknowledge the members of my graduate academic committee, including Dr. Andreas Holzenburg (former member of the committee) and especially Dr. Brian Shaw (committee chair), who each offered invaluable assistance, advice, and support throughout my doctoral studies and toward the completion of this dissertation. I would also like to acknowledge our collaborators in research, including: Dr. Zonghua Wang, Dr. Rosa Mouriño-Pérez, Dr. Wenhui Zheng, Ivan Murillo-Corona, Dr. Robert Roberson, and Tianyi Zhou. Additionally, I would like to acknowledge my colleagues in the Shaw laboratory, including Laura Quintanilla, Brigitte Bomer, Blake Commer, Tyler Johnson, Huijuan Yan, Edgar Vega, and Grace Cunningham. Finally, I would like to acknowledge my colleagues at Texas A&M University and elsewhere that assisted through thoughtful discussions, including: Dr. Xiaorong Lin, Dr. Xinping Xu, Srijana Upadhyay, Dr. Eli Borrego, and Dr. Stanislav Vitha.

Along with the people who assisted with my research, I would also like to acknowledge my family, including my parents Maria and Roger Schultz, my brother Jordan Schultz, and my grandparents Steve and Virginia Margeas, and my legion of pets (Adams, Ernie, Jefferson, Teddy, Winnie, and Zorro) for all of their support. At last, I would like to thank my wife, Janna Schultzhaus, for her limitless patience and intelligence, which she employed in assisting me in the completion of this degree.

CONTRIBUTORS AND FUNDING SOURCES

Contributors

This work was supervised by a dissertation committee consisting of Professor Brian D. Shaw (chair), Professor Daniel J. Ebbole, and professor Herman B. Scholthof of the Department of Plant Pathology and Microbiology and Professor Beiyan Nan of the Department of Biology.

The work completed in Chapter 4 was done, in part, under the supervision of Professor Zonghua Wang of the Fujian Agriculture and Forestry University in Fujian, Fuzhou, China, and Professor Rosa Mouriño-Pérez of the Centro de Investigación Científica y de Educación Superior de Ensenada in Ensenada, Baja California, México.

All other work conducted for the dissertation was completed by the student independently.

Funding Sources

Graduate study was supported by a Graduate Merit Fellowship from Texas A&M University, a Teaching Assistantship from the Department of Plant Pathology and Microbiology, and an East Asian Pacific Summer Institute Internship from the National Science Foundation.

This work was made also possible in part by the National Science Foundation under Grant Number No. DGE-1252521, as well as an East Asian Pacific Summer Institute funded by the National Science Foundation. Its contents are solely the

responsibility of the authors and do not necessarily represent the official views of the National Science Foundation.

This work was additionally made possible in part by Texas A&M University and Consejo Nacional de Ciencia y Tecnología (CONACyT) grant No. 2015-031. Its contents are solely the responsibility of the authors and do not necessarily represent the official views of Texas A&M University and CONACyT.

NOMENCLATURE

EE	Early Endosome
ER	Endoplasmic Reticulum
FF	Filamentous Fungi
FRAP	Fluorescence Recovery After Photobleaching
GARP	Golgi-Associated Retrograde Protein Complex
GFP	Green Fluorescent Protein
PC	Phosphatidylcholine
PE	Phosphatidylethanolamine
PS	Phosphatidylserine
PM	Plasma Membrane
PCR	Polymerase Chain Reaction
SNARE	Soluble N-ethylmaleimide-sensitive-factor Attachment REceptor
SPK	Spitzenkörper
SV	Secretory Vesicle
TGN	Trans-Golgi Network

TABLE OF CONTENTS

Page

LIST OF FIGURES

Page

CHAPTER I

INTRODUCTION AND LITERATURE REVIEW*

Overview: endocytosis and exocytosis in hyphal growth

Fungi are eukaryotic microorganisms that are widespread on Earth. The ubiquity and hardiness of these organisms presents society with unique opportunities and challenges. Some fungi, for example, are valuable biochemical factories used in industrial fermentation, while others cause devastating diseases of plants and animals. Understanding the biology of fungi is necessary for ensuring a beneficial relationship with these organisms in the future, and the work of thousands of cell biologists over the last two centuries has been completed toward this goal. However, fungi possess characteristics that make comparisons to other forms of life difficult, and many basic features of fungal biology are still unclear. One of these characteristics is the hypha, the predominant cell type of fungi. Fungal colonies are formed by the radiative growth of hyphae from an inoculation site. Individual hyphae, moreover, grow through deposition of membrane at a discrete region in the tip of their cells. This dissertation addresses how hyphae demarcate and maintain a region where membrane fusion and growth occurs.

Two ancient processes, endocytosis and exocytosis, are employed by eukaryotic cells to shape their plasma membrane and interact with their environment. Filamentous fungi have adapted them to roles compatible with their unique ecological niche and

morphology. These organisms are optimal systems in which to address questions such as how endocytosis is localized, how endocytosis and exocytosis interact, and how large molecules traverse eukaryotic cell walls. In the tips of filamentous (hyphal) cells, a ring of endocytosis encircles an apical crescent of exocytosis, suggesting that this area is able to support an endocytic recycling route, although both processes can occur in subapical regions as well. Endocytosis and exocytosis underlie growth, but also facilitate disease progression and secretion of industrially relevant compounds in these organisms. Here we highlight recent work on endocytosis and exocytosis in filamentous fungi.

Introduction: endocytosis and exocytosis in hyphal growth

Filamentous fungi (FF) are diverse organisms defined by the remarkably polarized growth of their characteristic cell type, the hypha. Underlying this lifestyle is an exquisite spatial control over two ubiquitous cellular processes: endocytosis and exocytosis (Araujo-Bazán, Peñalva, & Espeso, 2008; Caballero-Lima, Kaneva, Watton, Sudbery, & Craven, 2013; Shaw, Chung, Wang, Quintanilla, & Upadhyay, 2011; Taheri-Talesh et al., 2008; Upadhyay & Shaw, 2008). Endocytosis, or membrane internalization, and exocytosis, or secretion, govern a large portion of the interactions of cells with their environment. Both are highly regulated and complex, with endocytosis in budding yeast involving more than 60 proteins (Brach, Godlee, Moeller-Hansen, Boeke, & Kaksonen, 2014; J. Weinberg & Drubin, 2012; J. S. Weinberg & Drubin, 2014) and exocytosis employing conserved tethering complexes, lipids, and the cytoskeleton to overcome the energetic barrier for membrane fusion (**Figure 1.1 A, B**) (Finger &

Novick, 1998; He & Guo, 2009; Jahn & Südhof, 1999). Exocytosis has long been implicated in membrane expansion of vegetative cells in FF, but a role for endocytosis in maintaining hyphal shape has only recently been appreciated (Caballero-Lima et al., 2013; Hervás-Aguilar & Peñalva, 2010; Lee, Schmidtke, Dangott, & Shaw, 2008; Read & Kalkman, 2003; Upadhyay & Shaw, 2008). Much of what is known about these processes comes from studies in the budding yeast *Saccharomyces cerevisiae*, and a large portion of the machinery involved is conserved among eukaryotes. However, FF have some distinctions from yeast. For example, hyphae exhibit an enormous rate of exocytosis (Bartnicki-Garcia, Hergert, & Gierz, 1989; R. J. Howard, 1981). Moreover, filamentous ascomycetes and basidiomycetes possess a Spitzenkörper, an organelle that regulates secretion at the tips of growing hyphae (Brunswick, 1924; Dijksterhuis & Molenaar, 2013; Girbardt, 1957; Jones & Sudbery, 2010; Meritxell Riquelme & Sánchez-León, 2014). Additionally, endocytosis and exocytosis are clearly separated in growing hyphae (Sudbery, 2011; Taheri-Talesh et al., 2008). Here we summarize the most recent work done on endocytosis and exocytosis in FF, with a focus on growth and their importance in microbe-host interactions.

Exocytosis: vesicle tethering, secretion, and the Spitzenkörper

The exocytic machinery

Exocytosis is the process by which vesicles associate with the plasma membrane (PM) and empty their contents into the extracellular space (Finger & Novick, 1998; He & Guo, 2009; Jahn & Südhof, 1999). Membrane fusion in living cells involves donor

membranes (e.g. secretory vesicles) passing multiple tests for specificity with target membranes. These include at least three components for exocytosis in yeast (and, presumably, FF). The Rab GTPase Sec4p associates with secretory vesicles in its active GTP-bound form and interacts with the membrane fusion machinery (Guo, Roth, Walch-Solimena, & Novick, 1999). Next, a pair of Soluble N-ethylmaleimide-sensitive factor Attachment Receptor (SNARE) proteins, one on the vesicle (v-SNARE) and one on the target membrane (t-SNARE), are required to complete membrane fusion (Ferro-Novick & Jahn, 1994; Söllner, Bennett, Whiteheart, Scheller, & Rothman, 1993). Finally, exocytosis involves an octameric tethering complex, the exocyst, and associated Sec1/Munc18 (SM) proteins (Carr, Grote, Munson, Hughson, & Novick, 1999; Novick, Ferro, & Schekman, 1981). Strains with a disrupted exocyst accumulate secretory vesicles in the cytoplasm and are severely compromised in polarized growth, highlighting the importance of this complex in exocytosis and membrane expansion (Guo, Grant, & Novick, 1999). In fungi, the exocyst is composed of eight proteins, corresponding to *S. cerevisiae* Exo70p, Exo84p, Sec3p, Sec5p, Sec6p, Sec8p, Sec10p, and Sec15p (TerBush et al., 1996, Guo et al., 1999). Of these proteins, only Sec3 is dispensable in yeast (Haarer et al., 1996), which also holds true for *Aspergillus niger* and *Candida albicans* (Kwon et al., 2014; Li, Lee, Wang, Zheng, & Wang, 2007). In *N. crassa*, however, Sec-3 was essential and Sec-5 was not (Meritxell Riquelme et al., 2014), and both a *Magnaporthe oryzae* exo70 and a sec5 deletion were viable (Giraldo et al., 2013). These findings indicate that more work needs to be done to understand the assembly and structure of the exocyst in fungi.

Figure 1.1 Endocytic and exocytic machinery in hyphal tips. Exocytosis (**A**) drives growth at hyphal tips, and involves several components. Rho-GTPases including Rac1p and Cdc42p homologues (white) help polarize the actin cytoskeleton (green) and may directly localize the exocyst (orange). Specific lipids such as PIP_2 (yellow) that are enriched at the tip, and vesicle traffic may also contribute to exocyst placement (question marks). Secretory vesicles (blue) travel to the tip on microtubules (grey). Near the tip, vesicles associate with actin filaments and are tethered to the plasma membrane (black) by the exocyst. They eventually fuse with the membrane through interactions between vSNAREs (pink) and tSNAREs (red). Extracellular vesicles, additionally, may be released by fusion of specialized multivesicular bodies (MVB) with the plasma membrane. Endocytosis (**B**), is primarily seen at a subapical ring in growing hyphae. It involves the nucleation of actin (green) through interactions with Fimbrin (oval) and SlaB (pentagon) providing the force to invaginate the membrane, followed by scission, which involves BAR proteins such as the amphiphysins (rectangle). After internalization, endocytic vesicles travel to early endosomes (blue), and recycled cargo can then travel to late Golgi equivalents (yellow) to reenter the secretory pathway or possibly be sent back to the plasma membrane (orange arrow). Additional pathways of endocytosis in fungi include the endocytosis of Can1/CanA at MCCs/eisosomes (pink), and a possible clathrin-independent route regulated by Rho1p/RhoA (cloud) near the apex (red arrows).

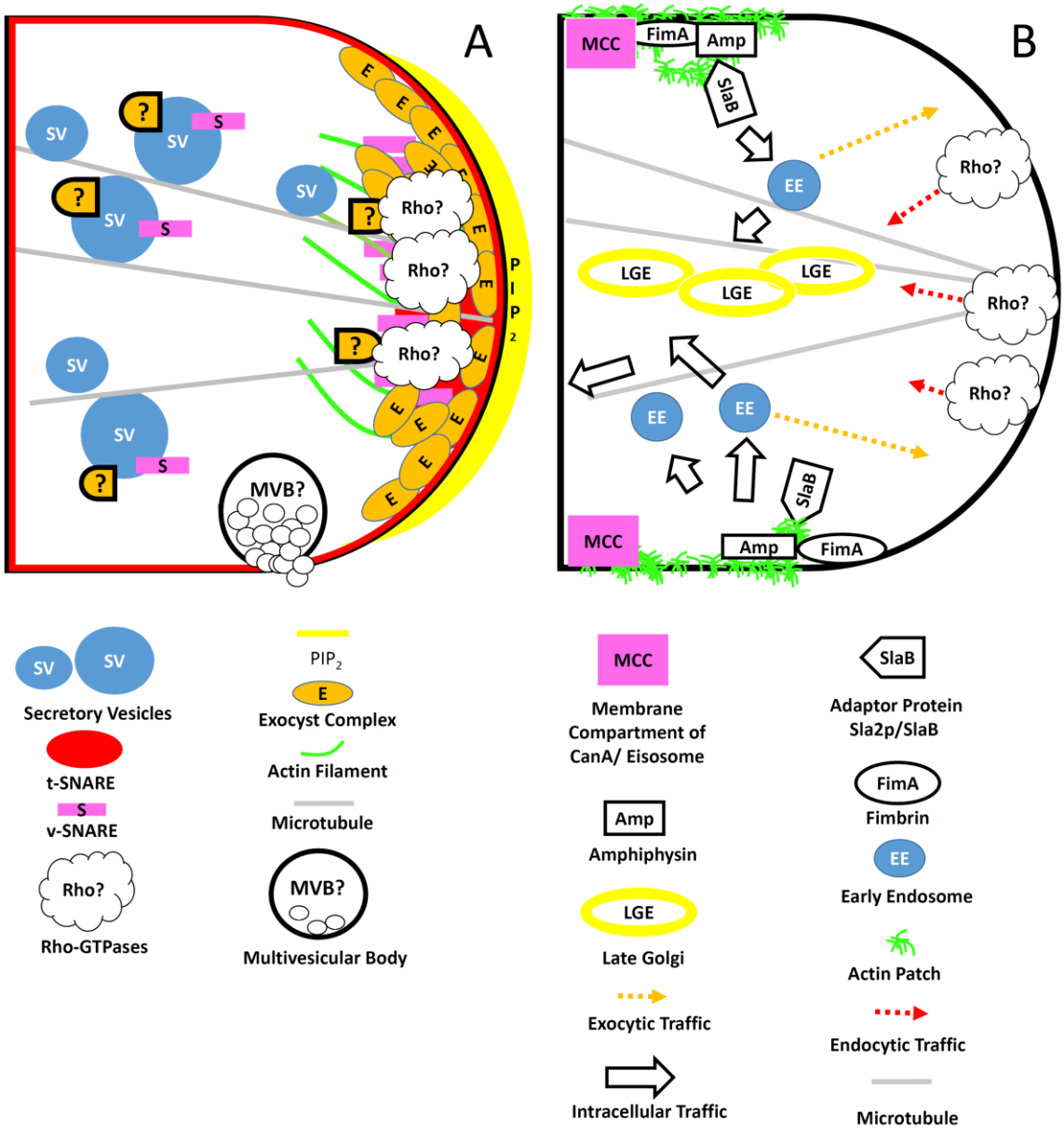
A
B
SV
S
?
Rho?
MVB?
E
PIP2
MCC
FimA
Amp
SlaB
EE
LGE
Secretory Vesicles
t-SNARE
v-SNARE
Rho-GTPases
Exocyst Complex
Actin Filament
Microtubule
Multivesicular Body
Membrane Compartment of CanA/ Eisosome
Amphiphysin
Late Golgi
Exocytic Traffic
Intracellular Traffic
Adaptor Protein Sla2p/SlaB
Fimbrin
Early Endosome
Actin Patch
Endocytic Traffic

Tethering complexes are important throughout eukaryotes for vesicle fusion with various cell destinations such as the PM, the Golgi, and the vacuole. The yeast homotypic fusion and vacuole protein sorting (HOPS) complex can increase lumenal mixing of SNARE-bearing proteoliposomes by 100-fold (Zick & Wickner, 2014). The role that the exocyst plays in fusion is not completely clear, but it appears to be able to associate with the Rab proteins on secretory vesicles, as well as promote binding between SNARE proteins on vesicles and the PM (Guo, Roth, et al., 1999; He & Guo, 2009; TerBush, Maurice, Roth, & Novick, 1996). Sso1/2p and Snc1/2p are the exocytic t- and v-SNARE proteins in *S. cerevisiae*, respectively (Valdez-Taubas & Pelham, 2003). Intriguingly, the Sso1p homologue is localized throughout the entire PM in nearly all eukaryotes, including FF (Guo, Sacher, Barrowman, Ferro-Novick, & Novick, 2000; Taheri-Talesh et al., 2008; Treitschke, Doehlemann, Schuster, & Steinberg, 2010; Valkonen et al., 2007). In general, however, the Snc1/2p homologues are only found at areas of growth (Hervás-Aguilar & Peñalva, 2010; Taheri-Talesh et al., 2008). Many t-SNAREs can interact with multiple v-SNAREs (Banfield, Lewis, & Pelham, 1995; Götte & Fischer von Mollard, 1998), but whether this occurs for Sso1/2p is not currently known. Currently, therefore, exocytosis in hyphae can be thought to be delimited by the location of the exocyst.

The earliest study of exocyst localization in hyphae was in *Aspergillus nidulans*, where SecC/Sec3p was localized to a small cap at hyphal tips (Taheri-Talesh et al., 2008). Next, *Ashbya gossypii* Exo70p, Sec3p, and Sec5p were observed, depending on growth rate, to a crescent at the apex (slow growth), or the Spitzenkörper (fast growth) (Köhli, Galati, Boudier, Roberson, & Philippsen, 2008). The exocyst of *C. albicans*

hyphae, on the contrary, forms a stable apical crescent even when the cytoskeleton is disrupted (Jones & Sudbery, 2010). More recently, Riquelme et al. (2014) observed that EXO-70 localizes to the periphery of the Spitzenkörper in an actin and microtubule-dependent manner in *N. crassa*, and these subunits may be responsible for tethering this organelle to the rest of the complex. This would be opposed to the situation in *S. cerevisiae* (He & Guo, 2009) and *Schizosaccharomyces pombe* (Bendezu, Vincenzetti, & Martin, 2012) where Exo70p and Sec3p bind to the PM and recruits the rest of the complex. It would, however, generally agree with the notion that the exocyst exists as two multimeric subunits, one of which travels on vesicles, that assemble at the PM in a reaction that promotes vesicle tethering (Guo, Grant, et al., 1999; Guo, Roth, et al., 1999; He, Xi, Zhang, Zhang, & Guo, 2007).

The Spitzenkörper and exocytosis

The Spitzenkörper is commonly viewed as a "vesicle supply center" that provides the membrane for tip growth in some fungi (Gierz & Bartnicki-Garcia, 2001; Meritxell Riquelme & Sánchez-León, 2014). Exocytic traffic from fungal Golgi equivalents (GEs) awaiting fusion with the PM provides a large part of the membrane for this organelle (Pantazopoulou, Pinar, Xiang, & Peñalva, 2014), which suggests that membrane fusion in the tip is limiting. This limitation may also influence the structure and size of the Spitzenkörper. Having exocyst proteins delivered to the tip on secretory vesicles could provide some of this regulation, if the fusion of subunits on vesicles with subunits on the PM was required for vesicle tethering, and PM-localized subunits were limited in quantify, for example. However, vesicles in the Spitzenkörper are also

organized into different layers, with large macrovesicles in the outer layer (termed by the authors the "Spitzenring") and smaller, microvesicles in the "core" (R. J. Howard, 1981; Meritxell Riquelme & Sánchez-León, 2014; Verdín, Bartnicki-Garcia, & Riquelme, 2009). In *N. crassa* these different layers are known to have different cargo, with the 1,3 β-glucan synthase GS-1 located in the outer layer and the chitin synthase Chs-1 present in the core (Verdín et al., 2009). *S. cerevisiae* also has distinct populations of high and low density vesicles that each have cargo destined for different locations (Harsay & Bretscher, 1995). It is possible that behavior among the different groups of vesicles could be different. Additionally, no studies to date in fungi have differentiated between exocytosis that results in full membrane fusion and the transient "kiss-and-run" exocytosis seen in animal and plant cells (Aravanis, Pyle, & Tsien, 2003; Weise, Kreft, Zorec, Homann, & Thiel, 2000). Analyzing these two populations of vesicles, as well as how they interact with the plasma membrane, will be key to gaining more insight into the nature of the Spitzenkörper and hyphal growth.

The cell wall and exocytosis

Along with membrane-building materials, secretory vesicles in fungi include proteins that are destined for the cell wall or the extracellular space. In yeast, this is represented by the subset of 100 nm "periplasmic" vesicles that include secreted proteins, such as the major exoglucanase Exg1p as cargo (Harsay & Bretscher, 1995). The cell wall is a formidable barrier to macromolecules, viruses, and bacteria (Moebius, Üzüm, Dijksterhuis, Lackner, & Hertweck, 2014), but fungi are clearly able to surpass this, as demonstrated by their prodigious production of secreted proteins, during nutrient

acquisition, disease progression in the host, secreted secondary metabolites, and a variety of antibiotics. Recently, more data has accumulated regarding trans-cell wall secretion. The presence of immunologically active vesicles in the culture supernatant of the basidiomycete pathogen *Cryptococcus neoformans*, as well as the ascomycetes *Histoplasma capsulatum* and *C. albicans*, are strong evidence for exocytosis being the preferred method of transport through walls (Albuquerque et al., 2008; Casadevall, Nosanchuk, Williamson, & Rodrigues, 2009; Rodrigues et al., 2007). This mechanism involves the fusion of organelles such as multivesicular bodies (MVBs) delivering cargo-loaded vesicles into the extracellular space. Aflatoxin B1, a carcinogenic secondary metabolite synthesized by some *Aspergillus* spp. is produced in vesicles termed "aflatoxisomes" trafficking to the PM. This may be a tactic that is conserved in many fungi to deploy a variety of molecules (Chanda et al., 2009b; Chanda, Roze, & Linz, 2010).

Endocytosis: the endocytic collar and hyphal morphogenesis

The endocytic machinery

Electron micrographs of budding yeast cells regularly reveal small (<200nm) invaginations of the PM associated with endocytic proteins. Surprisingly, these are rarely seen in similarly prepared images of hyphae, although the importance of endocytosis in fungi is well-established (Araujo-Bazán et al., 2008; Fischer-Parton et al., 2000; Upadhyay & Shaw, 2008). Endocytosis in yeast involves two phases. The earliest phase is variable (60-180 seconds) during which cargo congregate at nascent sites and the

clathrin coat is established around the invagination. The late phase is shorter and more ordered (~35 seconds) and in this step invagination is driven by actin nucleation, culminating in scission and movement away from the PM (W. Kukulski, Schorb, Kaksonen, & Briggs, 2012; W. Kukulski et al., 2011; J. Weinberg & Drubin, 2012). FF possess most of the endocytic proteins also present in yeast and mammals (**Figure 1.1 B**) (Read & Kalkman, 2003) and uptake endocytic markers regularly (Fischer-Parton et al., 2000), but the conservation of these phases may have diverged considerably, as seen for the scission step (Conibear, 2010).

Endocytic scission

Animals use the GTPase dynamin and the actin cytoskeleton for membrane bending and scission (van der Bliek & Meyerowrtz, 1991). In the absence of the yeast dynamin-1 homologue Vps1p, however, endocytosis proceeds normally. Vps1p also does not have an obvious PM localization (Peters, Baars, Bühler, & Mayer, 2004), which has led some to conclude that it does not participate in endocytosis. The *A. nidulans* Vps1p homologue, VpsA, was functionally characterized, and although endocytosis was not addressed, the deletion appeared to result in a pleiotropic effect as it does in *S. cerevisiae* (Tarutani, Ohsumi, Arioka, Nakajima, & Kitamoto, 2001). These results may have obfuscated its importance in fungal endocytosis, however, as recent studies incorporating electron microscopy have revealed defects in membrane invagination in Vps1p mutants (Smaczynska-de Rooij et al., 2010). These phenotypes have also been linked to another set of proteins, the amphiphysins Rvs161p and Rvs167p, which are known to act in scission in yeast (D. Wang, Sletto, Tenay, & Kim, 2011). In yeast,

amphiphysins arrive at endocytic sites just before scission, and may bind to and stabilize the invaginating endocytic bud through their F-BAR domains, which recognize membrane curvature (Meinecke et al., 2013). In the absence of Rvs161p or Rvs167p ~20% of invaginations retract to the membrane without undergoing scission, and endocytosis is greatly reduced (Kishimoto et al., 2011; Youn et al., 2010). Interestingly, some FF appear to have more amphiphysin-like proteins than in yeast (e.g., *Aspergillus nidulans* and *N. crassa* each possesses two proteins similar to the amphiphysin Rvs167 in yeast(Arnaud et al., 2012), and from data in *N. crassa* at least some appear to be dispensable for hyphal growth (**Figure 1.1B**) (Muñoz, Marcos, & Read, 2012). Alternatively, the unconventional Myosin Type I, MyoA, localizes to sites of endocytosis in *A. nidulans* (Yamashita, Osherov, & May, 2000) and interacts with Abp1p (Matsuo, Higuchi, Kikuma, Arioka, & Kitamoto, 2013). Additionally, a constitutively active allele of MyoA increased endocytosis at hyphal tips (Yamashita & May, 1998). The *S. cerevisiae* myosins Type I, Myo3p and Myo5p, have also been implicated in endocytosis (Geli & Riezman, 1996), but direct evidence is still lacking for a role in scission. More likely, their chief role is in actin patch regulation.

The lipid composition of endocytic invaginations also appears to play a role in vesicle scission through the activity of the synaptojanins. Several endocytic adaptor proteins have been shown to attach to Phosphatidylinositol (4,5) bisphosphate (PIP_2) on invaginating buds through Pleckstrin-Homology (PH) domains. Synaptojanins hydrolyze PIP_2 and deplete it at these sites. The differential lipid composition between the bud ends and the neck can then provide an interfacial force that may promote scission, as well as

uncoating of PH-domain proteins (Sun, Carroll, Kaksonen, Toshima, & Drubin, 2007). Most ascomycetes contain several, possibly redundant synaptojanin homologues, but as they regulate the intracellular PIP_2 level (Sun et al., 2007), which in turn is important for hyphal growth (Mähs et al., 2012; Sun & Drubin, 2012), their examination is warranted in future studies on endocytosis in filamentous fungi.

Alternate endocytic routes

Clathrin-mediated endocytosis is the best characterized internalization pathway in eukaryotes, but other types of endocytosis (e.g. phagocytosis) have been adapted in different organisms, collectively referred to as clathrin-independent endocytosis. In budding yeast, a clathrin-independent route for the uptake of FM4-64 was recently discovered (Prosser, Drivas, Maldonado-Báez, & Wendland, 2011). Surprisingly, it was independent of the Arp2/3p complex, which is critical for forming the actin patches that are commonly viewed as sites of endocytosis. Rather, it depended on the formin Bni1p, which nucleates actin filaments, and the GTPase Rho1p, which are generally associated with exocytosis. Indeed SepA, the only formin in *A. nidulans*, and the ortholog Bni-1 in *N. crassa*, are located in the Spitzenkörper and the apical dome and are thought to be mainly involved in producing actin filaments along which vesicle traffic is sent to the apex (Lichius, Yáñez-Gutiérrez, Read, & Castro-Longoria, 2012; Sharpless & Harris, 2002). Rho1p, additionally, interacts with the exocyst (Guo, Tamanoi, & Novick, 2001), and in *A. nidulans* its homologue RhoA is involved in cell wall deposition (Guest, Lin, & Momany, 2004). An endocytic internalization route occurring at the apex of hyphae would not be an unprecedented proposition, however, as multiple endocytic routes are

present in tip-growing plant cells (Bove et al., 2008; Ketelaar, Galway, Mulder, & Emons, 2008; Onelli & Moscatelli, 2013; Ovečka, Illés, Lichtscheidl, Derksen, & Šamaj, 2012). Intriguingly, in *C. albicans* clathrin and the arp2/3 complex, which assists in the formation of the actin patches that are thought to provide force for PM invagination, are not required for endocytosis (Epp et al., 2013). These mutants could not form hyphae, however, adding support for the importance of endocytosis in hyphal growth. Similar studies have shown endocytosis to concentrate in a region just behind the apex, and to be essential for normal growth in *A. oryzae*, *N. crassa*, *A. nidulans*, *A. gossypii*, and *Fusarium graminearum*. Disruption of the actin crosslinking protein Fimbrin in each of these organisms resulted in an almost complete block of endocytosis and compromised hyphae (Echauri-Espinosa, Callejas-Negrete, Roberson, Bartnicki-García, & Mouriño-Pérez, 2012; Higuchi, Shoji, Arioka, & Kitamoto, 2009; Jorde, Walther, & Wendland, 2011; Upadhyay & Shaw, 2008; Zheng et al., 2014).

The identification of clathrin-independent endocytic routes in FF could, therefore, be important for understanding the importance of endocytosis in hyphal growth. Recent studies indicate that such processes do exist, although their role in morphogenesis is not as clear as in *C. albicans*. First, the protein flotillin promotes clathrin-independent endocytosis in animal cells, and it localizes throughout the PM in *A. nidulans*, but is excluded from apical regions (Takeshita, Diallinas, & Fischer, 2012). Another study examined proteins that interacted with actin binding protein A (AbpA) in *Aspergillus oryzae* and identified the membrane compartment of CanA/eisosomes in subapical regions of hyphae (Matsuo et al., 2013). Deleting components of this

compartment did not have major effects on growth or FM4-64 uptake, but the internalization of AoCanA was disrupted. Eisosome disruption, moreover, did not obviously affect endocytic uptake in *A. gossypii* or *A. nidulans*, and their role in specialized endocytosis is still being explored in FF(Athanasopoulos, Boleti, Scazzocchio, & Sophianopoulou, 2013; Seger, Rischatsch, & Philippsen, 2011). In summary, endocytosis is conserved in filamentous fungi, but specific roles of endocytic proteins may be unique in these organisms. Investigating different endocytic routes in hyphae is a promising path for fungal cell biologists.

Endocytosis and exocytosis in polarized growth

Localization of exocytosis and endocytosis

Fungi are able to rearrange their growth axes in response to environmental cues (Brand et al., 2014; H. C. Hoch, Staples, Whitehead, Comeau, & Wolf, 1987; Stephenson, Gow, Davidson, & Gadd, 2014), and this involves a rapid dissolution and reorganization of the endocytic and exocytic machinery. How these processes become polarized and coupled, however, is unclear. In *S. cerevisiae*, endocytosis may polarize exocytosis by a dynamic "corralling" mechanism (Jose, Tollis, Nair, Sibarita, & McCusker, 2013), but in germling hyphae, these two process do not appear to be segregated (Sharpless & Harris, 2002; Taheri-Talesh et al., 2008; Upadhyay & Shaw, 2008). Additionally, in rapidly growing cells, the localization of many polarized proteins is growth rate dependent, and many components of hyphal tips rapidly mislocalize when cells stop growing, so any extremely deleterious mutation could cause the

mislocalization of any tip protein. For example, although in budding yeast Cdc42p was implicated in directional traffic of the exocyst component Sec6p (Adamo et al., 2001), it is unclear from that study whether the cells were growing when imaged. This is an important issue that should be addressed when assessing how any process is localized in hyphae.

Membrane composition can determine the location of exocytosis. In budding yeast, Exo70p and Sec3p bind PIP_2, which is polarized in the PM at sites of growth (He & Guo, 2009; He et al., 2007). In *N. crassa*, however, Exo-70 is associated with secretory vesicles and requires the actin cytoskeleton for its localization (Meritxell Riquelme et al., 2014), indicating a divergence of function between these proteins in filamentous fungi. PIP_2 concentration, as assessed by a fluorescent reporter, is somewhat polarized in hyphae, but forms a gradient that is much shallower than most tip components (Pantazopoulou & Peñalva, 2009; Vernay, Schaub, Guillas, Bassilana, & Arkowitz, 2012), although the PIP_2 synthase was required for *N. crassa* growth (Mähs et al., 2012). Exo84p was shown to be associated with Phosphatidylserine in *C. albicans*, and when it was phosphorylated it dissociated with this phospholipid and was released from the plasma membrane, which potentially allows it to be recycled back to the PM (Caballero-Lima & Sudbery, 2014). Filipin is a fluorescent marker for lipid rafts, and though staining with filipin is not accurate in live cells (Valdez-Taubas & Pelham, 2003), nearly all data to date indicate that these PM components are enriched at hyphal tips. It is possible that, as *S. cerevisiae* Exo70p recognizes PIP_2, some proteins may preferentially bind to lipid rafts. In animals, lipid rafts can mark sites of exocytosis

(Chamberlain, Burgoyne, & Gould, 2001; Salaün, James, & Chamberlain, 2004),and the presence of these domains can influence the integrity of the cytoskeleton in hyphae (Pearson, Xu, Sharpless, & Harris, 2004), but more work needs to be done to understand PM protein-lipid interactions in filamentous fungi.

Signaling the beginning of endocytosis

Endocytosis involves several dozen proteins and occurs in a sequential order, and in FF it is precisely localized. What directs this process to a specific space in the cell? The identity of a proteinaceous signal has been elusive, at least in fungi. Recently, the first seven proteins known to be involved in endocytosis were shown to be dispensable for endocytosis to localize and successfully complete in budding yeast (Brach et al., 2014). One possibility for the exclusion of endocytosis from the apical dome is that the high rate of exocytosis at the tip disallows buildup of the endocytic machinery. The process of endocytosis can take up to four minutes (W. Kukulski et al., 2011) which is unstable in a region with high membrane flux, such as the apex of hyphal tips. Supporting this is the observation that germlings, which experience much slower growth than mature hyphae, and thus less vesicle fusion at the tip, do not exhibit a separation of the exocytosis and endocytosis at the apex (Berepiki, Lichius, Shoji, Tilsner, & Read, 2010). However, this does not explain why endocytosis is highly concentrated at the collar, nor does it explain the relative stability of actin patches at the collar, both of which indicate that this region of the hypha is “marked” for endocytosis. The membrane composition at the collar is clearly important, but there are many other components that may play a role.

The lipid composition of the PM could determine the location of the collar. For example, in yeast, a mutant that lacked phosphatidylserine also lost the ability to polarize endocytosis, whereas the loss of PIP_2 had an effect on scission but not initiation of endocytosis (Sun & Drubin, 2012). Phosphatidylserine promotes polarization of Cdc42p (Fairn, Hermansson, Somerharju, & Grinstein, 2011), but this has not extended directly to the recruitment of endocytic proteins. Additionally, lipid rafts have been hypothesized to be involved in endocytosis (Parton & Richards, 2003), although they are generally present at the apex and taper off near the endocytic collar (Takeshita, Higashitsuji, Konzack, & Fischer, 2008). It is possible that a precise composition of lipid rafts or phospholipids is optimal for the attraction of endocytic proteins. One last hypothesis comes from two recent studies in budding yeast and *A. nidulans*, respectively, that looked at the role of the endoplasmic reticulum (ER) at the plasma membrane. In yeast it was observed that endocytosis occurred in areas that were devoid of a cortical-ER connection, so that the PM was segmented into domains that were either endocytic, carried lipid rafts, or were attached to the ER (Stradalova et al., 2012). Interestingly, the *A. nidulans* peripheral ER localizes near the endocytic collar, and it was hypothesized that the actin cytoskeleton associated with the endocytic collar may act to scaffold the peripheral ER in place to provide growing hyphal tips with secretory ER (Markina-Iñarrairaegui, Pantazopoulou, Espeso, & Peñalva, 2013).

Endocytic recycling in hyphae

The location of the endocytic collar suggests the presence of a recycling route near the hyphal apex. Endocytic recycling generally includes three phases. First,

membrane proteins are recognized at sites of endocytosis by cargo adaptor proteins and internalized. Next, they are sent to early endosomes, which tubulate and send traffic to late GEs. From there, they are able to be sorted back into the secretory pathway for exocytosis. Several proteins, including Snc1p (Valdez-Taubas & Pelham, 2003) and Wsc1p (Piao, Machado, & Payne, 2007) follow this pathway. The situation is different for filamentous fungi, however, as the Snc1p homologue SynA was still polarized in *A. nidulans* in a *vpt6/rabC* deletion, as well as an *rcyA* deletion, which presumably abolish most recycling traffic to late GEs. In mammals, recycling traffic travels through recycling endosomes, the Trans-Golgi Network (TGN), or is sent directly back to the PM through early endosomes in a so-called "quick recycling route" that is regulated by Rab4 (Grant & Donaldson, 2009), and it is likely that, if endocytic recycling does assist in hyphal growth, FF have adapted a more direct recycling route accommodate the rapid turnover that they likely require for some polarized proteins, although details of this route are unknown.

Some evidence has accumulated to support the presence of endocytic recycling in hyphal tips. Fischer-Parton et al. (2000) found that the endocytic marker FM4-64 localized to the Spitzenkörper soon after internalization in many fungi. Endocytic protein *Ao*End4 was discovered to be important for polarized growth as well as recycling of the v-SNARE *Ao*Snc1 in *A. oryzae* by Higuchi et al. (2008). Peñalva et al., additionally, showed that SynA was mislocalized to the PM when its endocytosis was blocked in *A. nidulans* (Hervás-Aguilar & Peñalva, 2010; Pantazopoulou & Peñalva, 2011). Most recently, Schultzhaus et al. showed that a plasma membrane flippase DnfA

was recycled through the late Golgi and endocytosed through an NPFxD motif in *A. nidulans* (Z. Schultzhaus, Yan, & Shaw, 2015b). Fluorescence Recovery After Photobleaching (FRAP) on tip components in *C. albicans* demonstrated that proteins that localize to the Spitzenkörper such as myosin light chain are more transient than proteins that form an apical crescent, such as the exocyst (Jones & Sudbery, 2010). These findings are in agreement with studies in yeast (Howell et al., 2012) that suggest that proteins that arrive at hyphal tips through vesicle trafficking, such as those trafficking via endocytic recycling, should accumulate in an area behind the membrane. Finally, Craven et al. performed an excellent description of the spatial orientation of the tip growth machinery in *C. albicans*, and determined that exocytosis and endocytosis were situated in a way that corresponded well with hyphal shape, although the specific identity and destination of the cargo of the endocytic collar has not been directly assessed (Caballero-Lima et al., 2013).

Recent studies suggest that, unlike the strict separation that occurs in hyphae, pollen tube tips uphold a complex current of vesicle traffic made of different endocytic and exocytic pathways, which are important for cell growth and shape (Bove et al., 2008; Helling, Possart, Cottier, Klahre, & Kost, 2006; Onelli & Moscatelli, 2013). This model is built from microscopic observations that suggested that the greatest area of cell expansion is not the extreme apex, but rather in an annular region around the very pole (Geitmann & Dumais, 2009). Additionally, clathrin-dependent and independent endocytosis occurs at different locations throughout the apical compartment of pollen tubes, and the route taken by cargo of these routes can be complex (Onelli & Moscatelli,

2013). The rate of endocytosis has been quantified in *Arabidopsis* pollen tubes. This revealed that an excess of vesicles large enough to accommodate almost a minute of growth is present in the apex of these cells (Ketelaar et al., 2008; Ovečka et al., 2012), but how much membrane was recycled was unclear. Such studies would be valuable for understanding growth in filamentous fungi.

Subapical endocytosis and exocytosis

In agreement with the idea that fungi regulate endocytosis and exocytosis to accomplish growth, the machinery for both processes is found at growing septa (**Figure 1.2**), as well as in new sites of branching. Septa represent subapical sites of polarization distinct from hyphal tip growth, and while the endocytic machinery can be seen intermittently throughout hyphae (likely for the internalization and recycling of a variety of transporters (Vlanti & Diallinas, 2008)) and secretion and growth (intercalary growth) have been observed occasionally in subapical compartments (Read, 2011), most studies focusing on the molecular machinery of endocytosis and exocytosis in these regions have centered around what occurs at septa (Diego Luis Delgado-Álvarez, Bartnicki-García, Seiler, & Mouriño-Pérez, 2014; Hayakawa, Ishikawa, Shoji, Nakano, & Kitamoto, 2011; Mouriño-Pérez, 2013). As reviewed in Mouriño-Pérez (2013) the formation of a septum is a process that coordinates many influences, including cell wall growth, the cytoskeleton, and mitosis. Endocytosis and exocytosis at these locations are subject to different constraints than the hyphal tip. First, from studies on the septation machinery, proteins begin at the cell wall and move inward as the septum is made, following a structure called the contractile actin ring

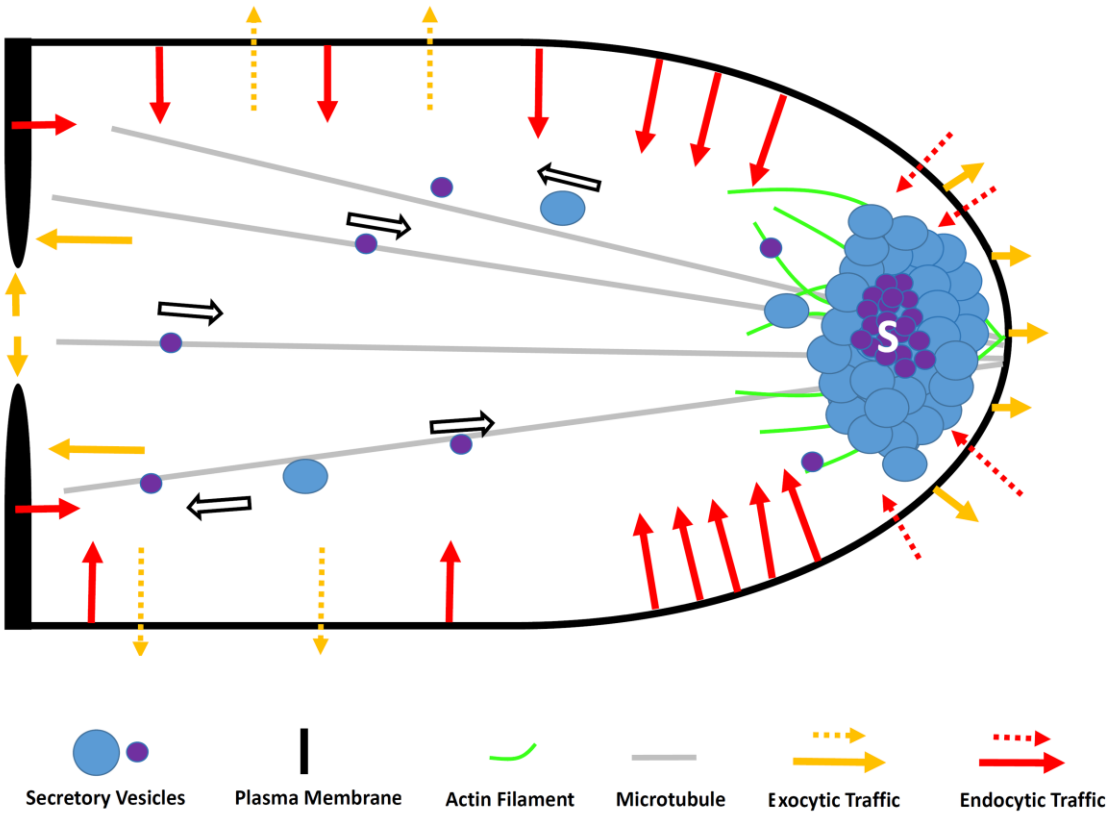

Figure 1.2 Pathways of membrane flow in fungal hyphae. Raw materials for the plasma membrane, as well as membrane proteins and other molecules, are brought to hyphal tips on microtubules (grey). At the tip, they can traffic back to subapical compartments, or enter the Spitzenkörper (S) and be sent to the plasma membrane on actin filaments (green). At the apex, vesicles can fuse, causing growth to occur (orange arrows), or transiently associate with the plasma membrane (not shown). Molecules in the plasma membrane can be endocytosed through either clathrin-dependent or independent endocytosis at the collar (red arrows). Endocytosis and exocytosis also occurs at septa (far left), and may even occur at other places in the cell through an unexplored mechanism (orange and red dotted arrows).

(Diego Luis Delgado-Álvarez et al., 2014). The exocytic machinery will therefore overlap or be removed as the septum contracts, and the curvature of the membrane at septa will be greater. Additionally, there is probably less microtubule traffic to the septa, as they are anchored at the tip, making actin more important for exocytosis at septa. This could explain why the well-studied formin s*epA*, when deleted in *A. nidulans*, completely blocks septum formation but not tip growth, although in *N. crassa*, the formin Bni-1 arrives after actin cables at septa (Mouriño-Pérez, 2013).

Endocytosis and exocytosis and pathogenesis

Effectors and the interfacial layer between pathogen and host

An important tool in the fungal pathogen repertoire is an effector, which is a secreted molecule that contributes to disease progression. These are so common that some fungal pathogens such as *Ustilago maydis* produce more than 150 potential effectors, all of which may have different targets in the host (Mueller et al., 2008). Effectors are secreted into their host, which is important as the molecules may have distant targets and even may be toxic to the pathogen. Interestingly, *M. oryzae*, the destructive rice blast pathogen, is able to deliver proteins to distinct extracellular regions, either into the host-pathogen interface or into the host cell, using two distinct mechanisms that require either the conventional Golgi-directed secretory machinery, or one that is Brefeldin A-insensitive and requires some components of the exocyst (Giraldo et al., 2013). Additionally, hyphae that grow inside plants are usually bulbous and misshapen in comparison to hyphae growing on media. Some changes in shape

could be the result of the physical barriers encountered when growing inside a host, but a concomitant reorganization of exocytosis and endocytosis could also play a role in this change. Endocytosis, for example, is important for morphology as well as virulence in such diverse pathogens as *U. maydis* (Fuchs, Hause, Schuchardt, & Steinberg, 2006), *F. graminicola* (Zheng et al., 2014), and the mammalian pathogen *C. albicans* (Douglas, Martin, & Konopka, 2009).

Endocytosis and drug resistance and mating

Endocytosis could also be a common route into cells for signaling molecules and antifungal drugs. Interestingly, amphiphysins were recently discovered in two independent screens to identify genes controlling Conidial Anastamosis Tube formation (Fu et al., 2011), as well as resistance to antifungal peptides (Muñoz et al., 2012). Amphiphysins, as mentioned in section 3.2, seem to be much less important in filamentous fungi than in yeast, and these recent studies may provide some evidence that these organisms take advantage of different forms of endocytosis for the variety of different tasks that they perform in their life cycles.

A promising method being developed to treat plant diseases is host-induced gene silencing using RNA Interference (RNAi), in which pathogens are exposed to short interfering double-stranded RNAs that mediate silencing of important genes in their genome, leading to dysfunction or death (McDonald, Brown, Keller, & Hammond, 2005; Nakayashiki et al., 2005; Nunes & Dean, 2012). How the genetic material is transported into the pathogen in this case is not currently known, and it is not effective for all fungal pathogens, but at least for *A. nidulans*, it is able to be absorbed from the

media (Khatri & Rajam, 2007), and the endocytic pathway may be the method of internalization, as seen in *Drosophila melanogaster* (Saleh et al., 2006).

Conclusion: endocytosis and exocytosis in hyphal growth

It is now clear that membrane flux and traffic through the PM are complex, underlying processes that define the filamentous lifestyle of filamentous fungi (**Figure 1.2**), but each new study brings with it new questions. How important is the coordination between exocytosis and endocytosis for development? What methods do different tip proteins use to maintain their localization (e.g. by endocytic recycling or some other mechanism), and how does this relate to protein function? What role does the plasma membrane play in localizing these processes? How do they contribute to growth inside hosts, and translocation of signaling molecules and antifungal compounds? Finally, how do proteins assemble within, or traverse through the thick cell wall? FF are ideal models in which to explore these questions, which are of interest to all of eukaryotic cell biology. With efficient gene-targeting techniques already established for model systems, and increasingly being adapted for more economically important organisms, it is only a matter of time before these are addressed.

CHAPTER II

CLATHRIN LOCALIZATION AND DYNAMICS IN *Aspergillus nidulans**

Overview: clathrin localization and dynamics in *A. nidulans*

Cell growth necessitates extensive membrane remodeling events including vesicle fusion or fission, processes that are regulated by coat proteins. The hyphal cells of filamentous fungi concentrate both exocytosis and endocytosis at the apex. This investigation focuses on clathrin in *Aspergillus nidulans*, with the aim of understanding its role in membrane remodeling in growing hyphae. We examined clathrin heavy chain (ClaH-GFP) which localized to three distinct subcellular structures: late Golgi (*trans*-Golgi equivalents of filamentous fungi), which are concentrated just behind the hyphal tip but are intermittently present throughout all hyphal cells; the region of concentrated endocytosis just behind the hyphal apex (the "endocytic collar"); and small, rapidly moving puncta that were seen trafficking long distances in nearly all hyphal compartments. ClaH localized to distinct domains on late Golgi, and these clathrin "hubs" dispersed in synchrony after the late Golgi marker PH^{OSBP}. Although clathrin was essential for growth, ClaH did not colocalize well with the endocytic patch marker fimbrin. Tests of FM4-64 internalization and repression of ClaH corroborated the observation that clathrin does not play an important role in endocytosis in *A. nidulans*. A

---

*This chapter is reprinted with permission from "Clathrin localization and dynamics in *Aspergillus nidulans*" by Schultzhaus, Z. S., T. B. Johnson, and B. D. Shaw. 2017. 103(2): 299-318.

minor portion of ClaH puncta exhibited bidirectional movement, likely along microtubules, but were generally distinct from early endosomes.

Introduction: clathrin localization and dynamics in *A. nidulans*

Intracellular traffic occurs primarily through vesicle intermediates that move among individual organelles and the plasma membrane. The diversity of cargo and destinations that these trafficking intermediaries possess suggests the existence of subsets of vesicles and proteins dedicated to the transport of certain molecules. Moreover, it renders maintenance of vesicle integrity and specificity essential. Assisting in the formation and budding of membranes are coat proteins, which form around nascent vesicles and promote the energy-intensive membrane bending associated with vesicle formation.

Mirroring the diversity of intracellular vesicles, there are different types of coat proteins. Among these are the coat proteins complexes (COP) I and II, which function in traffic between the endoplasmic reticulum and the early Golgi, and clathrin, which works at later stages in the secretory pathway, as well at the plasma membrane as a prime component of endocytosis (Bonifacino & Glick, 2004; McMahon & Mills, 2004; Schekman & Orci, 1996). Clathrin is the most well-characterized coat protein complex. It was discovered and named in 1976 (Pearse, 1976) and has been the subject of intense investigations (Robinson, 2015). It is composed of two proteins, the clathrin "heavy" and "light" chains, that combine into a triskelion that includes three copies of each subunit.

Multiple triskelia organize into a lattice at sites of membrane budding to provide structural support for membrane bending through the natural curvature of the lattice, as well as support for vesicle fission (Frances M Brodsky, 1988; Frances M Brodsky, Chen, Knuehl, Towler, & Wakeham, 2001; W. Kukulski, Andrea Picco, Tanja Specht, John AG Briggs, and Marko Kaksonen, 2016). Clathrin performs this function primarily at the late/*trans*-Golgi and at the plasma membrane, with resulting vesicles being sent to early endosomes in both cases (Bonifacino & Glick, 2004; Costaguta, Stefan, Bensen, Emr, & Payne, 2001; Hinners & Tooze, 2003; Puertollano et al., 2003; Raiborg et al., 2002; Raiborg, Bache, Mehlum, Stang, & Stenmark, 2001). Thus, clathrin is a major component of both the endocytic (plasma membrane budding) and the secretory (Golgi budding) machinery in eukaryotes (Daboussi, Costaguta, & Payne, 2012; Gall et al., 2002; Kaksonen, Toret, & Drubin, 2005; Newpher, Smith, Lemmon, & Lemmon, 2005).

In an effort to understand the molecular basis of the filamentous growth of fungi, we are working to characterize the endocytic machinery in the fungus *Aspergillus nidulans*. In hyphae, the tip-growing cells produced by filamentous fungi, endocytosis is highly concentrated at a specific region behind the site of growth. The annulus of endocytosis stretching from 1-5μm behind the apex, termed the "endocytic collar," thus represents endocytic "hot spots" seen in mammalian cells, where the membrane appears to be marked for constitutive endocytosis (Cao, Krueger, & McNiven, 2011; Diego L Delgado-Álvarez et al., 2010; Hervás-Aguilar & Peñalva, 2010; Saffarian, Cocucci, & Kirchhausen, 2009; Z. Schultzhaus, Quintanilla, Hilton, & Shaw, 2016; Z. S. Schultzhaus & Shaw, 2015; Shaw et al., 2011; Sudbery, 2011; Taheri-Talesh et al.,

2008; Upadhyay & Shaw, 2008; C.-L. Wang & Shaw, 2016). Only proteins known to be involved in the middle and late stages of endocytosis have been studied in filamentous fungi. These proteins generally arrive and leave the plasma membrane with consistent lifetimes, whereas "early stage" endocytic proteins, including clathrin, are more variable and can be dependent on factors such as the amount of cargo associated with patches (Carroll et al., 2012; Kaksonen et al., 2005; J. Weinberg & Drubin, 2012).

Clathrin is therefore an ideal protein for investigating the molecular processes at the hyphal tip. The function and localization of clathrin has not been determined in filamentous fungi. Clathrin-dependent and clathrin-independent endocytosis occur in both the budding yeast *Saccharomyces cerevisiae* (Lemmon & Jones, 1987; Tuo, Nakashima, & Pringle, 2013), and the fungal pathogen *Candida albicans* (Epp et al., 2013; Xu et al., 2007), and clathrin is not strictly essential for viability in either of these organisms. In *C. albicans*, however, inhibiting a component of clathrin-mediated endocytosis had the specific effect of abolishing the formation of hyphae (Epp et al., 2010). Studying clathrin in filamentous fungi is potentially informative for several reasons. First, fungal cell biologists and pathologists have focused on intracellular trafficking as a major player in overcoming host defenses, production of mycotoxins, polarized growth, and development (Chanda et al., 2009b; Pinar, Pantazopoulou, Arst, & Peñalva, 2013; Z. Schultzhaus, Yan, & Shaw, 2015a; Z. S. Schultzhaus & Shaw, 2015; Steinberg, 2007b; Wedlich-Söldner, Bölker, Kahmann, & Steinberg, 2000). Second, the elongate cells of filamentous fungi are excellent for imaging long distance trafficking, as well as the interplay of endocytosis and exocytosis (Abenza, Pantazopoulou, Rodríguez,

Galindo, & Peñalva, 2009; Becht, König, & Feldbrügge, 2006; Caballero-Lima et al., 2013; Echauri-Espinosa et al., 2012; Feldbrügge, Kämper, Steinberg, & Kahmann, 2004; Jones & Sudbery, 2010; Lee et al., 2008; Lee & Shaw, 2008; Pantazopoulou & Peñalva, 2009; Meritxell Riquelme et al., 2014; Sánchez-León et al., 2011; Sánchez-León et al., 2015; Steinberg, 2007a, 2007b; Sudbery, 2011; Taheri-Talesh et al., 2008; Wedlich-Söldner et al., 2000). Third, the endocytic collar that just precedes the hyphal tip is a uniquely fungal structure that is important for the maintenance of somatic fungal growth, and little is known about endocytic protein dynamics there (Araujo-Bazán et al., 2008; Diego L Delgado-Álvarez et al., 2010; Echauri-Espinosa et al., 2012; Lee et al., 2008; Z. Schultzhaus et al., 2016; Z. S. Schultzhaus & Shaw, 2015; Taheri-Talesh et al., 2008; Upadhyay & Shaw, 2008). Finally, membrane progression through Golgi is coupled to polarized growth and is easily visualized in filamentous fungi, allowing for the examination of any clathrin structures that might be found at this organelle (Bowman, Draskovic, Freitag, & Bowman, 2009; Bracker, 1967; Cole, Davies, Hyde, & Ashford, 2000; Dargent, Touze, Rami, & Montant, 1982; Harris, 2013; Hohmann-Marriott et al., 2006; R. J. Howard, 1981; J. J. Kim, Lipatova, Majumdar, & Segev, 2016; Pantazopoulou, 2016; Pantazopoulou & Peñalva, 2009; Pantazopoulou et al., 2014; Pinar et al., 2013; M Riquelme, Roberson, & Sánchez-León, 2016; Sánchez-León et al., 2015).

Here, we examined clathrin function and localization in *A. nidulans*. Clathrin decorated late Golgi (the *trans*-Golgi equivalents of filamentous fungi) and exhibited distinct dynamics during late Golgi maturation. In addition, clathrin weakly labeled endocytic sites, and disruption of clathrin had minimal effects on endocytosis. Finally,

small structures labeled with clathrin, possibly representing transitory vesicles moving from sites of clathrin budding, exhibited long distance movement throughout hyphae.

Experimental Procedures: clathrin localization and dynamics in *A. nidulans*

Cultivation of A. nidulans

All *A. nidulans* strains used in this study were cultivated on standard, solid minimal medium with the appropriate nutritional supplements (Kaminskyj, 2001) unless otherwise noted. For transformation, ~10^9 freshly harvested conidia were grown overnight in standard, liquid complete medium with appropriate supplements. Selection occurred on minimal medium with 1.2M sorbitol and the appropriate supplements added. Germlings were cultivated on sterile coverslips in liquid minimal medium with the appropriate supplements added. *alcA*::*mCherry*::*rabA* was induced by culturing spores on solid or liquid minimal medium with 1% ethanol as a carbon source. *niiA*::*claH* was cultured in solid minimal medium with either 40mM $NaNO_3$ (expressing) or 40mM NH_4Cl (repressing) as a nitrogen source. Crosses were performed on minimal medium with appropriate supplements using standard *A. nidulans* mating techniques (Kaminskyj, 2001).

Genetic analyses and genetic manipulation of A. nidulans

Sequence of the *claL*, *claH*, and *fimA* coding sequences for the creation of primers and for sequence homology analysis were obtained through the *Aspergillus* genome database (www.aspgd.org) (Cerqueira et al., 2013). Sequence homology analysis was performed by the Basic Local Alignment Search Tool for nucleotide and protein

sequences on the National Center for Biotechnology Information website (http://www.ncbi.nlm.nih.gov/).

All *A. nidulans* strains used and constructed in this study are listed in **Supplemental Table ST2.1**. The primers and plasmids used to obtain these strains are listed in **Supplemental Tables ST2.2** and **ST2.3**, respectively**.** The protocol used to perform fusion PCR-based amplification of knockout and GFP/mCherry transformation constructs, as well as the protocol for polyethylene glycol transformation of protoplasts was previously published (Oakley, Edgerton-Morgan, & Oakley, 2012). The *claL* deletion mutant was obtained in the strain TNO2A7 (Nayak et al., 2006) using *A. fumigatus riboB* as a selectable marker to replace the complete *claL* coding sequence. All fluorescent protein constructs were expressed as the sole copy of the gene under the control of their native promoters through insertion of the GFP or mCherry coding sequence just before the stop codon of each respective coding region. These strains were constructed in this manner to ensure native levels of expression for all fluorescent constructs. ClaH-GFP and ClaL-GFP in strain TNO2A7 were obtained by inserting a fragment including the *GFP* coding sequence followed by the *A. fumigatus pyrG* gene amplified from plasmid pFNO3(Yang et al., 2004) immediately after the *claH* or the *claL* coding sequence. The FimA-mCherry and ClaH-mCherry in the strain NkuNU (Z. Schultzhaus et al., 2015a) were obtained by inserting a fragment including the *mCherry* coding sequence followed by the *A. fumigatus pyroA* gene amplified from plasmid pHL85 (H.-L. Liu, De Souza, Osmani, & Osmani, 2009) immediately after the *fimA* or the *claH* coding sequence. *claH* was placed under the control of the *niiA* promoter by

insertion of a construct encoding the *A. fumigatus pyrG* gene followed by the *niiA* promoter amplified from plasmid 1863 (Hervás-Aguilar & Peñalva, 2010) immediately preceding the *claH* locus through homologous recombination. For each transformation, eight primary transformants were analyzed to confirm the presence of similar phenotypes for deletion or knockdown mutants, or for similar fluorescence localization and the wild type-like growth in GFP and mCherry fusion strains.

Preparation for imaging, and pharmaceutical and dye application

For imaging of clathrin at late Golgi and at the endocytic collar in mature hyphae, conidia were streaked in the center of a plate of minimal medium and incubated overnight at 30ºC. On the next day, a square of agar containing the leading edge of the growing colony approximately the size of a 22mm x 22mm cover slip was cut out and placed on a glass slide. Next, 15µl of liquid minimal media were applied to the cells on the block of agar, and a coverslip was gently added to minimize damage to the cells; finally, the cells were incubated at 30ºC for 20 minutes to allow for equilibration, and imaged at ~23ºC. Imaging of rapidly growing (approximately 1.3 µm/minute), leading hyphae could take place for at least three hours after the addition of the cover slip before the space between the agar and the coverslip began to become desiccated. Imaging of germlings, alternatively, began within five minutes of placing the coverslip, with germlings attached, on the microscope slide with no additional liquid minimal medium, as performed previously (Shaw, Momany, & Momany, 2002). For chilling of germlings, spores germinated on coverslips in liquid minimal medium at 30ºC overnight were

placed in 4ºC for 30 minutes before being placed on microscope slides pre-cooled to ~1ºC and maintained on ice until just before imaging.

For benomyl treatment, 15µl of liquid minimal media with a final concentration of 5µg/mL benomyl from a stock of 500 µg/mL in 100% ethanol was added to the cells before the addition of the coverslip. Cytochalasin A was added at a final concentration of 200µg/mL from a stock of 10mg/mL DMSO in a similar manner. The cells were then incubated for 20 minutes and imaged. A similar procedure was followed using an appropriate amount of 2% DMSO or 1% ethanol to strains expressing Lifeact-tagRFP or GFP-TubA to confirm the effects of these drugs on actin and microtubule, respectively. 15µL of liquid minimal medium with a 300µg/ml Brefeldin A (BFA) was added for observations on ClaH-GFP at late Golgi, and imaging took place immediately. FM4-64, finally, was applied at a final concentration of 20µM in 15µm of liquid minimal medium before applying the coverslip to the hyphae, or by injecting a similar volume of medium with a similar concentration of FM4-64 to equilibrated cells situated between the surface of the agar and the coverslip using a Hamilton syringe. Imaging beginning immediately after application.

Imaging and image analysis

All images and videos presented here are of medial optical planes captured with epifluorescence microscopy. Imaging was done on using a system described previously (Z. Schultzhaus et al., 2015a; Shaw & Upadhyay, 2005). This included an Olympus BX51 microscope (Olympus, Tokyo, Japan) with appropriate GFP and RFP/mCherry filter sets, a cooled Hamamatsu Orca ER camera (Hamamatsu Photonics, Hamamatsu

City, Japan), Slidebook imaging software (Intelligent Imaging Innovations/3i, Denver, Colorado, USA) for interfacing with the microscope and for deconvolution when appropriate, FIJI/ImageJ (Rasband, 1997; Schindelin et al., 2012) for image analysis, Adobe Photoshop (Adobe, San Jose, California, USA) for processing and formatting. When appropriate (e.g. when presenting images or videos of dim ClaH-GFP structures such as endocytic sites or moving puncta), videos and images are presented in inverted greyscale.

To analyze progression from mRFP-PH^{OSBP} fluorescence on an individual late Golgi cisterna to ClaH-GFP fluorescent signal, ten two-color time-lapse image sequences of at least one mature hypha each were captured at a rate of 15 images/min for up to eight minutes, taking into account the average late Golgi lifetime of ~ 120 seconds (Pantazopoulou, 2016; Pantazopoulou et al., 2014). Late Golgi cisternae that exhibited a clear transition from mRFP-PH^{OSBP} to ClaH-GFP in this time period and were sufficiently distant from other GFP and mCherry signal during their lifetimes such that their fluorescent signal would not be augmented by signal from surrounding structures in the cytoplasm were chosen for data collection, which went as follows: mean fluorescence levels for each channel (green and red) were measured using ImageJ for regions of interest that included the complete late Golgi. Measurements were taken over the period from when mRFP-PH^{OSBP} fluorescence reached maximum levels until the late Golgi cisterna was no longer visible. The mean fluorescence intensity for each channel at each time point was then corrected for background fluorescence levels and the relevant intensity data was normalized for maximum and minimum fluorescence

intensity of each channel during the entire image sequence to enable graphical representation of mRFP-PH^{OSBP} to ClaH-GFP transition. A quantitative assessment of colocalization was obtained as a Pearson's Correlation Coefficient through "Mask Statistics" in Slidebook 5.0 by measuring GFP and mCherry overlap in a filled in region of mature hyphae of interest expressing relevant GFP and mCherry constructs.

The lifetimes of FimA-GFP and ClaH-GFP endocytic patches were measured using time-lapse sequences with single plane images for up to two minutes at a rate of 1s/image. ClaH-GFP lifetimes were primarily calculated for patches as close to the endocytic collar as possible, while FimA-GFP patch lifetimes were calculated for patches present throughout the cell. Patch lifetimes were calculated from the time a patch was first visible until no signal was present. Colocalization between FimA-mCherry and ClaH-GFP was determined by obtaining time-lapse sequences (15 images/minute) of strains that produced both of these proteins, and determining whether GFP signal was present or absent before the appearance of a FimA-mCherry patch. Density of FimA-mCherry patches was calculated by observing the number of new patches that appeared in one minute within a 5µm site corresponding to the endocytic collar, or a site of the same size 15µm away from the apex. The patches that arrived in this time period were also measured for their maximum size and their fate (fusion, fission, lateral movement outside of the 5µm window, or disappearance) for each zone (apical and subapical).

Kymographs were created using Slidebook by reslicing images along a segmented line drawn through the length of hyphae. At least ten videos of cells expressing ClaH-

GFP and exposed to liquid minimal medium with 2% DMSO, 1% ethanol, Cytochalasin A, or benomyl were taken, at ~500ms/frame and 20 frames, and the number of videos in which trafficking of puncta could be seen was tallied and compared between the treatments. Colocalization of ClaH-GFP with mCherry-RabA and FM4-64 was assessed by taking time-lapse sequences at 4s/image and assaying whether puncta in the RFP channel overlapped with puncta in the GFP channel for 3 or more frames in a row, to minimize the possibility of false positives.

Results: clathrin localization and dynamics in *A. nidulans*

Identification of clathrin components in A. nidulans

Clathrin is a major, conserved component of the endocytic and secretory machineries in eukaryotes (Tomas Kirchhausen, 2000; Tom Kirchhausen, Owen, & Harrison, 2014; Pearse, 1976; Robinson, 1994; J. Weinberg & Drubin, 2012). The homologues of the clathrin heavy and light chain are encoded by *A. nidulans* AN4463 and AN2050, respectively (Bourett, James, & Howard, 2007; Goldman & Osmani, 2007; Sánchez-Ferrero & Peñalva, 2007). Below, we use the name given to them previously (Sánchez-Ferrero & Peñalva, 2007), and refer to the clathrin heavy chain/AN4463 as c*laH* and the clathrin light chain/AN2050 as c*laL*. The *claH* gene is composed of 5416 nucleotides, including 6 exons, and is predicted to encode a protein of 1676aa in length. *claL* is composed of 906 nucleotides, including 4 exons and is predicted to encode a protein of 240aa in length (Cerqueira et al., 2013).

Fungi (including *Neurospora crassa*, *S. cerevisiae*, *C. albicans*, *Ustilago maydis* and *A. nidulans*) appear to encode one copy each of the heavy and light chain proteins, as opposed to animals and plants, which possess at least two copies of each gene (Epp et al., 2013; D.-U. Kim et al., 2010; Read & Kalkman, 2003; Wakeham et al., 2005; J. Weinberg & Drubin, 2012). Clathrin light chain proteins, overall, appear to be much less conserved than heavy chain proteins, particularly in the N-terminal ~50% of the protein. ClaL, for example, shares ~25% similarity with both *Homo sapiens* clathrin light chain A and clathrin light chain B, but all of the similarity is within the last 200aa of the 240aa ClaL for LCb and the last 120aa for LCa. The same holds true when comparing the ClaL with the light chain homologue in *U. maydis*, which shares almost no similarity with the first 80aa of ClaL. This can be accounted for by the observation that binding of the light chain to the heavy chain occurs primarily within the center and the C-terminal regions of the light chain (F. M. Brodsky et al., 1991; C. Y. Chen et al., 2002). In the 22aa stretch on the N-terminus that is completely conserved among vertebrate light chains, a phenylalanine and a leucine (at position 29-30 in ClaL) appear to be conserved throughout fungi and animals (as an FLxRE motif in fungi, **Supplemental Figure SF2.1**).

General localization of clathrin in A. nidulans

To view general clathrin dynamics in *A. nidulans*, we constructed a strain expressing either *claH*::*GFP* or *claL*::*GFP* as the sole copy of the gene at their respective loci under control of their native promoters by adding the GFP sequence immediately before the stop codon. In previous studies, an N-terminal fusion for

labelling the clathrin light chain was used (Newpher et al., 2005). Here, C-terminal fusions were used. All tested transformants were similar to wild type in growth (**Supplemental Figure SF2.2**), and exhibited consistent fluorescent signals, and ClaH-GFP was used for the following experiments, unless otherwise noted.

ClaH-GFP localized to a variety of structures, several of which will be examined in detail below. Among these, the most pronounced were fragmented, cytosolic rings that proceeded with the growing tip (**Figure 2.1A and Movie 2.1**). These structures undulated, with portions of the rings moving in and out of focus during video acquisition. Although they were highly pleiomorphic, they shared some characteristics, including: the presence of one or several bright puncta where ClaH-GFP was presumably highly concentrated within the structure, the appearance of a semicircular or circular backbone along which the puncta were arranged, and their steady positioning relative to the apex (**Fig. 2.1A**).

Next, we noted that in growing cells ClaH-GFP appeared to localize weakly to the endocytic collar, but ClaH-GFP structures were absent from the most apical 1-3µm of the cytoplasm in growing cells (**Movie 2.1 and Fig. 2.1B**). This could be seen clearly when FM4-64 was used to stain cells expressing *claH*::*GFP* (**Fig. 2.1B**). In filamentous fungi, FM4-64 is internalized primarily through endocytosis and slowly labels many intracellular membranes including, but not always, the Spitzenkörper, a spherical body in the hyphal apex that is composed of exocytic and recycling vesicles (Fischer-Parton et al., 2000; Fuchs et al., 2006; Grove & Bracker, 1970; Hoffmann & Mendgen, 1998; R. J. Howard, 1981; Jones & Sudbery, 2010; Meritxell Riquelme, 2013; Meritxell Riquelme

et al., 2007; Meritxell Riquelme et al., 2014; Sánchez-León et al., 2015; Verdín et al., 2009). A Spitzenkörper is a hallmark of a healthy, rapidly-growing hypha in ascomycetous filamentous fungi, and in **Fig. 2.1B** this is shown with a Spitzenkörper labeled with FM4-64 imaged concurrently with ClaH-GFP which showed a zone of ClaH-GFP exclusion that was present within the hyphal tip (**Fig. 2.1B**). Alternatively, in non-growing cells, both the zone of exclusion and the Spitzenkörper were absent (**Fig. 2.1B**) (Araujo-Palomares, Castro-Longoria, & Riquelme, 2007; Löpez-Franco & Bracker, 1996). The ClaH-GFP exclusion zone seen in growing cells was similar to that seen with late Golgi equivalents in *A. nidulans* (Pantazopoulou, 2016; Pantazopoulou & Peñalva, 2009; Pantazopoulou et al., 2014; Pinar et al., 2015).

By taking videos of clathrin dynamics with frame rates of ~5/second, we observed several small puncta exhibiting directional movement near the edges of hyphae (**Fig. 2.1C**). The movement was saltatory, and the structures were small and dim so that they were frequently obscured by larger ClaH-GFP structures during image capture, but they were seen and recorded frequently enough that it became clear that a separate population of clathrin was continuously trafficking along the length of the hyphae. The highest concentration of ClaH-GFP structures were present within 15µm from the growing tip (**Movie 2.1 and Fig. 2.1D**). Finally, we checked the localization of both ClaL and ClaH proteins in a strain that contained both ClaL::mCHerry and ClaH-GFP. As expected, the proteins colocalized well (**Fig. 2.1E**), although colocalization was not entirely complete, likely due to movement occurring in the time frame (~2 seconds)

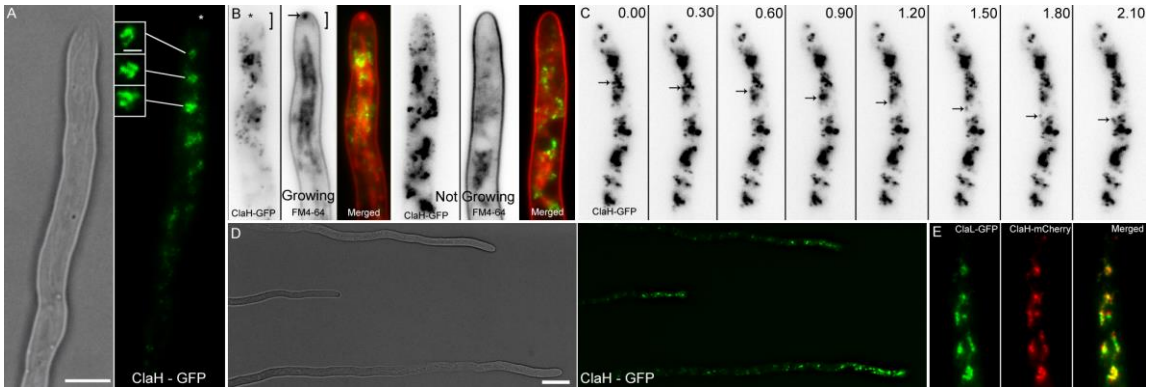

Figure 2.1 General ClaH-GFP/clathrin localization in *Aspergillus nidulans*. A. ClaH-GFP localizes to bright cytosolic structures, illustrated in the right panel and enlarged 2x in the insets (* = hyphal tip). **B.** ClaH-GFP is absent from the tip in growing cells (left three panels), while this exclusion zone is not seen in non-growing cells (right three panels, brackets = area with minimal ClaH-GFP presence, arrow = Spitzenkörper, red and green channels are presented in inverted greyscale). **C.** Small clathrin structures (arrows) were also seen moving long distances within hyphae (time in seconds, presented in inverted greyscale). **D.** ClaH-GFP is concentrated within the region ~15µm from the hyphal tip (right panel). **E.** Colocalization of ClaL-GFP and ClaH-mCherry (Pearson's Correlation Coefficient = 0.92 for this image, likely <1.0 because of time difference between GFP/mCherry channel capture). Scale bar= 5µm, except bar in insets = 2 µm.

between the capture of each channel. Next, we analyzed each class of ClaH-GFP localization more thoroughly.

Clathrin localizes to dynamic hubs on late Golgi

Clathrin is known to act as a coat protein for vesicles budding from the *trans*-Golgi network (Frances M Brodsky, 1988; Draper, Goda, Brodsky, & Pfeffer, 1990; Griffiths & Simons, 1986; Tom Kirchhausen et al., 2014; Le Borgne & Hoflack, 1997; Newpher et al., 2005; Rothman & Orci, 1990; Salamero, Sztul, & Howell, 1990). This led us to hypothesize that a major cytosolic population of clathrin, likely the fragmented rings shown in **Fig. 2.1A**, would localize to the late Golgi. To assess whether these structures were indeed ClaH-GFP associating with the late Golgi, we constructed strains that expressed both ClaH-GFP and the late Golgi marker mRFP-PH^{OSBP} (Pantazopoulou & Peñalva, 2009) simultaneously. As shown in **Fig. 2.2, A-C and Movies 2.2 and 2.3**, ClaH-GFP localized on mRFP-PH^{OSBP} – labeled late Golgi. Across several images and time lapse sequences, we did not observe any late Golgi that did not associate with some ClaH-GFP at some point during its lifetime (**Fig. 2.2A, C, and Movie 2.2**). Interestingly, instead of being arranged over the surface of the Golgi, ClaH-GFP was arrayed on the organelles in a variety of patterns. For example, circular cross-sections were seen with 1 - 8 ClaH puncta (generally depending on the size of the mRFP-PH^{OSBP}-labeled late Golgi) arranged symmetrically, resulting in the appearance of "hubs" on late Golgi: specific sites that appeared to be dedicated to clathrin-associated budding **(Fig. 2.2, A-C)**. Alternatively, late Golgi that did not form rings were sometimes completely covered with ClaH-GFP (**Fig. 2.2C**). To confirm that ClaH-GFP was associating with late Golgi,

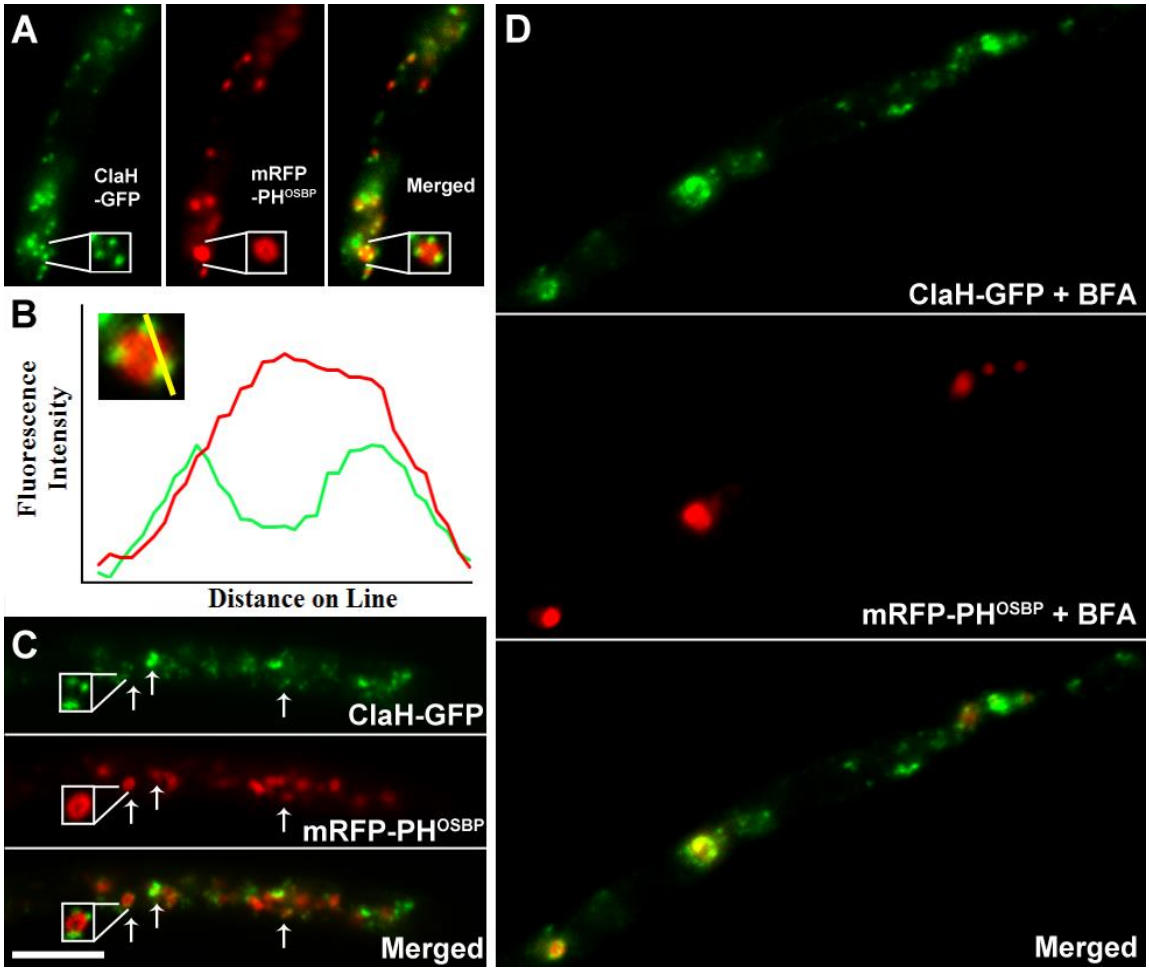

Figure 2.2 ClaH-GFP/clathrin decorates *A. nidulans* late Golgi equivalents. A. ClaH-GFP puncta arranged on circular late Golgi in a germling (and 2x magnification inset). **B.** Fluorescence intensity along a line drawn through the late Golgi shown in **A** with graph showing ClaH-GFP localization around mRFP-PH^{OSBP}-labeled late Golgi. **C.** A variety of ClaH-GFP localization patterns on mRFP-PH^{OSBP} labeled late Golgi. **Left arrows and insets** show three separate ClaH-GFP hubs on late Golgi, **center arrows** show ClaH-GFP brightly localized over an entire late Golgi, and **right arrows** show a late Golgi with one ClaH-GFP hub. **D.** A portion of ClaH-GFP segregates into "Brefeldin bodies," marked here by mRFP-PH^{OSBP}, when hyphae were exposed to Brefeldin A. Scale bar = 5µm.

we treated ClaH-GFP and mRFP-PH^{OSBP} expressing strains with Brefeldin A. In *A. nidulans*, BFA causes late Golgi to collapse into large, bulbous cytosolic bodies (Lee & Shaw, 2008; Pantazopoulou & Peñalva, 2009). When added to a strain expressing ClaH-GFP and mRFP-PH^{OSBP}, BFA caused the expected collapse of mRFP-PH^{OSBP}. ClaH-GFP, moreover, strongly associated with these structures, although there was some residual ClaH-GFP signal (**Fig. 2.2D**).

To obtain a better understanding of the interplay of clathrin and late Golgi dynamics we captured dual-channel image sequences of strains expressing ClaH-GFP and TGN-mRFP over a time limit that could capture the entire lifetime of a late Golgi while limiting phototoxicity on our system (~3-4 minutes total, imaging every 4 seconds). As shown in **Movie 2.2, 2.3** and **Fig. 2.3**, ClaH-GFP appeared to be associated with all late Golgi at some level throughout the lifetime of the organelle. However, as the late Golgi began to dissipate, ClaH-GFP fluorescence intensity increased until just after mRFP-PH^{OSBP} could no longer be seen. Between 2-4 frames (10-20 seconds) after mRFP-PH^{OSBP} could not be seen, ClaH-GFP would dissipate. This behavior is represented in **Fig. 2.3, A-C** as a recording of relative ClaH-GFP and mRFP-PH^{OSBP} fluorescence intensities over time on individual late Golgi, showing that ClaH-GFP intensity reaches its peak just after mRFP-PH^{OSBP} disappears. Specifically, ClaH-GFP signal was highest on average 8 +/- 2 seconds (s) (N=14) after mRFP-PH^{OSBP} signal dissipated.

Clathrin localization at sites of endocytosis

Clathrin plays a well-known role in endocytic site establishment and

maintenance, as well as vesicle fission (Granseth, Odermatt, Royle, & Lagnado, 2006; Kaksonen et al., 2005; W. Kukulski, Andrea Picco, Tanja Specht, John AG Briggs, and Marko Kaksonen, 2016; Newpher et al., 2005; Robinson, 1994; J. Weinberg & Drubin, 2012), although clathrin-independent endocytosis has also been documented in many organisms (Epp et al., 2013; Mayor, Parton, & Donaldson, 2014; Prosser et al., 2011). Endocytosis is generally thought to be essential for hyphal growth, and a characteristic feature of growing hyphae is a "collar" of endocytic sites concentrated behind the hyphal tip (Fischer-Parton et al., 2000; Fuchs et al., 2006; Z. Schultzhaus & Shaw, 2016; Z. Schultzhaus et al., 2015a; Shaw et al., 2011; Sudbery, 2011; Taheri-Talesh et al., 2008; Upadhyay & Shaw, 2008).

Therefore, we attempted to track ClaH-GFP at endocytic sites in this region. Interestingly, unlike in budding yeast, where clathrin and most other endocytic proteins can be seen as puncta at the plasma membrane, and in contrast to the high concentrations of other endocytic proteins in the endocytic collar, no strong ClaH-GFP cortical localization could be seen (**Fig. 2.4A**), even with significantly higher exposures than those used for viewing Golgi signal. Instead, ClaH-GFP was primarily localized to a haze with a few puncta where the endocytic collar would normally be located (bracket in **Fig. 2.4A**), behind which the bright cytosolic structures corresponding to late Golgi could be seen (**Fig. 2.4A**). Clathrin acts early in the endocytic process (Kaksonen et al., 2005; Newpher et al., 2005; J. Weinberg & Drubin, 2012). To compare localization of this early endocytic protein with that of a protein from later in the process, we obtained a strain in which ClaH-GFP and the actin cross-linking protein FimA-mCherry (Fimbrin)

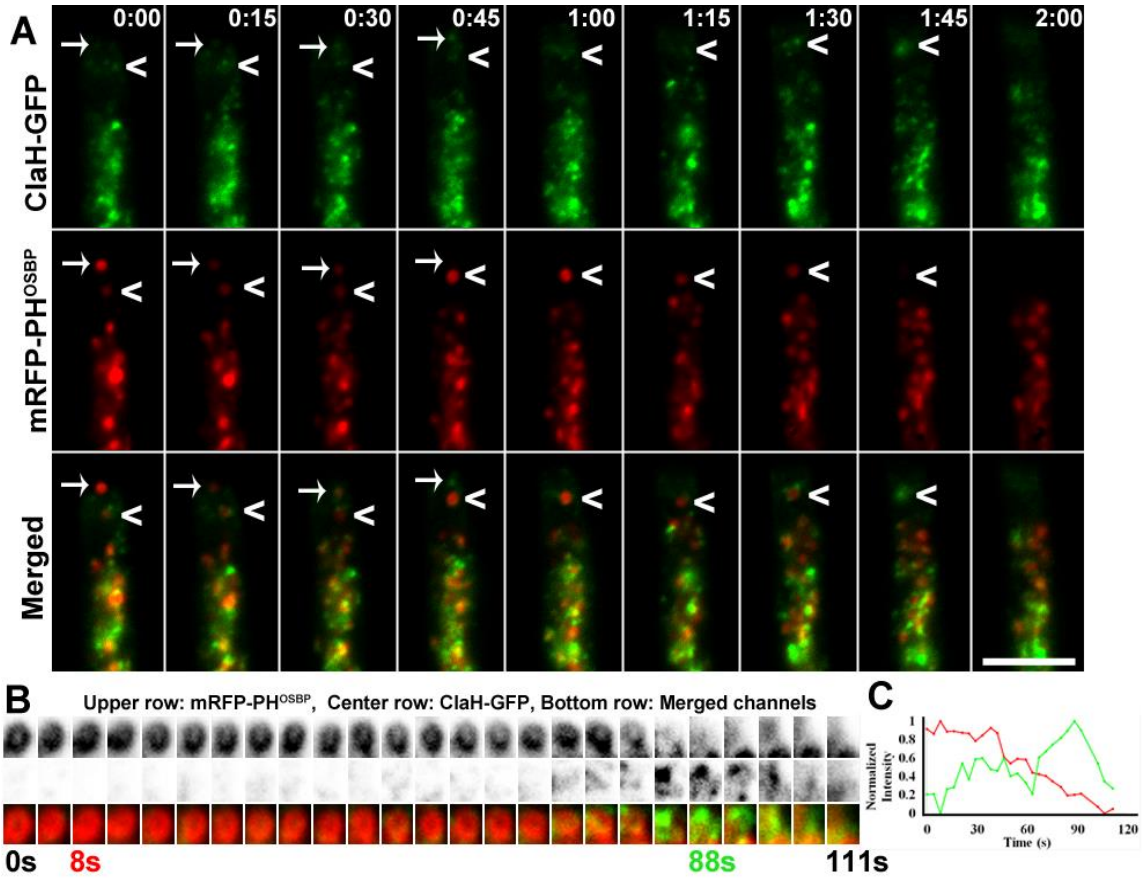

Figure 2.3 ClaH-GFP dynamics during late Golgi progression. A. As mRFP-PH^{OSBP}/ late Golgi dissipate, ClaH-GFP, which is present on late Golgi throughout its lifetime, increases in concentration (arrows and arrowheads = two separate events of ClaH-GFP progression, 15 seconds between each image). **B.** An individual late Golgi progressing through a transition from mRFP-PH^{OSBP} (top row) to ClaH-GFP (middle row). Red and green channels are presented in inverted greyscale. **C.** Normalized fluorescence intensity of ClaH-GFP (green line) and mRFP-PH^{OSBP} (red line), during a time period corresponding to the mRFP-PH^{OSBP} – ClaH-GFP transition. Scale bar = 5µm.

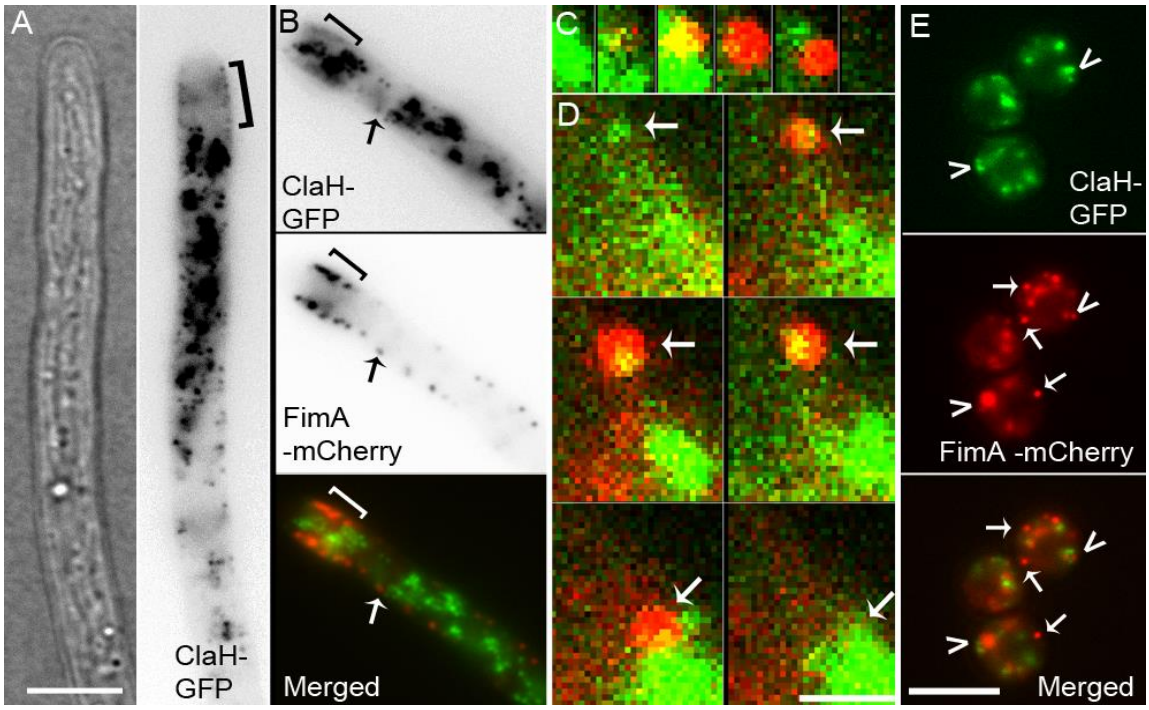

Figure 2.4 ClaH-GFP/clathrin localization at sites of endocytosis. A. ClaH-GFP patches at the endocytic collar (**bracket**). Cytosolic ClaH-GFP structures were generally present in highest density within or just behind the endocytic collar. Green channel presented in inverted greyscale. **B.** ClaH-GFP expressed together with endocytic protein FimA-mCherry (**bracket** = endocytic collar, **arrows** = subapical punctum with both ClaH-GFP and FimA-mCherry. Red and green channels presented in inverted greyscale. **C.** A ClaH-GFP patch progressing into a FimA-mCherry-labeled patch (images taken at 4s/frame interval, plasma membrane is in upper right quadrant of frames, where FimA-mCherry originates). **D.** A FimA-mCherry patch appearing and moving laterally, while associated with a ClaH-GFP patch (images taken at 4s/frame interval, arrow = ClaH-GFP patch, plasma membrane is in upper right quadrant of frames). **E.** ClaH-GFP colocalized only weakly with a portion of FimA-mCherry patches in swollen conidia (**arrows** indicate no colocalization, **arrowheads** indicate some signal overlap). Scale bars for **A, B, and E** = 5µm, scale bars in **C**, **D** = 1µm.

were co-expressed at their native loci by their native promoters. We also imaged FimA-GFP individually for analysis of actin patch dynamics. FimA-mCherry/GFP localized to bright, cortical puncta and was highly enriched in the endocytic collar, as seen previously (Upadhyay & Shaw, 2008). When imaged together, ClaH-GFP and FimA-mCherry exhibited only minor colocalization at the collar, with FimA-mCherry much brighter and more discrete while ClaH-GFP signal was a haze only slightly above background (**Fig. 2.4B**). In fact, only 57.7% (N=45/78) of FimA-mCherry in subapical regions (>15µm behind the apex) were preceded or colocalized with ClaH-GFP signal tosome extent. In the endocytic collar, ClaH-GFP did form puncta, but these did not obviously give rise to FimA-mCherry puncta, and because both of these proteins were extremely dynamic in the endocytic collar, to FimA-mCherry at a patch, as seen at endocytic sites in yeast (Kaksonen et al., 2005; Newpher et al., 2005), was rare in this region (**Movie 2.4 and see below**).

To see if brighter structures were obscuring colocalization between clathrin and fimbrin, we also analyzed several videos of patches at distal regions of hyphae, where there was much less cytosolic fluorescence. Again, only a minor relationship between ClaH-GFP and FimA-mCherry was shown. **Fig. 2.4C** shows one FimA-mCherry patch arising near a large ClaH-GFP patch with the ClaH-GFP dissipating around the same time as FimA-mCherry, and in **Fig. 2.4D** which captures a FimA-mCherry patch appearing at the same location just after a patch labeled with ClaH-GFP, then moving with ClaH-GFP before disappearing.

Finally, we reasoned that endocytic patches could be observed within conidia that are swollen just prior to germ tube emergence, which do not have regions of highly concentrated endocytosis. Therefore, we incubated spores on minimal medium for 2.5 hours (a time after dormancy is broken, but before a polarized germ tube emerges). At this time, each spore had 11.3 +/- 0.41 endocytic sites (N=30) as determined by Z-stacks of FimA-mCherry (**Movie 2.5**). Again, however, FimA-mCherry and ClaH-GFP did not show strong colocalization (**Fig. 2.4E and Movie 2.5**). Some FimA-mCherry patches were associated with ClaH-GFP, but the ClaH-GFP signal was significantly dimmer, and some ClaH-GFP patches that appeared to be associated at first with FimA-mCherry moved independently of them in subsequent frames (**Movie 2.5**). In conclusion, ClaH-GFP localizes to the endocytic collar, but it does not consistently colocalize or precede FimA-mCherry patches.

Dynamics of endocytosis in A. nidulans *hyphae*

To understand the dynamics of these "early module" and "late module" endocytic proteins (Kaksonen et al., 2005), we compared the movements and lifetimes of individual puncta labeled by either FimA-GFP or ClaH-GFP in mature hyphae and in germlings. ClaH-GFP puncta were quantified in the collar, where they were most likely of endocytic nature, and exhibited significantly longer lifetimes than distinct FimA-GFP patches, which could be easily seen throughout hyphae (24 +/- 1.5s, N= 34 for ClaH-GFP vs 10 +/- 0.4s for FimA-GFP) (**Fig. 2.5A**). Some larger plaques of both proteins were not added to these counts as they were often composed of several patches fusing and breaking apart, so the individual lifetime was difficult to ascertain. These dynamics

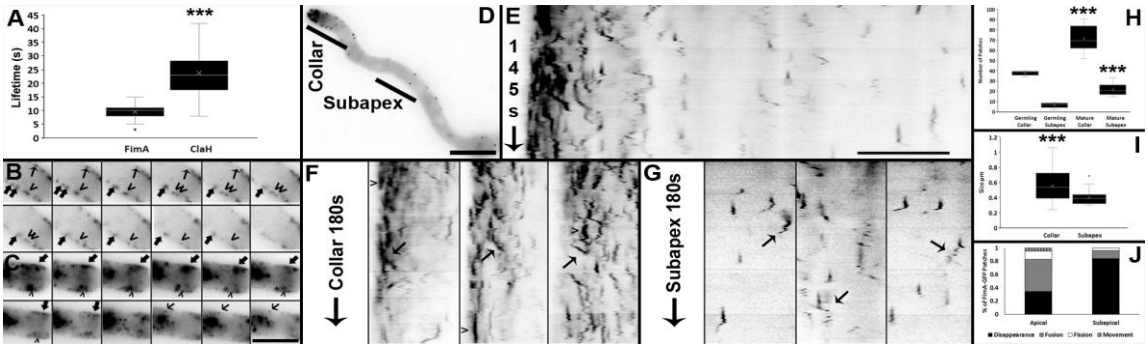

Figure 2.5 Endocytic patch dynamics in *A. nidulans.* **A.** Lifetimes of FimA-GFP and ClaH-GFP puncta at the plasma membrane. **B.** FimA-GFP patch dynamics at the endocytic collar, with images taken every one second (different arrows and arrowheads indicate individual patches of interest within image sequence). **C.** ClaH-GFP patch dynamics at the endocytic collar with images taken every one second (different arrows and arrowheads indicate individual patches of interest within image sequence). **D, E.** Kymograph of FimA-GFP patches generated from a time lapse video obtained from the germinated spore pictured in panel **D**. **F.** Kymograph of FimA-GFP patches at the endocytic collar (**arrows** indicate overlap of two or more patches, **arrowheads** indicate large, intensely fluorescent endocytic patches). **G.** Kymographs of FimA-GFP patches in a subapical region (>15µm from the apex. **Arrows** indicate lateral movement on the plasma membrane just before dissipating. **H.** Number of FimA-GFP patches arising in one minute in the endocytic collar compared to a subapical region of the plasma membrane in germlings compared to mature hyphae. **I.** Size of FimA-GFP patches in the endocytic collar compared to a subapical region of the plasma membrane. **J.** "Fate" of FimA-GFP patches in the subapical region, Black indicates disappearance of the patch, grey indicates fusion with another patch, white indicates fission into two patches, and vertical lines indicates lateral movement out of the 5µm region being analyzed. Scale bar = 5µm, bars in each graph indicate +/- standard error, asterisks indicate a Student's t-Test p-value of <0.001. All microscope images presented in inverted greyscale.

are discussed below. We did not find a correlation between FimA-GFP distance from the apex and patch lifetime (not shown), which is in agreement with data from yeast that progression through the later endocytic ("actin") module is more rapid and regular than the earlier module (Kaksonen et al., 2005). In **Fig. 2.5B** the dynamics of several FimA-GFP patches in the endocytic collar over time are presented. In the upper panels of this figure, a patch is seen as a distinct spot that slowly disappears, likely because it is internalized. On the opposite region of the membrane, distinct puncta can be seen moving laterally, and possibly fusing or splitting into several patches.

ClaH-GFP showed different dynamics at the collar (**Fig. 2.5C**). Rather than labelling specific puncta, we observed that much of the signal was present in transient plaques that extend into the cytoplasm, in addition to more static patches near the membrane. This is demonstrated in the upper panels of **Fig. 2.5C**, in which several puncta appear that are too close to be resolved, and then can be seen forming a plaque. On the opposite side of the plasma membrane, puncta are obscured by these larger "plaques," which disappear, leaving the puncta behind (see also arrowhead on lower panels). Additionally, in **Movie 2.6**, typical, elongate ClaH-GFP structures, rather than distinct patches, can be seen localizing from the edge of the cell at the endocytic collar to the center of the cytosol.

Because the subapical collar appears to be marked for endocytosis, we next tested if any other regions of the subapical plasma membrane were marked for endocytosis. As shown in **Fig. 2.5E, F, and G**, endocytic patches, in general, do not appear to assemble consistently at specific sites in subapical regions, although there are

exceptions in which large FimA-GFP structures were seen persisting for longer than most puncta and giving rise to multiple patches (**Movie 2.7**).

These observations provided more evidence that the endocytic collar is a unique, marked "hotspot" for endocytosis, and led us to characterize the difference in frequency, size, and fate of endocytic sites occurring at the collar. From videos of FimA-GFP, we obtained videos showing several rounds of endocytosis at either the endocytic collar (~1-5µm from the apex **Fig. 2.5F**) or a similarly sized region 15µm away from the apex (**Fig. 2.5G**). Kymographs from subapical regions allowed for a visualization of individual patch dynamics, which become more active and move along the membrane and into the cytosol near the ends of their lifetimes, giving the characteristic endocytic patch "J-shape" on a kymograph (**Fig. 2.5G**) (Newpher et al., 2005). We measured the number of new FimA-GFP sites in these two areas (apex and subapex) over one minute in germlings (with no septa present between the hyphal tip and the spore) and leading hyphae. As shown in **Fig. 2.5H**, significantly more patches were formed in the collar than in the subapex at all time points, as expected, and more patches were formed per minute for the collar (71.33 +/- 5.5 patches/minute collar, mature; 37.8 +/- 1.07 patches/minute collar, germlings) and the subapex (21.78 +/- 2.7 patches/minute, subapex, mature; 6.4 +/- 1.21 patches/minute, subapex, germling; N=6 mature hyphae and N=5 germlings, **Fig. 2.5H**). Patches in the collar of mature hyphae were also larger on average (0.55 +/- 0.032µm, collar, N=41 and 0.4 +/- 0.017µm, N=30, **Fig. 2.5I**), which is apparent in kymographs of the collar (**Fig. 2.5F**) as wide structures of high intensity.

Finally, because we had seen evidence of patches interacting (fusing, splitting), we documented the fate of patches in the collar compared to the subapex. **Fig. 2.5J** shows that patches arising in the collar are more likely to be seen fusing with another patch when compared to those in the subapex (48% collar patches, N=41 vs 12% subapical patches, N=25), whereas subapical patches were more likely to arise and disappear without significant lateral movement or interaction with another patch (84% subapical patches, N=25 vs 34% collar patches, N =41). Finally, patches in the collar were more likely to undergo fission into two or more particles than subapical patches (12% collar patches, N=41 vs 4% subapical patches, N=25) or to undergo lateral movement to a spot outside of the 5µm window used for analysis (5% collar patches, N=41 vs 0% subapical patches, N=25). In conclusion, the endocytic collar gives rise to more FimA-GFP patches over time. These patches are, larger and more dynamic than patches that arise in subapical regions, and are more likely to interact with each other. The degree to how these characteristics affect endocytic progression and vesicle size are areas for future study.

The role of clathrin in endocytosis

We next tested whether clathrin plays a role in endocytosis. First, we attempted to delete *claH* and *claL*. Three individual transformations were unsuccessful in isolating a homokaryotic *claH* deletion, suggesting that this gene is essential. A *claL* deletion was isolated, but its growth and development was extremely disrupted (**Fig. 2.6A**). Interestingly, however, FM4-64 uptake did not appear to be strongly inhibited in a *claL* deletion (**Fig. 2.6B**). This phenotype is not completely diagnostic of the presence of

endocytosis, as FM4-64 may enter the cell through other means, but it is important to note that internalization of FM4-64 was almost completely abolished in a *fimA* deletion (Upadhyay & Shaw, 2008). To test whether clathrin is involved in endocytosis in a more direct manner, we looked at FimA-mCherry when *claH* was downregulated using the *niiA* promoter. The *niiA* promoter is well-characterized and allows expression when nitrate is present as a nitrogen source (Cove, 1966; Hervás-Aguilar & Peñalva, 2010; Osherov, Mathew, & May, 2000; Punt et al., 1995; Z. Schultzhaus et al., 2016; Z. Schultzhaus & Shaw, 2016; Z. Schultzhaus et al., 2015a), but is strongly repressed when the nitrogen source provided is ammonium.

As expected, when a strain containing both FimA-mCherry and *niiA*::*claH* was grown with sodium nitrate as the nitrogen source, hyphae were normal and FimA-mCherry was strongly concentrated at the endocytic collar (**Fig. 2.6C**). When this strain was grown with ammonium chloride as the nitrogen source, growth was also extremely debilitated (**Supplemental Figure SF2.2**). After an overnight incubation, several germlings were seen that were highly vacuolated, with fluorescence spread throughout the cytoplasm (**Fig. 2.6D**). Other hyphae, however, exhibited FimA-mCherry patches (**Fig. 2.6D** and **Movie 2.8**). Interestingly, the lifetimes of these patches did not significantly differ on either *claH* expressing or repressing conditions (10 +/- 0.6s, N=26; and 10 +/- 0.5s, N=24, respectively). Representative kymographs of FimA-mCherry in each of these conditions are given in **Fig. 2.6E**.

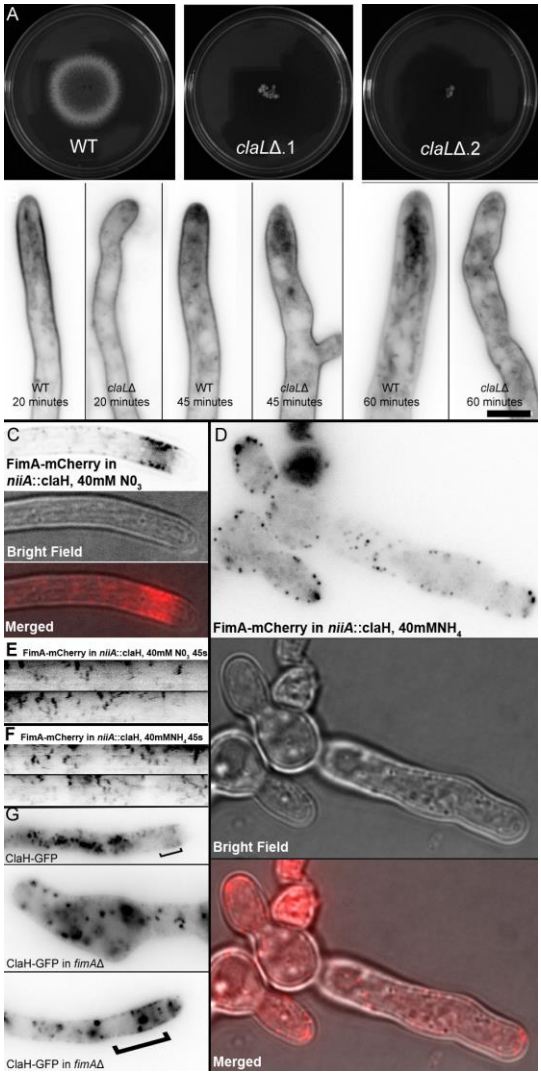

Figure 2.6 Role of *claL* and *claH* in growth, FM4-64 internalization, and FimA patch dynamics. A. General phenotype of colonies of *claL* deletion mutant. **B.** Time course of FM4-64 internalization for a *claL* deletion compared to wild type. **C.** FimA-mCherry localization in a strain with *claH* under control of the *niiA* promoter in expressing conditions. **D.** FimA-mCherry localization in a strain with *claH* expression repressed by the *niiA* promoter in repressed conditions. **E.** Kymograph demonstrating FimA-mCherry patch dynamics when *claH* is expressed and **F.** repressed. **G.** Localization of ClaH-GFP in a *fimA* deletion mutant. Scale bars = 5μm. All images except merged bright field/mCherry are presented in inverted greyscale.

We hypothesized that ClaH-GFP may accumulate on the plasma membrane and be easier to view if endocytic site progression is stalled, so we looked at ClaH-GFP in a *fimA*Δ strain produced previously (Upadhyay & Shaw, 2008). In this strain, most conidia produce aberrant germ tubes and short, swollen hyphae, although some normal but slow-growing hyphae are also produced (Upadhyay & Shaw, 2008). In the absence of *fimA* in swollen germlings, ClaH-GFP was still strongly localized to internal cytosolic structures, with little evidence of a proliferation of plasma membrane localization (**Fig. 2.6G** and **Movie 2.9**). Remarkably, however, in some normal-shaped hyphae, patches were seen accumulating in the plasma membrane, near and beyond where the endocytic collar would generally be located (**Fig. 2.6G** and **Movie 2.9**). In time lapse videos these patches were dim and relatively static (**Movie 2.9**).

Vesicle trafficking

Finally, we observed structures labeled with ClaH-GFP undergo rapid, directed movement. This movement included the presence of a population of small, dim puncta that was only a minor portion of total ClaH-GFP signal, and it was observed occurring over distances of greater than 10μm (**Fig. 2.7, A-C Movie 2.10**). This movement was bidirectional and rapid (2.04+/s 0.17 μm/sec, N=21), as judged by time lapse videos of these movements in several hyphae (**Movie 2.10, Fig. 2.7, A-C**). These puncta were also frequently observed changing directions, stopping, and appearing to associate with other larger structures. (**Movie 2.10 and Fig. 2.7, A-C**). These behaviors suggested that the puncta were trafficking along microtubules. Such movement has been extensively characterized in hyphae, and clathrin has been implicated in Golgi-endosome trafficking

in other organisms (Abenza et al., 2009; Costaguta et al., 2001; Hinners & Tooze, 2003; Lauvrak, Torgersen, & Sandvig, 2004; K. Liu, Surendhran, Nothwehr, & Graham, 2008). To test this hypothesis, we first looked at the effect that various cytoskeletal disrupting agents had on the long distance trafficking by determining how frequently we could detect the movement under various conditions. The results of this experiment, presented in **Fig. 2.7D** and **Movie 2.11**, are as follows. In control conditions (see **Experimental Procedures**), long distance movement, as defined by directional movement of a punctum over at least three frames, could be detected in 84.2% of videos captured (N=19). When cytochalasin A was added to inhibit actin trafficking, growth halted, but ClaH-GFP movement could still be seen in 81.5% of videos (N=27). However, when benomyl was added, which abolishes microtubule trafficking in filamentous fungi, ClaH-GFP trafficking was only observed in 3.8% of the captured image sequences (N=26, **Movie 2.11**).

To further confirm that clathrin was localized to structures that undergo long distance movement on microtubules, we attempted to colocalize ClaH with microtubules with a strain expressing GFP-TubA and ClaH-mCherry at their native loci. The velocity of movement of the small puncta, however, made imaging of traffic along microtubules difficult on our system, as did the observation that long distance traffic was primarily accomplished by small, dim structures, which were even more difficult to image with an mCherry fluorescent label. To assist with image capture of this rapid process, then, we took advantage of a previous observation (Abenza et al., 2009) that vesicle trafficking is slower in germlings that have been chilled and placed on a microscope slide. Using this

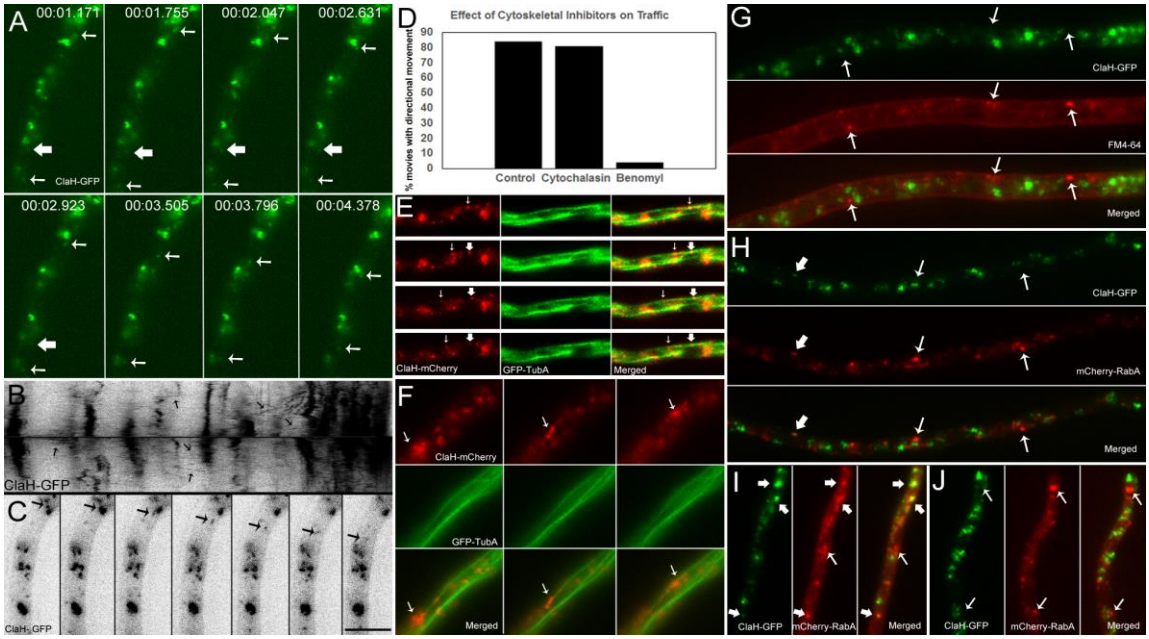

Figure 2.7 ClaH-GFP/clathrin trafficking dynamics. A. Image sequence showing ClaH-GFP puncta (**thin arrows**) moving linearly over a long distances within the cytoplasm (images taken from **Movie 2.10**) while another punctum remains static (**thick arrows**), time in mm:ss.msmsms. **B.** Kymographs of ClaH-GFP trafficking near the opposite edges of one hyphal cell. **Arrows** indicate directional movement in the kymograph. Images taken every 300ms for one minute. **C.** Representative trafficking event from the video used to create kymographs in **B** (Kymograph and time lapse images presented in inverted greyscale)**. D.** Percent of image sequences in which linear traffic of puncta over 5µm was observed when cells were exposed to cytoskeletal disrupting agents (cytochalasin A - microfilaments or benomyl - microtubules) or relevant controls. **E.** Small ClaH-mCherry punctum moving along a microtubule (**thin arrows**) after appearing to break off from a larger, static punctum (**thick arrows**). **F.** Large ClaH-mCherry structure (arrows) moving along a microtubule, as labeled by GFP-TubA (images acquired every 4s). **G.** Early FM4-64 staining in cells expressing ClaH-GFP, **arrows** indicate FM4-64-labeled structures. **H.** Image of mature hyphal cells expressing ClaH-GFP and mCherry-RabA simultaneously, **thick arrows** indicate colocalization, **thin arrows** indicate mCherry-RabA structures with no ClaH-GFP. **I, J.** Germlings of strains expressing ClaH-GFP and mCherry RabA showing both structures that colocalize (**thick arrows**), and structures that do not colocalize (**thin arrows**). Scale bars = 5µm.

technique, we observed colocalization of ClaH-mCherry puncta on microtubules labeled by GFP-TubA, and also some evidence of trafficking (**Fig. 2.7E**). Larger structures, presumably Golgi, could also be observed travelling along microtubules labeled with TubA-GFP (**Fig. 2.7F**).

Next, we tested the hypothesis that the trafficking ClaH-GFP was associated with endosomes. We approached this experiment in two ways. First, we attempted to see if the earliest FM4-64 labeled structures colocalized with ClaH-GFP. FM4-64 is primarily internalized through endocytosis and labels early endosomes within the first 10-15 minutes after addition (Abenza et al., 2009; Fischer-Parton et al., 2000; Hoffmann & Mendgen, 1998; M. A. Peñalva, 2005). FM4-64, and ClaH-GFP did not show colocalization at these earliest time points (5/45, 11.1% FM4-64-labeled structures also had ClaH-GFP signal that persisted for 3 or more images, 4s/image, **Fig. 2.7G**). To test the localization of ClaH-GFP on endosomes more directly, we colocalized ClaH-GFP with the early endosome marker mCherry-RabA, which is under the control of the *alcA* promoter (Abenza et al., 2009; Zhang, Qiu, Arst, Peñalva, & Xiang, 2014).

Under inducing conditions (MM with 1% ethanol as a carbon source), trafficking of ClaH-GFP and mCherry-RabA puncta could be easily observed (**Movie 2.12**). However, we were again unable to detect any strong colocalization (14/114, 12.2% mCherry-RabA endosomes had ClaH-GFP signal that persisted for 3 or more images, 4s/image, **Fig. 2.7H**). Finally, we attempted to slow down endosomal trafficking by imaging germlings mounted on chilled microscope slides in liquid MM, as previously described (Abenza et al., 2009). In this instance, we observed an increase in

colocalization of patches in those germlings characterized by minimal trafficking (34/88 mCherry-RabA endosomes had ClaH-GFP signal that persisted for 3 or more image, 4s/image, **Fig. 2.7I, J**). Importantly, ClaH-GFP that colocalized with mCherry-RabA was generally larger and brighter than the rapidly-moving ClaH-GFP puncta, which were frequently just large enough to be resolved by our microscope (**Movies 2.11 and 2.12**). These results suggested that clathrin associates somewhat with endosomes, but that the moving puncta were separate from endosomes.

Discussion: clathrin localization and dynamics in *A. nidulans*

Our effort to explore the importance of endocytosis in filamentous fungi led us to investigate clathrin in *A. nidulans*. To date, little is known about the localization or function of clathrin in filamentous fungi, despite the roles endomembrane trafficking and endocytosis have in fungal growth, development, and pathogenicity. In fact, few endocytic proteins have been characterized, and those that have are generally associated relatively late stages of endocytosis.

Analysis of endogenously tagged ClaH-GFP revealed several structures that exhibited predictable behaviors over time. In conidia, ClaH-GFP localization is almost indistinguishable from clathrin heavy chain in budding yeast (Newpher et al., 2005), where it is present as cortical and cytosolic puncta that are relatively static. However, ClaH-GFP is substantially different in hyphae.

Clathrin associated with late Golgi in A. nidulans

Clathrin formed large, fragmented rings that punctuated the cytosol. Because

clathrin is a coat protein for vesicles budding from late Golgi (Daboussi et al., 2012), and because the location of late Golgi is well known in *A. nidulans* (Pantazopoulou & Peñalva, 2009; Pantazopoulou et al., 2014; Pinar et al., 2015), we reasoned that these clathrin structures represented clathrin localization on late Golgi. In yeast, clathrin overlaps strongly with late Golgi markers (Daboussi et al., 2012; Newpher et al., 2005), and this is the case for most proteins previously localized to the late Golgi in filamentous fungi, which also cover the structures indiscriminately (Pantazopoulou & Peñalva, 2011; Z. Schultzhaus et al., 2015a).

Clathrin, on the other hand, is concentrated to specific regions of late Golgi in hyphae. This suggests compartmentalization in the cytosolic leaf of the late Golgi membrane. One reason for this observation may be because there is almost certainly an increase in the diversity and the amount of cargo traveling into and out of late Golgi, both from earlier on in the secretory pathway (both early and late Golgi are relatively polarized (Pantazopoulou & Peñalva, 2009)) and from endosomes (e.g. endocytic recycling from the endocytic collar). Organization at the late Golgi may be critical for properly handling this volume of traffic.

An obvious question that arises from this observation is: how do late Golgi support such organization? Many mechanisms could offer an explanation. The actin cytoskeleton, for example, is responsible for the polarization of late Golgi in *A. nidulans* (Pantazopoulou & Peñalva, 2009), and is also involved in segregating cargo at the yeast late Golgi (Curwin, von Blume, & Malhotra, 2012). However, clathrin was still

organized at discrete spots on late Golgi, rather than spread throughout the organelles, in the presence of Cytochalasin A (**Movie 11**, and personal observations).

Lipid composition is also coupled to protein dynamics at the Golgi. Ergosterol is enriched in low density secretory vesicles in yeast (Surma, Klose, Klemm, Ejsing, & Simons, 2011). To our knowledge, there is currently no effective live-cell marker developed for ergosterol, but several sterol transport proteins were recently visualized in *A. nidulans* and did not appear to exhibit similar organization at the late Golgi (Bühler, Hagiwara, & Takeshita, 2015). Phosphatidylinositol 4-Phosphate (PtdIns(4)P) levels at the late Golgi, on the other hand, can be visualized in part by mRFP-PH^{OSBP}, which also requires binding to ArfA/Arf1p for labelling (Levine & Munro, 2002). Again, both ArfA and PH^{OSBP} appeared to localize to Golgi membranes evenly, rather than to distinct domains, and when PtdIns(4)P levels are artificially decreased in yeast, clathrin and adaptor proteins still arrive at the late Golgi and exhibit the same organization and sequential progression (Daboussi et al., 2012; Lee & Shaw, 2008). Whether manipulation of PtdIns(4)P levels in hyphae would change the overall organization of clathrin on late Golgi in *A. nidulans* remains to be seen.

Phosphatidylserine (PS) is also a constituent of late Golgi membranes, and may play a role in budding clathrin-coated vesicles there (Mioka, Fujimura-Kamada, & Tanaka, 2014; Takeda, Yamagami, & Tanaka, 2014). For example, many adaptor proteins associate with basic, negatively charged molecules such as PS (Fairn & Grinstein, 2010; Fairn et al., 2011; Yeung et al., 2008). Additionally, PS has previously been shown to stimulate ArfA/Arf1p activity in the recruitment of AP-1 and subsequent

formation of clathrin-coated vesicles (Zhu, Drake, & Kornfeld, 1999). Finally, the lipid flippase Drs2p, which contributes to PS asymmetry at the late Golgi and in post-Golgi vesicles, is required for the formation of a subset of clathrin coated secretory vesicles, and interacts physically with AP-1 in the sorting of several secreted proteins in yeast (Gall et al., 2002; K. Liu et al., 2008). Although DnfB, the *A. nidulans* Drs2p homolog, shows strong localization to the late Golgi, it does not show the organization associated with clathrin, and PS only appears to be present in significant amounts on the outside of secretory vesicles (i.e. after late Golgi exit) (Z. Schultzhaus et al., 2015a). A PS-flip may contribute to the budding off of clathrin-coated vesicles, but it likely is not the only factor in the spatial organization of clathrin at this location.

Recent experiments in *A. nidulans* have demonstrated that the end of the late Golgi life cycle is typified by the exchange of PH^{OSBP} for RabE, after which the organelle rapidly dissociates into smaller vesicles bound for the Spitzenkörper (Pantazopoulou et al., 2014; Pinar et al., 2015). Our results place the time of clathrin recruitment (and likely, clathrin budding) at the late Golgi to just after PH^{OSBP} depletion on all late Golgi, and given the data on RabE dynamics at late Golgi, the disappearance of clathrin is likely concomitant with the dissolution of the late Golgi into vesicles. This suggests that there might be synchronization between the production of exocytic vesicles and the production of clathrin-coated vesicles at the late Golgi. Clathrin budding could also be initiated by an overall change in late Golgi composition, which would explain why ClaH-GFP puncta on individual late Golgi arrive and leave with synchronicity even though they do not appear to be physically connected. It will be interesting to see

whether Golgi adaptor proteins behave similarly. Additionally, it is necessary to get a more time-resolved picture of the peak-peak times of fluorescence intensity for several late Golgi and post-Golgi markers, as done in Daboussi *et al*. (2012). Our imaging system did not allow for the rapid capture needed for this analysis.

Clathrin involvement in endocytosis in A. nidulans *and other filamentous fungi*

The clathrin coat is one of the longest-lived components of the endocytic machinery that contains >60 proteins. It is recruited by ENTH-domain containing proteins such as Ent1/2p, as well as the AP-2 adaptor complex, early in the endocytic process, after which the coat assembles and is maintained on forming vesicles until they undergo fission and move into the cytosol (Carroll et al., 2012; W. Kukulski, Andrea Picco, Tanja Specht, John AG Briggs, and Marko Kaksonen, 2016; J. Weinberg & Drubin, 2012).

We previously published details of the endocytic marker FimA in *A. nidulans* (Upadhyay & Shaw, 2008) which did not include an examination of the lifetime of fimbrin endocytic patches. Fimbrin has since been shown to show similar localization in a variety of filamentous fungi (Castillo-Lluva, Alvarez-Tabarés, Weber, Steinberg, & Pérez-Martín, 2007; Diego L Delgado-Álvarez et al., 2010; Gupta et al., 2015). Here, we observed that these structures appear to dissipate more rapidly in hyphae than in budding yeast (~9 seconds vs ~12 seconds) (K. Kim et al., 2006). Importantly, clathrin could not be seen colocalizing with many FimA patches, including nearly 60% of subapical endocytic sites. In the endocytic collar, clathrin did not form puncta, but rather localized to a haze, whereas in spores and subapical compartments only rarely colocalized with

FimA endocytic patches. Additionally, the *claL* deletion mutants, though extremely impaired in growth, could internalize FM4-64 at rates similar to wild type, suggesting the presence of a clathrin-independent endocytic pathway in *A. nidulans.* In parallel experiments looking at the interdependence between ClaH and FimA, ClaH depletion, although clearly disruptive to cells, did not appear to change FimA patch dynamics. *fimA* disruption produced a different effect on ClaH: ClaH accumulation occurred at the endocytic collar. The structures that accumulated, however, were still much larger, dimmer, and more stable than FimA patches (**Fig. 6E** and **Movie 9**). In all, these suggested that clathrin, and possibly other "early" endocytic proteins, have a unique structure and dynamic from later endocytic proteins, and are possibly always present at sites of endocytosis at a low level, which makes them undetectable or having a negligible role at these sites.

Despite the supposed ubiquity of clathrin in eukaryotic endocytosis, coated vesicles have rarely been seen in micrographs produced by transmission electron microscopy in hyphae and other filamentous fungal cell types (Bourett et al., 2007; Bracker, 1967; Fischer-Parton et al., 2000; Grove & Bracker, 1970; Hoffmann & Mendgen, 1998; Hohmann-Marriott et al., 2006; R. J. Howard, 1981; That, Hoang-Van, Turian, & Hoch, 1987), and whether endocytosis in filamentous fungi is primarily clathrin-dependent or independent has remained unresolved. Mechanisms for clathrin-independent endocytosis are well known in mammals and have recently been analyzed in yeast, where they are controlled by proteins generally associated with actin cables, such as formin (Mayor et al., 2014; Prosser et al., 2011). The sole formin in *A. nidulans*,

SepA, can be seen at the endocytic collar (our unpublished observations), and is important for hyphal growth (Harris, Hamer, Sharpless, & Hamer, 1997; Sharpless & Harris, 2002). However, the clathrin-independent pathway in yeast was not dependent upon fimbrin, whereas FimA appears required for nearly all endocytosis (including FM4-64 internalization) in *A. nidulans* (Lucena-Agell, Galindo, Arst, & Peñalva, 2015; Z. Schultzhaus & Shaw, 2016; Upadhyay & Shaw, 2008).

One potential indication that clathrin-independent endocytosis or trafficking is occurring in fungi is the filasome. These are small vesicles that are associated with cell wall components, and seen surrounded by microfilaments (H. Hoch & Howard, 1980; R. J. Howard, 1981; T. Takagi, Ishijima, Ochi, & Osumi, 2003) that were later shown to be primarily composed of actin (Bourett & Howard, 1991; Bourett et al., 2007; Roberson, 1992). Actin is a major component of the endocytic machinery, and filasomes have been seen in the periphery of the cell, suggesting that they might be originating from the plasma membrane (Kübler & Riezman, 1993). Whether they are associated with clathrin, however, has not been resolved, and more recent studies have provided evidence against them being of endocytic nature, at least in terms of trafficking to the vacuole (Ayscough, 2000; Mulholland, Konopka, Singer-Kruger, Zerial, & Botstein, 1999; Mulholland et al., 1994; T. Takagi et al., 2003). Notably, fimbrin patches are not always associated with the plasma membrane, as some are observed undergoing long distance directional movement within the cytoplasm in *A. nidulans* (Upadhyay & Shaw, 2008). Most recently, filasomes were described in *Coemansia reversa*, but interestingly appeared to have a more regular coat rather than the indistinct mass of filaments surrounding the

microvesicle cores of previous images of filasomes. In short, there is little direct evidence for filasome participation in endocytosis, but the role of filasomes, and whether clathrin itself is completely dispensable for endocytosis in fungi, remain unresolved. The use of methods to disrupt clathrin specifically at the plasma membrane are likely necessary to shed light on the latter issue, although discovering such a method that lacks significant pleiotrophic effects is difficult (Dutta & Donaldson, 2012; Vercauteren et al., 2010).

Vesicle trafficking of clathrin in A. nidulans

The historic absence of clathrin-coated vesicles seen using electron microscopy, however, did not preclude us from observing a lively network of clathrin trafficking within the cytosol. These led us to hypothesize that clathrin may be acting on early endosomes, both due to the speed and bidirectionality of the trafficking puncta, and by observations suggesting movement was on microtubules. Clathrin could potentially affect early endosomes in three ways: first, by facilitating the transfer of cargo from the late Golgi to endosomes, second, by assisting in the formation of endocytic vesicles, which fuse with early endosomes, and third, because clathrin is known in mammalian cells to produce a specific class of vesicles from early endosomes. In plants, the late Golgi and early endosomes are part of a continuous network and share membrane identity (Viotti et al., 2010). However, they are spatially resolved in filamentous fungi which has allowed for their extensive characterization (Abenza et al., 2009; Steinberg, 2007b; Zhang et al., 2014).

Early endosomes in *A. nidulans* are composed of two separate populations: large, less motile structures and smaller, bidirectionally motile, rapid structures that move over long distances (Abenza et al., 2009). The highly motile ClaH-GFP puncta have the characteristics of the smallest set of early endosomes, and we did observe some colocalization between ClaH-GFP and the early endosomal marker mCherry-RabA. Movement of these proteins together on the same organelles, however, still needs to be established. It is possible that ClaH-GFP trafficking, which is able to stop abruptly and occasionally appears to occur from puncta breaking off of larger structures (and notably does not enter the hyphal apex, as opposed to early endosomes), is representative of transient association of ClaH-GFP with vesicles immediately after budding. Further investigations into clathrin in filamentous fungi should make use of biochemical characterization of isolated and purified early endosomes. Pharmaceuticals that target clathrin-mediated endocytosis but not other roles of clathrin would also be extremely useful in future studies.

CHAPTER III

Aspergillus nidulans FLIPPASE DNFA IS CARGO OF THE ENDOCYTIC COLLAR AND PLAYS COMPLEMENTARY ROLES IN GROWTH AND PHOSPHATIDYLSERINE ASYMMETRY WITH ANOTHER FLIPPASE, DNFB*

Overview: flippases DnfA and DnfB in *A. nidulans*

Endocytosis and exocytosis are strictly segregated at the ends of hyphal cells of filamentous fungi, with a collar of endocytic activity encircling the growing cell tip, which elongates through directed membrane fusion. It has been proposed that this separation supports an endocytic recycling pathway that maintains polar localization of proteins at the growing apex. In a search for proteins in the filamentous fungus *Aspergillus nidulans* that possess an NPFxD motif, which signals for endocytosis, a Type 4 P-Type ATPase was identified and named DnfA. Interestingly, NPFxD is at a different region of DnfA than the same motif in the *Saccharomyces cerevisiae* ortholog, although endocytosis is dependent on this motif for both proteins. DnfA is involved in asexual sporulation and polarized growth. Additionally, it is segregated within the Spitzenkörper from another Type 4 P-type ATPase, DnfB. Next, the phosphatidylserine marker GFP-Lact-C2 was expressed in growing hyphae, which revealed that this

---

*This chapter is reprinted with permission from "*Aspergillus nidulans* flippase DnfA is cargo of the endocytic collar and plays complementary roles in growth and phosphatidylserine asymmetry with another flippase, DnfB" by Schultzhaus, Z.S., H.Yan, and B. D. Shaw. 2015. Molecular microbiology, 97(1): 18-32.

phospholipid is enriched on the cytosolic face of secretory vesicles. This distribution is affected by deleting either *dnfA* or *dnfB*. These findings provide evidence for the spatial and temporal segregation of Type4-ATPases in filamentous fungi, and the asymmetric distribution of phosphatidylserine to the Spitzenkörper in *A. nidulans*.

Introduction: flippases DnfA and DnfB in *A. nidulans*

The vegetative cells, or hyphae, of filamentous fungi are ideal models for studying cell polarity. Hyphae colonize substrata through tip growth, a process that is supported by directed membrane fusion and cell wall synthesis (Wessels, 1986). This polarized exocytosis is also responsible for the secretion of a multitude of compounds that fungi use to facilitate disease, gather nutrients, and discern the mating competency of other individuals. Because these organisms germinate and produce ornate reproductive structures in response to external stimuli (i.e. light, nutrient limitation, the presence of certain oxylipins), filamentous fungi also present a system in which to study cellular differentiation (Herrero-Garcia, Garzia, Cordobés, Espeso, & Ugalde, 2011; Mooney & Yager, 1990; Röhrig, Kastner, & Fischer, 2013). Understanding how fungi localize their growth machinery will inform models of fungal pathogenicity, as well as research into basic cell biology.

The importance of directed secretion is highlighted in higher filamentous fungi by the presence of the Spitzenkörper, an organelle unique to higher filamentous fungi, through which membrane flows to the hyphal apex (Grove & Bracker, 1970). The nature of this organelle is somewhat elusive, as it is composed of individual secretory vesicles,

but functions as one unit (e.g. retracting or meandering in the apical region of hyphae) (Grove & Bracker, 1970; Löpez-Franco & Bracker, 1996; Verdín et al., 2009). From previous studies in *Neurospora crassa*, it is clear that at least two types of vesicles with different cargo are present in the Spitzenkörper, and that some of them may to be endocytic vesicles (Fischer-Parton et al., 2000; Sánchez-León et al., 2015; Verdín et al., 2009). This has also been seen in apical regions of *Aspergillus nidulans* (Hohmann-Marriott et al., 2006; Torralba, Raudaskoski, & Pedregosa, 1998). Different growth proteins exhibit distinct patterns of localization in hyphal tips, both in the Spitzenkörper and in the plasma membrane (Sudbery, 2011), and how proteins maintain position in a bilayer that is constantly being remodeled has not been resolved.

Recently, a zone of endocytosis, termed the sup-apical collar, that encircles the tip of growing hyphae was discovered in *Aspergillus nidulans*, *N. crassa*, and other filamentous fungi (Caballero-Lima et al., 2013; Echauri-Espinosa et al., 2012; M. Á. Peñalva, 2010; Shaw et al., 2011; Taheri-Talesh et al., 2008; Upadhyay & Shaw, 2008), similar to the localization of endocytosis almost exclusively to new buds in *Saccharomyces cerevisiae* (Mulholland et al., 1994). In hyphae, however, endocytosis and exocytosis appear to be strictly segregated at the tip (Araujo-Bazán et al., 2008; Taheri-Talesh et al., 2008). Without endocytosis, hyphal growth ceases, and it has been proposed that this endocytic region is necessary to maintain certain markers at the hyphal apex (Hervás-Aguilar & Peñalva, 2010; Shaw et al., 2011). Endocytosis could thus counteract the high amount of membrane deposition at the site of growth, which would act to diffuse proteins away from the tip (Caballero-Lima et al., 2013). Some

proteins might then also be recycled back to the plasma membrane, and thus use the endocytic collar in part to maintain polarization. How endocytosis and exocytosis segregation in hyphal tips is established and contributes to cell shape are central issues to be addressed in the emerging model of tip growth.

Intriguingly, although endocytosis is polarized in hyphae, a distinct early signal for endocytosis in fungi remains elusive, as endocytosis is still initiated when the seven earliest known endocytic proteins are deleted in *S. cerevisiae* (Brach et al., 2014). Observations in yeast and mammalian cells indicate that the phospholipid composition of membranes may play a role in promoting endocytosis, as deletion of the phosphatidylserine (PS) synthase *cho1* in budding yeast completely depolarized endocytic sites (Sun & Drubin, 2012), and in reconstituted mammalian cells clathrin-coated pits are not formed in the absence of phosphatidylinositol 4,5 bisphosphate (PIP_2) (Antonescu, Aguet, Danuser, & Schmid, 2011; Boucrot, Saffarian, Massol, Kirchhausen, & Ehrlich, 2006; Cocucci, Aguet, Boulant, & Kirchhausen, 2012). PIP_2 was shown to be polarized in *N. crassa*, but PS distribution has not been examined in filamentous fungi (Mähs et al., 2012).

To date, only one protein, the Soluble N-ethylmaleimide Attachment factor Receptor Protein (SNARE) SynA, has been shown to be cargo of the endocytic collar in filamentous fungi (Pantazopoulou & Peñalva, 2011). Here, DnfA is identified as another protein that is endocytosed and recycled in the hyphal tip of *A. nidulans*. DnfA is a flippase (Type 4 P-Type ATPase) that was discovered to have roles in growth and conidiation. These proteins regulate phospholipid asymmetry in eukaryotic cells, which

has, in turn, been suggested to play a large role in the membrane bending required for secretory vesicle formation(Takeda et al., 2014). DnfA and another P4-ATPase, DnfB, were also seen to regulate PS distribution.

Experimental Procedures: flippases DnfA and DnfB in *A. nidulans*

Identification of A. nidulans *flippase genes*

A. nidulans DnfA-D were identified first as the orthologs of Dnf1p-3p, Drs2p and Neo1p from *S. cerevisiae* in the *Aspergillus* genome database website (www.aspgd.org), and confirmed using reciprocal best-hit results on NCBI BLAST. Percentage identities among there obtained using Clustal Omega. Other genes were identified in a similar manner.

Fungal genetic techniques

All fungal strains used in this study are listed in **Supplemental Table ST3.1**. Plasmids and primers are listed in **Supplemental Table ST3.2.** Transformation and fusion PCR were carried out as described previously (Oakley et al., 2012). *dnfA* and *dnfB* deletion mutants were constructed using *A. fumigatus riboB* to restore riboflavin prototrophy, and were complemented by inserting the appropriate coding region into the mutant at the native locus using the *A. fumigatus pyrG* gene, resulting in complemented mutants prototrophic for pyrimidines and riboflavin. For each strain created, five primary transformants were analyzed to confirm the presence of similar phenotypes, and one strain was chosen for experiments. All transformants used were streaked for single spore colony isolation twice and validated by PCR using flanking primers or Southern

blot to confirm the presence of a single insertion at the correct locus. Crosses were performed using standard *Aspergillus* mating techniques (Kaminskyj, 2001). Fluorescent mutants were created using similar techniques, fusing the *gfp::pyrG* or the *mCherry::pyroA* sequence from the plasmid pFNO3 (GFP) (Yang et al., 2004) or pHL85 (mCherry, FGSC), respectively, to the 3'end of the gene, and targeting the fusion construct to the appropriate native locus. GFP-Lact-C2 was amplified from plasmid Lact-C2-GFP-p416 (Yeung et al., 2008), which was obtained from Addgene (www.addgene.org) and fused to the *niiA* promoter from plasmid p1863 (Hervás-Aguilar & Peñalva, 2010). Its Spitzenkörper localization was similar when expressed as one copy from the *pyrG* locus, or inserted in an untargeted manner into strain A773. The DnfA^{AAFxD}-GFP mutant was inserted at the *dnfA* locus, which was confirmed by diagnostic PCR of the whole construct (using primers situated outside of the construct), followed by digestion of this construct with *Sph*I to confirm that the proper mutation was present.

Media and sample preparation for imaging

All experiments were performed on standard minimal medium, with nutritional supplements added as needed. In experiments with GFP-Lact-C2, ammonium chloride was added from a 1M stock to the appropriate concentration in minimal medium, following previous techniques (Hervás-Aguilar & Peñalva, 2010). Unless otherwise specified, all images were acquired from live cells grown on agar blocks as follows: a square of agar containing the leading edge of a 16-24-hour old colony was excised from a plate and put on a glass slide; 15µl of liquid minimal media was applied to the block of

agar and a coverslip was gently added. Next, the cells were incubated at 30ºC for 30 minutes before viewing to equilibrate after encountering the glass surface. For benomyl treatment, 15µl of liquid minimal media containing either 1% ethanol or benomyl in ethanol to bring to a final concentration of 10µM. FM4-64 was also applied at a final concentration of 10µM in liquid minimal medium under the cover slip after equilibration, using a syringe.

Quantification of dnfA*Δ growth rate, conidiation, and germination*

*dnfA*Δ mutants growth rates were obtained by processing cells for imaging in a similar manner to that described above, followed by measuring the distance traveled by the extreme apex of >20 hyphae in 5 minutes using Slidebook 5.0 software. Conidiation was measured by removing the center of 10 day old colonies (N=10) grown on minimal medium at 30ºC with a 1 cm diameter cork borer, placing the agar plug into 1ml of 0.2% Tween in water, and vortexing for one minute before counting. Images of plates were taken of colonies grown from 10^3 spores for 10 days at 30ºC. Images of conidiophores were captured by collecting young conidiophores with a dissecting needle from a two day old plate and suspending them into liquid minimal media on a glass slide for analysis, or by using Riddell mounts (Riddell, 1950). Quantifying primary and secondary germ tube emergence was done by plating 10^3 spores of TNO2A7 (*dnfA*$^+$), the *dnfAΔ* mutant, or the complement on solid medium and counting the percentage of spores with one or more germ tubes each hour until ~100% of *dnfA*$^+$ and complemented spores had produced more than one germ tube. Germination experiments were repeated twice with >100 spores counted each hour.

Microscopy

Microscopy was performed as previously described on an Olympus BX51 microscope (Shaw & Upadhyay, 2005; Upadhyay & Shaw, 2008), and images were captured with a Hamamatsu Flash Orca-ER cooled CCD camera.

Image analysis and preparation

All images were captured using Slidebook 5.0 software. Fluorescence intensity data was gathered using the Line Intensity Statistics tool Slidebook 5.0 to measure the intensity of pixels across the lines drawn through relevant portions of the images. Measurements of Spitzenkörper sizes were taken from pictures of similar intensity and exposure times. All images were prepared for publication using Adobe Photoshop CS5.1.

Results: flippases DnfA and DnfB in *A. nidulans*

The type 4 P-Type ATPase DnfA is polarized in A. nidulans *hyphae and germinating conidia*

To look for proteins that could be cargo of the endocytic collar, the *A. nidulans* complete protein sequence (Cerqueira et al., 2013) was queried for proteins that harbor an NPFxD motif, using the EMBOSS Fuzzpro package (Rice, Longden, & Bleasby, 2000). This motif has been shown to mediate binding to the endocytic protein Sla1p in budding yeast (J. P. Howard, Hutton, Olson, & Payne, 2002; Tan, Howard, & Payne, 1996), and this site is conserved in the Sla1p homologs of filamentous fungi (Mahadev et al., 2007). In total, there are 37 *A. nidulans* proteins that contain this motif. All are

listed in **Supplemental Table ST3.3,** along with four others that encode a DPFxD motif that likely performs a similar function (Olmo & Grote, 2010). Notable members of this list are four endocytic proteins: MyoA, an essential Type I Myosin (McGoldrick, Gruver, & May, 1995; Yamashita & May, 1998); AN2492, the homolog of budding yeast Pal1p, a protein that is present early at endocytic sites (Carroll et al., 2012; Ge, Chew, Wachtler, Naqvi, & Balasubramanian, 2005); Coronin, a major component of the endocytic machinery in fungi, including *N. crassa* (Echauri-Espinosa et al., 2012); and AN0697, the Syp1p homolog, which acts with the arp2/3 complex to organize actin patches during endocytosis in yeast (Boettner et al., 2009; Stimpson, Toret, Cheng, Pauly, & Drubin, 2009). The presence of this motif in proteins of the endocytic machinery will be examined elsewhere. To find candidates for endocytic recycling at hyphal tips, the 14 proteins with predicted transmembrane domains were examined more closely. One particularly interesting member was AN8672, which encodes a Type 4 P-type ATPase (hereafter P4-ATPase). These proteins are flippases that facilitate the movement of phospholipids such as phosphatidylcholine (PC), phosphatidylethanolamine (PE), and PS between membrane leaflets in eukaryotic cells (Backer & Dawidowicz, 1987; Baldridge & Graham, 2012; Mioka et al., 2014; Pomorski et al., 2003).

A. nidulans and all other filamentous fungi examined encode four P4-ATPases that correspond to the *S. cerevisiae* Drs2-Neo1-Family genes dnf1/2 (AN8672/*dnfA*), drs2 (AN6112/*dnfB*), dnf3 (AN2011/*dnfC*), and neo1 (AN6614/*dnfD*). Each of these proteins contains between seven and ten transmembrane domains and are relatively large

(>1000 amino acids). All P4-ATPases except for Neo1p homologs also associate with a small (~300aa) β-subunit of the Cdc50p family (Bryde et al., 2010; Poulsen et al., 2008; Saito et al., 2004). Interestingly, while *S. cerevisiae* possesses three Cdc50p paralogs (Cdc50p, Lem3p, and Crf3p) that associate exclusively with individual α-subunits (Drs2p, Dnf1/2p, and Dnf3p, respectively) (Mioka et al., 2014), most filamentous fungi appear to possess single Cdc50p homologs. Comparisons of the *A. nidulans* and *S. cerevisiae* P4-ATPase proteins are provided in **Supplemental Table ST3.4**, and the structure of each P4-ATPase of *A. nidulans* is provided in **Supplemental Figure SF3.1**.

If DnfA is cargo of the endocytic collar, it should be present at sites of growth. To determine this, the eGFP coding sequence was inserted in frame at the 3' end of the native *dnfA* locus. The resulting transformants were not different from the parent strain (TNO2A7) in growth or development. One strain was selected for further studies. In growing hyphae, DnfA-GFP was polarized to the apical plasma membrane (**Figure 3.1A**). It was also observed in the Spitzenkörper where it localized to an area greater than that stained with FM4-64 (1.2µm and 0.8µm, respectively, N=24 hyphal tips; **Fig. 3.1B**). Additionally, a small area of exclusion that was detectable in medial focal planes as a decrease in fluorescence intensity could be seen at the center of the DnfA-GFP-labelled Spitzenkörper (**Figs. 3.1C, D**). Resolving this central void was often difficult due to its size and the dynamic movement of the *A. nidulans* Spitzenkörper. Finally, in germinating conidia, DnfA-GFP localized to the germination site and to the tip of new germ tubes (**Fig. 3.1E**).

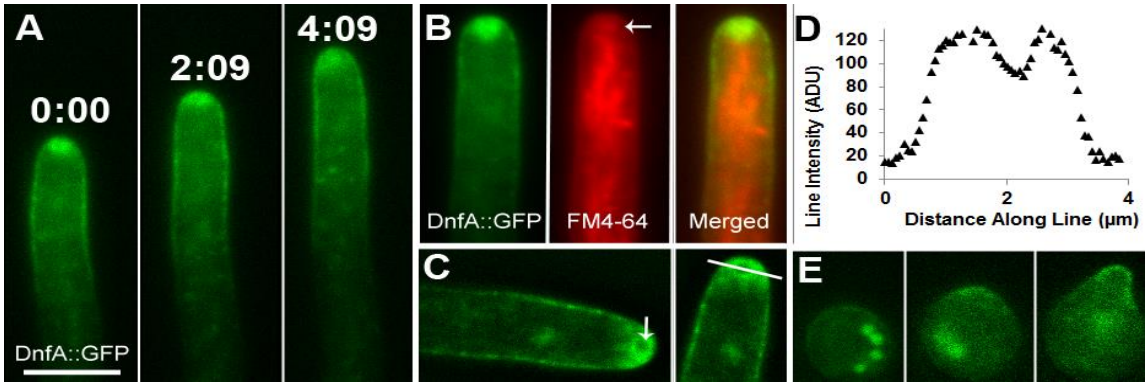

Figure 3.1 Localization of the P4-ATPase DnfA in *A. nidulans*. DnfA-GFP localized to the apical plasma membrane as well as the Spitzenkörper in growing hyphal tips (**A**). **B**, DnfA-GFP (**left panel**) occupies a somewhat larger region than FM4-64 (**arrow, center panel**) in the Spitzenkörper (**right panel**). **C** an example of an exclusion zone near the center of the Spitzenkörper (**arrow, line**). This exclusion accompanied a moderate but clear drop in fluorescence intensity in this region (**D, fluorescence along line in C**). DnfA-GFP localized to the site of germination, during the earliest stages of germ tube emergence (**E**). Scale bar = 5µm.

An NPFxD motif mediates endocytosis of DnfA at hyphal tips

DnfA-GFP localizes to the plasma membrane within 11.8 ± 2.5 μm (N=19) from the cell apex (**Figure 3.2A**). This suggested that it could be cargo of the endocytic collar. Single or combinatorial mutations of the Arginine (N), Proline (P), or Phenylalanine (F) residues to Alanine (A) in this motif halt endocytic uptake (Tan et al., 1996), so the DnfA NPFxD was mutated to AAFxD to make DnfA^{AAFxD}::GFP, and expressed it at the native locus the only copy of *dnfA.* Although some hyphae had a larger diameter (data not shown), the DnfA^{AAFxD}-GFP strain did not have an obvious phenotype at the colony level. Strikingly, however, DnfA^{AAFxD}-GFP lost polarization and localized throughout the plasma membrane. It was also not uniform in the plasma membrane, something which could be faintly discerned with DnfA-GFP (**Fig. 3.1**) but was accentuated with DnfA^{AAFxD}-GFP. Rather, it was present in foci of heterogeneous size, as well as at septa (**Fig. 3.2B**). DnfA^{AAFxD}-GFP was also no longer prominent in the Spitzenkörper, indicating that its endocytosis is important for accumulation in that organelle. Interestingly, *S. cerevisiae* Dnf1p, the DnfA homolog, contains an N-terminal NPFxD motif, and it mediates Dnf1p endocytosis and recycling (K. Liu, Hua, Nepute, & Graham, 2007). P4-ATPases are highly conserved throughout eukaryotes, but through a comparison of homologs in the filamentous Ascomycetes, this is not present at this location on DnfA homologs outside of the aspergilli (data not shown). Additionally, it is conserved as DPFxD, rather than NPFxD, in all of the other sequenced *Aspergillus* spp.

DnfA-GFP was also observed in a deletion of the *A. nidulans vps54* homolog, AN7993, which is part of the Golgi Associated Retrograde Protein (GARP) complex,

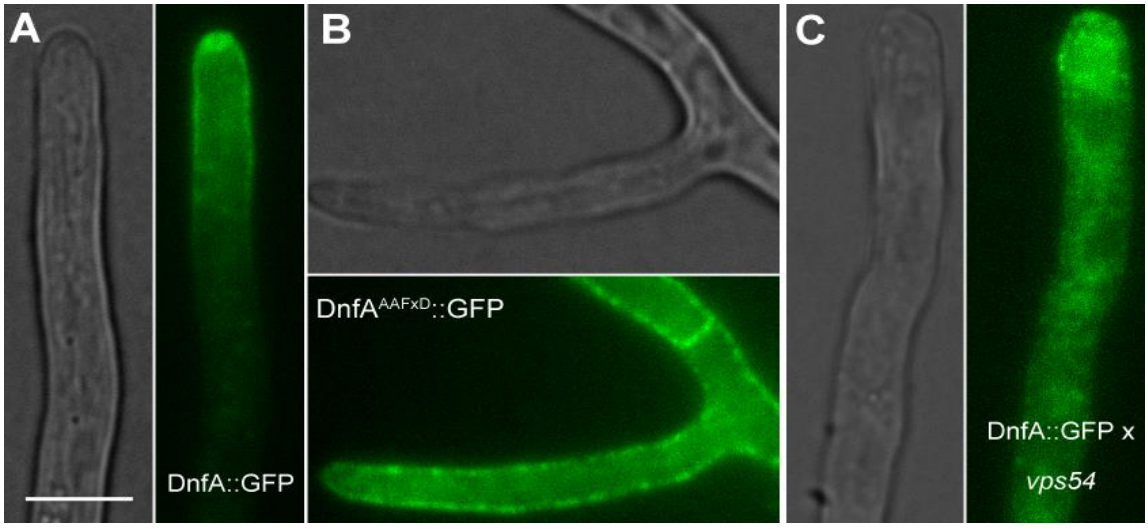

Figure 3.2 DnfA recycled in hyphal tips requires an NPFxD motif. A. DnfA-GFP is polarized in growing cells, and localizes to a portion of the plasma membrane. **B.** DnfA^{AAFxD}-GFP loses this localization and is instead present throughout the plasma membrane, including at septa, but not in the Spitzenkörper. **C.** In a *vps54* deletion, DnfA-GFP also loses polarization, instead showing diffuse cytoplasmic localization. Scale bar = 5µm.

also known as the Vps Fifty-Three (VFT) complex. This complex is responsible for tethering traffic from endosomes to the TGN/ late Golgi, and therefore the recycling of proteins from early endosomes back to the plasma membrane (Siniossoglou & Pelham, 2001). In the *vps54* mutant, DnfA-GFP was no longer polarized, and instead was mislocalized to the cytosol (**Fig. 3.2C**). These results show that DnfA uses endocytic recycling to maintain its polarization in the hyphal tip.

dnfA *has roles in spore pigmentation and hyphal growth*

P4-ATPases have been implicated in secretion, endocytic recycling, and polarized growth in budding yeast (Alder-Baerens, Lisman, Luong, Pomorski, & Holthuis, 2006; Pomorski et al., 2003), and the presence of DnfA-GFP in the Spitzenkörper suggested that some of these roles may be shared in *A. nidulans*. To explore this possibility, *dnfA* was deleted. *dnfA* deletions exhibited slow growth (**Supplemental Figure SF2A**) and diminished conidiation (**Supplemental Figure SF2B**). Although germination proceeded normally (data not shown), a large portion of germlings were delayed or blocked in the formation of a second germ tube. This phenotype resulted in many *dnfAΔ* mutant spores germlings with a single, wide germ tube (**Figures 3.3B, C**) when compared with the thin proto-hypha seen in TNO2A7 at a similar time point (**Fig. 3.3A**). Only 37% produced a second germ tube by18 hours when nearly all of the germlings of the parent strain and the complemented strain had at least two germ tubes (94%, N=200). Mature *dnfAΔ* hyphae were unable to maintain the stable growth axis that is seen in wild type (**Fig. 3.3D**), resulting in cells that were irregular in shape (**Figs. 3.3E**). In contrast to reports from yeast that suggested a role of Dnf1p in

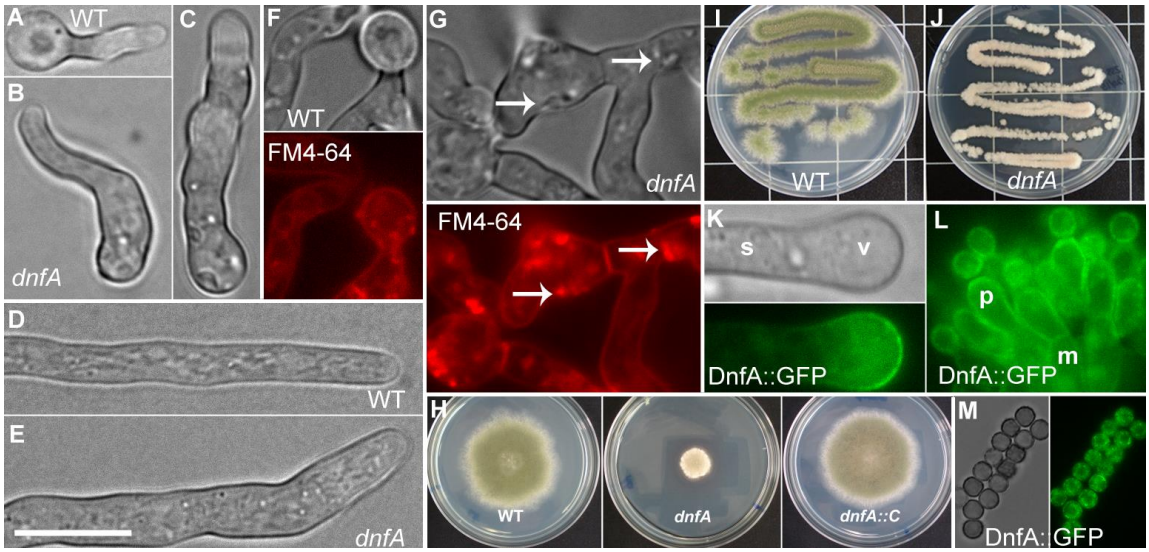

Figure 3.3 Phenotypes of *dnfA*Δ. **A.** Germ tube of parent strain. **B-C** Germ tubes of *dnfA* deletions, these were frequently wider than hyphae at their base, and irregularly shaped. *dnfA*$^{+}$ parent strain hyphae (**D**) are straight and grow along one axis, whereas hyphae of *dnfAΔ* (**E**) meander and exhibit irregular structures in their cytoplasm. This is seen clearly with FM4-64 labelling of the parent *dnfA*$^{+}$ (**F**) and *dnfAΔ* (**G**) hyphae, as *dnfAΔ* accumulates membranous structures along the membrane of subapical compartments (**G, arrows**). **H, I**. *dnfAΔ* colonies after growth on minimal media for 7 days (**H**) to accentuate the growth defect and 3 days (**I**) to show the conidial pigmentation phenotype. DnfA-GFP accumulates in the plasma membrane of the entire conidiophore (**K, L**), as well as in newly formed conidia (**M**). Scale bars = 5µm.

endocytosis (Pomorski et al., 2003), FM4-64 internalization was not perturbed in these mutants, although labelling with this dye revealed the accumulation of abnormal membranous plaques in subapical regions of *dnfAΔ* mutants, which could also be seen on bright field (**Figs. 3.3G**), but were generally absent from TNO2A7 (**Fig. 3.3F**).

Another phenotype exhibited by these mutants was the dramatic change in spore pigmentation. Conidia of these strains were nearly colorless (**Figs. 3.3, H-J)**. Supporting the claim that DnfA functions during conidiogenesis, DnfA-GFP was located in cytosolic puncta and the plasma membrane throughout conidiophores during several stages of conidiation (**Figs. 3.3K, L**), as well as in young conidia (**Fig. 3.3M**). Conidiophore structure, however, appeared normal in *dnfAΔ* mutants. Two differences, however, were exhibited in conidiophores at the cellular level. First, echoing the decrease in conidiation, chains of conidia were rarely seen after three days, and only three to four conidia were observed on conidiophores after seven days (**Supplemental Figure SF2C**), compared with the long, melanized chains seen in the parent strain, and wild type *A. nidulans* (**Supplemental Figure SF2D**). Conversely, many conidiophores exhibited branching of the aerial stalk (**Supplemental Figure SF2E, F**). This phenotype was never observed in the parent strain or the complemented strain conidiophores. This data demonstrates that *dnfA* has multiple functions in *A. nidulans*, including germination, hyphal growth, asexual reproduction, and spore pigmentation.

DnfA and DnfB localize to distinct parts of the Spitzenkörper and have non-overlapping functions in A. nidulans

Two budding yeast P4-ATPases, Dnf1p and Drs2p, have functional overlap but minimal spatial overlap (Alder-Baerens et al., 2006; Hua, Fatheddin, & Graham, 2002). Hyphae have well-defined endomembrane systems, so observing both proteins simultaneously in these cells may provide some clarity on their possibly disparate regulation. To test this idea, *A. nidulans* AN6112 (*dnfB*) was identified as the drs2 homolog, and *DnfB-mCherry* or *DnfB-GFP* was inserted at the *dnfB* locus under the control of the *dnfB* promoter. Both showed similar subcellular distributions, and no difference was seen in growth and development between each strain and the parent strain. In hyphae, DnfB-GFP localized to the apical plasma membrane, some cytosolic structures, and a compact locus just behind the cell tip (**Figure 3.4A**). This locus was smaller than DnfA-GFP (0.8µm and 1.3µm, respectively, N=21) and overlapped well with FM4-64 (0.7 µm each, N=22, **Fig. 3.4A**). In addition, it was hypothesized that DnfA and DnfB would act at late Golgi, given their role in secretion in other organisms, and the similarity between this organelle and the shape of cytosolic structures labeled by both proteins. Therefore, the late Golgi marker mRFP::PH^{OSBP} (Pantazopoulou & Peñalva, 2009) was used to label this organelle in DnfA-GFP and DnfB-GFP strains (**Figs. 3.4B, C**). Both proteins co-localized well with mRFP-PH^{OSBP}, although for DnfA this association was more prominent near the apex, whereas DnfB could be seen on cytosolic bodies corresponding to late Golgi over a large area of hyphae (**Figs. 3.4B, C**).

Figure 3.4 DnfB and other Spitzenkörper localized proteins in *A. nidulans.* A. DnfB-GFP localizes (**left panel**) to the center of the Spitzenkörper, the plasma membrane, and cytosolic structures. In the Spitzenkörper, it is labeled with FM4-64 (**center and right panel**). **B.** DnfA-GFP and DnfB-GFP (**left panels**) (**C**) colocalize with mRFP-PH^{OSBP} (**center panels**) at late Golgi (**arrows, right panels**). DnfA-GFP (**left panels**) and DnfB-mCherry (**center panels**) overlapped in hyphal tips (**right panels**) (**D**) and in new branches (**E**). **F.** GsaA-GFP (**upper panel**) and DnfB-mCherry (**center panel**) in growing hyphae (**bottom panel**). **G.** GFP-SynA (**upper panel**) and DnfB-mCherry (**center panel**) in growing hyphae (**bottom panel, merged**). **H.** Model of Spitzenkörper organization. Microtubules (**black lines**) extend the length of hyphae, along which secretory vesicles (**blue and gold circles**) travel to the apex, where they enter the Spitzenkörper. There, they are organized with DnfB in the center (**orange cloud**) and GsaA and DnfA around the periphery (**blue cloud**). SynA, as shown previously, labels the entire region (not shown). **Arrows** represent membrane flow out of (exocytosis) and into (endocytosis) the cell. **I-J.** Spitzenkörper showing the DnfA-GFP exclusion zone (**top panel**), which is covered completely by DnfB-mCherry (**center panel**), as demonstrated by fluorescence intensity of each along the line drawn through the Spitzenkörper (**bottom panel, I**). Orange triangles are DnfB-mCherry values, blue triangles are those of DnfA-GFP. Scale bars = 2.5µm for **C** alone, 2.5 µm for all others.

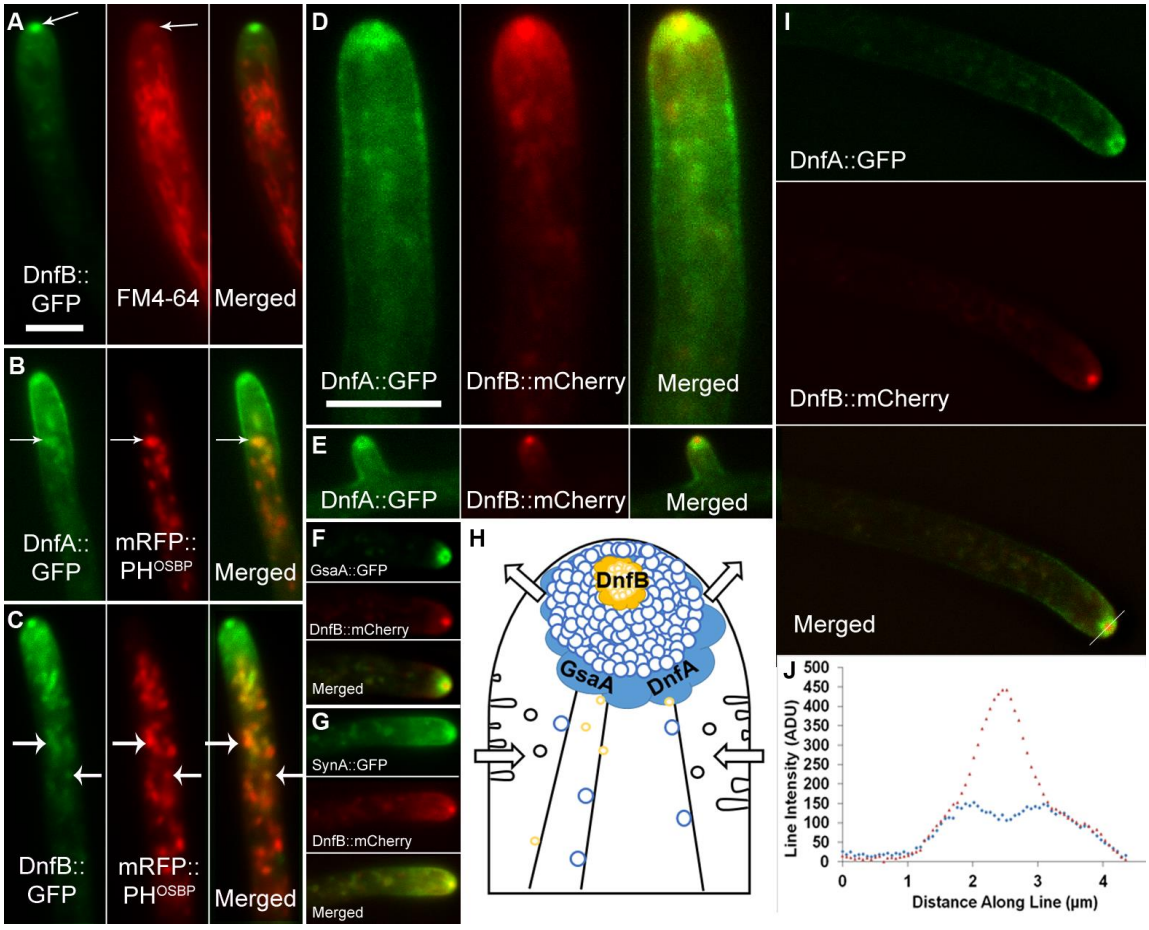
A
DnfB::
GFP
FM4-64
Merged
B
DnfA::
GFP
mRFP::
PHOSBP
Merged
C
DnfB::
GFP
mRFP::
PHOSBP
Merged
D
DnfA::GFP
DnfB::mCherry
Merged
E
DnfA::GFP
DnfB::mCherry
Merged
F
GsaA::GFP
DnfB::mCherry
Merged
G
SynA::GFP
DnfB::mCherry
Merged
H
DnfB
GsaA
DnfA
I
DnfA::GFP
DnfB::mCherry
Merged
J
Line Intensity (ADU)
500
450
400
350
300
250
200
150
100
50
0
0
1
2
3
4
Distance Along Line (μm)

These data are in agreement with observations in other organisms placing P4-ATPases at the *trans*-Golgi (Bryde et al., 2010; Hua et al., 2002; Poulsen et al., 2008).

The difference in localization between DnfA and DnfB suggested that they may be segregated to different parts of the Spitzenkörper. To test this, *DnfB-mCherry* was expressed at the native locus in the DnfA-GFP strain, and imaged in growing hyphal tips. Strikingly DnfB-mCherry localized to the center of the DnfA-GFP apical structure (**Figs. 3.4D, E**).

Although it is established that hyphal tips are complex cellular compartments, with several proteins exhibiting widely differential localizations that correspond to their function (Sudbery, 2011), only the organization of the *N. crassa* Spitzenkörper has been studied in any detail using fluorescent proteins in live cells. To understand if such organization was conserved in *A. nidulans* as well, the localization of two proteins was compared: GsaA-GFP (AN8846), part of the 1, 3 β-glucan synthase machinery, and the synaptobrevin homolog (v-SNARE) GFP-SynA, together with DnfB-mCherry. GsaA-GFP (**Fig. 3.4F**) forms a ring that completely encircles DnfB-mCherry (size = 1.1µm and 0.8µm, respectively, N=25). GsaA-GFP, additionally, does not label the subapical plasma membrane. In contrast, SynA-GFP (**Fig. 3.4G**) always completely overlapped DnfB-mCherry, although it was spread throughout a larger area of the Spitzenkörper (1.0µm vs 0.7µm, respectively, N=25). For clarity, these localization patterns are represented in a model (**Fig. 3.4H**). Finally, the regions of the Spitzenkörper where DnfB-mCherry and DnfA-GFP were most concentrated were exclusive of each other

(**Figs. 3.4I, J**). In many cases, however, exclusion was imperfect, due to the small size and dynamic nature of the *A. nidulans* Spitzenkörper.

DnfA and DnfB have different dynamics during growth and reproduction

Two types of vesicles are found in the Spitzenkörper. In electron micrographs that capture this organelle intact, large macrovesicles (size in *A. nidulans* ~45nm) generally populate the outer layer, while the inner "core" is occupied by smaller microvesicles (~20nm) (Grove & Bracker, 1970; Hohmann-Marriott et al., 2006; Löpez-Franco & Bracker, 1996; Torralba et al., 1998; Verdín et al., 2009). The presence of different vesicles has been proposed to function as a method for spatial or developmental regulation of secretion (Verdín et al., 2009). Indeed, the Spitzenkörper is absent from germ tubes (Araujo-Palomares et al., 2007). Both DnfA-GFP and DnfB-GFP (or mCherry) exhibited movement reminiscent of vesicles throughout the length of hyphae (**Movie 3.1**), and their orientation suggested that these proteins may be present on these different types of vesicles, so next, DnfA-GFP and DnfB-mCherry were localized at different stages of development.

In dormant conidia, both proteins localized to small puncta that only moderately overlapped, with DnfB-mCherry exclusively in the cytosol and DnfA-GFP also in the plasma membrane and as cortical patches (**Figure 3.5A**). When germination commenced and spores swelled, DnfB-mCherry was barely detectable, and DnfA-GFP mobilized to the plasma membrane (**Fig. 3.5B**). In germ tubes, DnfA-GFP maintained this apical plasma membrane localization until the Spitzenkörper developed. DnfB-mCherry was more erratic. In early germ tubes DnfB-mCherry was absent, but over time it could be

Figure 3.5 DnfA-GFP and DnfB-mCherry localization at different stages of development. A-C. DnfA (**center left panels**) and DnfB (**center right panels, right panels**) exhibited partial co-localization in early developmental stages such as newly formed conidia (**A**), swollen conidia (**B**), and young germ tubes (**C**). **Arrows** in **B** shows DnfA-GFP on the plasma membrane of swollen conidia. **Arrows in C** indicate cytosolic structures where both proteins colocalize. **D.** Fully developed conidiophore in bright field (**top left panel**), with DnfA-GFP (**top right panel**), DnfB-mCherry (**bottom left panel**), and both channels merged (**bottom right panel**). **E-F.** DnfA-GFP (**second panel from top**) and DnfB-mCherry (**third panel from top**) on the plasma membrane (DnfA-GFP) and colocalizing on diffuse structures with DnfB-mCherry in the cytosol of stalks and vesicles (**E, F**) and metullae (**arrows in E**). Bottom panels of **E** and **F** are merged images of GFP and mCherry. Scale bars = 5 μm for **A-C**, 5 μm for **D-F**.

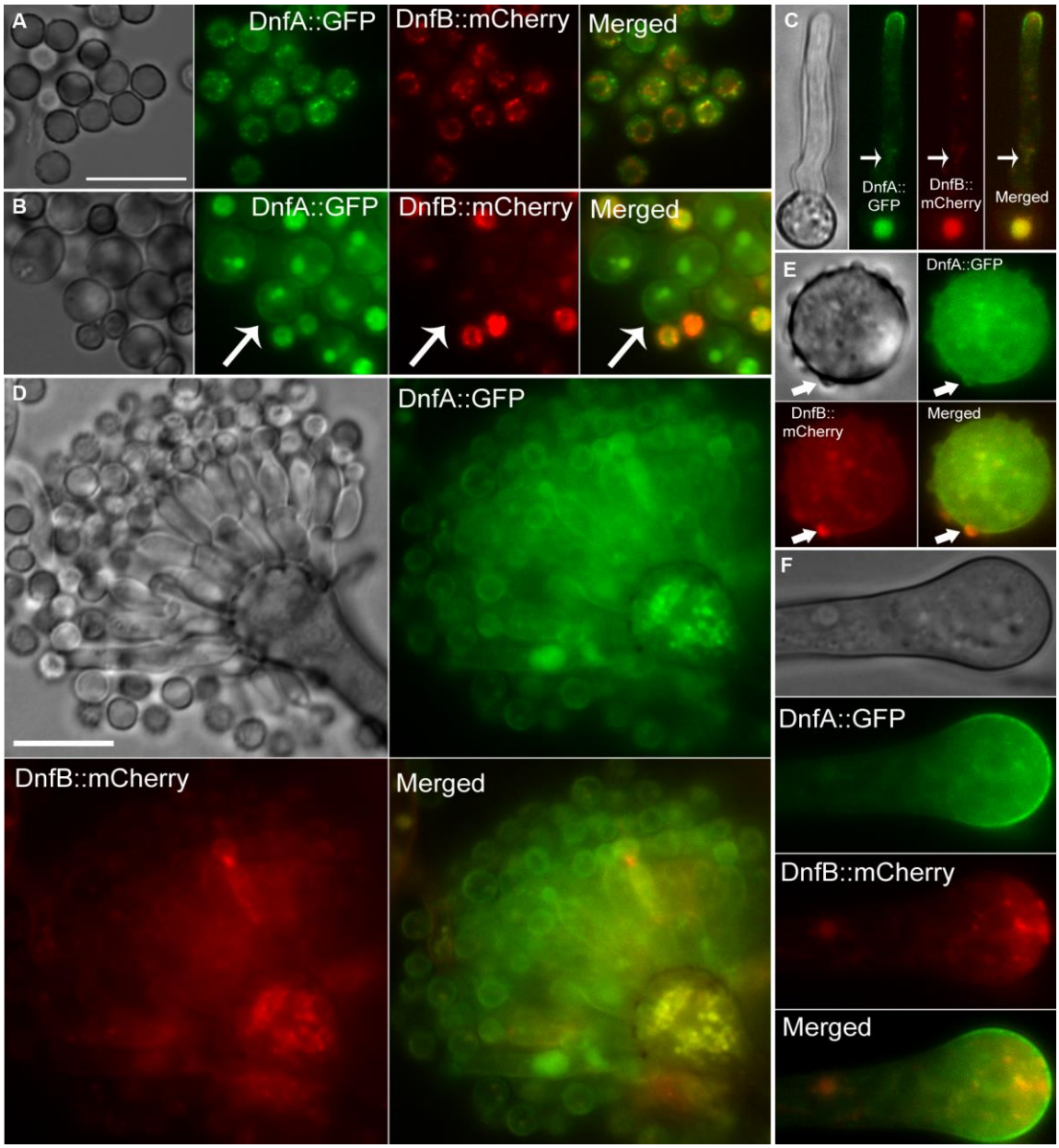
A
DnfA::GFP
DnfB::mCherry
Merged
B
DnfA::GFP
DnfB::mCherry
Merged
C
DnfA:: GFP
DnfB:: mCherry
Merged
D
DnfA::GFP
DnfB::mCherry
Merged
E
DnfA::GFP
DnfB:: mCherry
Merged
F
DnfA::GFP
DnfB::mCherry
Merged

seen in intracellular structures as well as discrete foci on the plasma membrane, in contrast to the more continuous distribution of DnfA-GFP at germling tips (**Fig. 3.5C**). In general, DnfA was more diffuse at all stages, although both proteins co-localized frequently to cytosolic structures (**Fig. 3.5C**). The localization of DnfA and DnfB was also examined during conidiation. In conidiophores, while DnfA-GFP was seen in the periphery of nearly all cell types (**Fig. 3.5D**), DnfB-mCherry was only seen at the earliest stages of conidiophore development, during aerial hyphae formation and the **3.5E, F**). DnfB-mCherry was primarily absent from the plasma membrane, unlike DnfA-GFP, but rather localized to cytoplasmic structures, some of which co-localized with DnfA-GFP. This suggested that DnfB did not have a role in regulating conidiation. Indeed, the *dnfB*Δ mutant appeared to produce relatively normal levels of conidia with normal pigmentation, although deleting *dnfB* appeared to promote sexual reproduction, as indicated by the presence of cleistothecia in *dnfB*Δ colonies after 5 days (**Supplemental Figure SF3.3A-D**).

DnfA and DnfB behave similarly in the absence of microtubule trafficking

Vesicles are thought to reach the Spitzenkörper on microtubules, and indeed the post Golgi/ secretory vesicles associated with RabE in *A. nidulans* have been shown to move along microtubules to the Spitzenkörper, where they interact with the Myosin V MyoE to be delivered on F-actin to the plasma membrane for exocytosis (Pantazopoulou et al., 2014). For these vesicles, movement towards and away from the tip was seen, particularly if they could not associate with F-actin, such that these vesicles moved along microtubules as along a conveyer belt. RabE appears to label the entire Spitzenkörper in

A. nidulans, but, interestingly, corresponds to YPT-31 in *N. crassa*, which associates to the periphery of the Spitzenkörper in that organism (Sánchez-León et al., 2015). If DnfA and DnfB associate with different types of vesicles, they may respond to a disruption of microtubules differently. To determine this, the microtubule-destabilizing drug benomyl was applied to growing hyphae expressing DnfA-GFP and DnfB-mCherry. Fifteen minutes after benomyl exposure, which was enough time to observe complete disruption of the microtubule cytoskeleton of GFP-TubA (not shown), there were distinct changes to the localization of these proteins. First, both DnfA and DnfB exhibited an increased concentration at the Spitzenkörper. Next, this structure slowly elongated, with one end appearing to remain attached to the tip (**Supplemental Figure SF3.4A**). DnfA-GFP and DnfB-mCherry, notably, colocalized in this structure, such that retraction of it as one unit was observed (**Supplemental Figure SF3.4B**). Additionally, DnfA and DnfB aggregated together in the cytosol (**Supplemental Figure SF3.4C**).

DnfA and DnfB regulate phosphatidylserine asymmetry in A. nidulans

Phospholipids exhibit asymmetric distributions in eukaryotic cells, which can be exploited for a multitude of polarized cellular processes (Alder-Baerens et al., 2006; Fairn & Grinstein, 2010; Pomorski et al., 2003; Takeda et al., 2014). P4-ATPases play an important role in regulating this asymmetry. *S. cerevisiae* Dnf1p and Drs2p, for example, can act on PS, although Drs2p has greater activity towards PS (Baldridge & Graham, 2012). Removal of PS by deleting cho1 orthologs (the budding yeast phosphatidylserine synthase) disrupted polarized growth in *S. cerevisiae* as well as *Schizosaccharomyces pombe* and *Candida albicans* (Y. L. Chen et al., 2010; Fairn &

Grinstein, 2010; Luo et al., 2009). These findings suggested that PS distribution may be important for hyphal growth. Attempts to delete AN10701, the *A. nidulans* ortholog of budding yeast cho1, were unsuccessful, with the only primary transformants (in four independent transformations) being heterokaryons, as seen using the heterokaryon rescue method (Osmani, Oakley, & Osmani, 2006) (**Supplemental Figure SF3.3E**). This was true even in the presence of choline and ethanolamine, which restore growth to *cho1* mutants in other fungi (Y. L. Chen et al., 2010; Fairn & Grinstein, 2010; Luo et al., 2009), suggesting that it is an essential gene.

The C2-domain of bovine lactadherin binds specifically to PS, and GFP-Lact-C2 has been developed as a marker to view PS dynamics in live cells (Andersen, Berglund, Rasmussen, & Petersen, 1997; Yeung et al., 2008). PS is polarized to sites of growth in budding yeast, but has not been examined in hyphae. To observe PS distribution in *A. nidulans*, GFP-Lact-C2 was expressed under the control of the *A. nidulans niiA* promoter, which controls a nitrate reductase that is strongly repressed in the presence of ammonium (Cove, 1966; Punt et al., 1995). Similar localization was seen in >10 individual transformants, and one was chosen for further analysis. With the *niiA* promoter, excellent control over GFP-Lact-C2 expression was obtained over a wide range of ammonium levels (**Figure 3.6A**). When grown on media lacking NH_4, GFP-Lact-C2 labeled a large, bulbous mass at the tip of the cell, as well as smaller, subapical masses (**Fig. 3.6A**). Above 10mM NH_4Cl, GFP-Lact-C2 production was minimal and

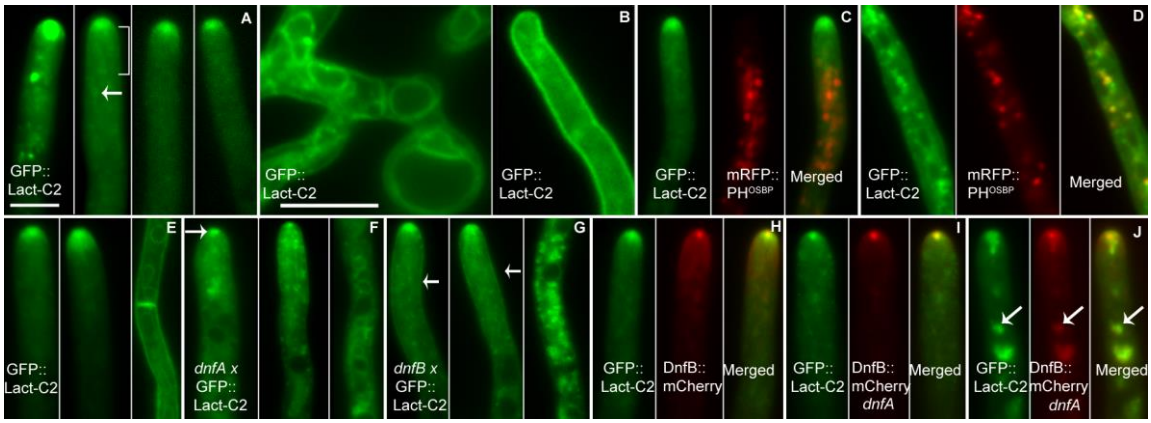

Figure 3.6 Phosphatidylserine distribution, as labeled by GFP-Lact-C2, in *A. nidulans* growing hyphae, and *dnfAΔ* and *dnfBΔ* mutants. A. GFP-Lact-C2 (**A**) marked the Spitzenkörper over a large range of expression levels, from minimal medium (no ammonium, **left panel**) to 1mM, 5mM, and 10mM of added NH_4Cl (**center left, center right, and right panel, respectively**). The plasma membrane around the apex was never labeled in wild type (**bracket**). However, some intracellular structures (**arrow**), similar to late Golgi, could be seen. Polarized localization was lost in subapical regions (**B, left panel**), or non-growing cells (**B, right panel**). **C.** GFP-Lact-C2 (**left panel**) did not obviously colocalize with mRFP-Ph^{OSBP} (**center panel**) on late Golgi near the apex. However, they became more aligned in subapical compartments (**D**). Phosphatidylserine in *dnfA*$^+$*dnfB*$^+$ hyphae (**E**) was disrupted in *dnfAΔ* mutants (**F**), and *dnfBΔ* mutants (**G**). **Arrows** in **F** point to the smaller Spitzenkörper in *dnfAΔ* cells, and in **G** mark the plasma membrane where GFP-Lact-C2 fluorescence can be seen. **H.** Colocalization of GFP-Lact-C2 (**left panel**) with DnfB-mCherry (**center panel**). **I, J.** GFP-Lact-C2 (**left panels**) and DnfB-mCherry (**center panels**) overlap well in the Spitzenkörper of the *dnfAΔ* mutant, as well as in the cytoplasm (**arrow**) at higher levels of GFP-Lact-C2 expression. Scale bars = 5 µm. **6B** is shown 2x larger than other figures to distinguish intracellular membrane labelling.

difficult to see, so all further images of GFP-Lact-C2 in were taken in minimal medium with 1mM NH_4Cl added.

Interestingly, GFP-Lact-C2 did not label the plasma membrane in mature, growing hyphae at any expression level, except possibly at the apex (**Fig. 3.6A**). Rather, the marker labeled the Spitzenkörper and some small puncta that could be seen moving rapidly into and out of the apical region (**Movie 3.2**). In subapical regions and non-growing cells, however, GFP-Lact-C2 was distributed throughout the plasma membrane without any obvious polarity, and also labeled endomembrane that appeared to be endoplasmic reticulum and vacuoles (**Fig. 3.6B**). GFP-Lact-C2 also does not strongly co-localize with mRFP-PH^{OSBP} on late Golgi (**Fig. 3.6C**), indicating that PS may be exposed to the cytosol at or after leaving this organelle. In sub-apical regions, however, overlap with late Golgi is more apparent (**Fig. 3.6D**).

To determine the role of DnfA and DnfB in PS distribution, GFP-Lact-C2 was inserted into *dnfAΔ* and *dnfBΔ* mutants. Compared to a $dnfA^+$ $dnfB^+$ strain (**Fig. 3.6E**), the aggregation of vesicles at the tip was much smaller (**Figs. 3.6F, G**). Subapical localization, moreover, was disrupted in *dnfAΔ* mutants, where little labelling of the plasma membrane could be seen (**Fig. 3.6F, Movie 3.3**). A similar pattern was seen in germlings. At early stages of germination in the parent strain, GFP-Lact-C2 strongly labeled the plasma membrane along with many endomembrane such as the endoplasmic reticulum and vacuoles (**Supplemental Figure SF3.5A**). The only obvious polarity in these cells, moreover was an accumulation of GFP-Lact-C2 subtending the apex, which was strikingly similar to the localization of GFP-Lact-C2 in *S. cerevisiae* early buds

(Fairn et al., 2011). *dnfAΔ* germlings, however, appeared to have PS exposed only in the plasma membrane opposite the germination site (**Supplemental Figure SF3.5B**). Deletion of *dnfB* also had a subtle, but different effect. In this mutant, GFP-Lact-C2 labeled the Spitzenkörper and cytosol similarly to *dnfB*$^+$ cells in germlings (**Supplemental Figure SF3.5C**), but, strikingly, also could frequently be seen on the plasma membrane in growing hyphal tips, unlike in wild type (**Fig. 3.6G, Movie 3.4**).

Finally, the diminished Spitzenkörper observed in *dnfAΔ* cells suggested that vesicles labeled with GFP-Lact-C2 may represent those associated with DnfB only, so DnfB-mCherry and GFP-Lact-C2 were expressed together in *dnfAΔ* cells. Indeed, in contrast to the situation in *dnfA*$^+$*dnfB*$^+$ cells, where GFP-Lact-C2 labeled a larger portion of the Spitzenkörper (**Fig. 3.6H, Movie 3.5**), DnfB-mCherry colocalized completely with the GFP-Lact-C2 apical body in *dnfAΔ*, even when the marker aggregated in subapical regions under high levels of expression (**Figs. 3.6I, J**). In summary, PS is located throughout the inner plasma membrane in non-growing cells, but in rapidly growing hyphae is on the cytosolic side of vesicles in the Spitzenkörper. *dnfA* and *dnfB*, additionally, appear to play complementary roles in vesicle trafficking to the Spitzenkörper, and regulating PS distribution in the plasma membrane.

Discussion: flippases DnfA and DnfB in *A. nidulans*

DnfA is endocytosed and recycled in hyphal tips

The NPFxD endocytic motif was first seen in yeast on Kex2p, a resident Golgi protein that undergoes endocytosis mediated through this motif when mislocalized to the

plasma membrane (Tan et al., 1996). More recently, it has been shown to assist in the endocytosis of Dnf1p (K. Liu et al., 2007) and the cell wall stress sensor Wsc1p (Piao et al., 2007). However, its conservation in other organisms has not been explored, and its presence in *A. nidulans* DnfA is surprising in several ways. First, N/DPFxD is present in the DnfA orthologs of all sequenced *Aspergillus* spp., but is completely absent from organisms just outside this group (e.g. *Penicillium* spp.), although P4-ATPases are relatively well-conserved throughout eukaryotes (our unpublished observations).

N/DPFxD is, importantly, only one of many endocytic motifs available to eukaryotes. For example, although two NPFxD sequences are present in Drs2p in yeast, their deletion does not result in an observable change in Drs2p localization (K. Liu et al., 2007). In *A. nidulans*, DnfB lacks the motif, but is also present in the plasma membrane, and actually trails off much earlier than DnfA, suggesting that it may have an even more efficient method for extraction back into the cytosol. It will be interesting to explore more thoroughly the determinants for endocytosis from the fungal plasma membrane by completing systematic mutations on a variety of hypha tip proteins. Alternatively, multiple forms of endocytosis may be present in hyphae, as seen in pollen tubes (Onelli & Moscatelli, 2013; Ovečka et al., 2012).

In budding yeast, Dnf1p travels through the late Golgi on the way back to the plasma membrane, similar to the recycling pathway that Snc1p, the yeast v-SNARE takes (K. Takagi et al., 2012; Valdez-Taubas & Pelham, 2003). Here DnfA was shown to traverse a similar route. The Snc1p homolog in *A. nidulans*, SynA, however, is still polarized when retrograde traffic to the late Golgi is abolished (Pantazopoulou &

Peñalva, 2011). It is tempting to think that this discrepancy implies an important role for DnfA at the late Golgi that is not shared by SynA. In any case the observations above provide more evidence for the existence of multiple recycling routes exist in *A. nidulans*, although a fungal organelle analogous to the recycling endosomes present in mammals has yet to be identified.

dnfA *has roles in reproduction, hyphal growth, and germination*

The deletion of *dnfA* had several effects. Each, however, could possibly be explained by a role for *dnfA* in secretion. First, growth was decreased, and because growth is driven by secretory vesicle fusion at the apex, this could be because of a concomitant disruption in the secretory vesicle trafficking. More interesting was the dramatic reduction in conidiation and conidium pigmentation. This is likely the result of a deficiency in melanization, which could be from disrupted melanin deposition or the production of less melanin overall. Melanin is a common secondary metabolite responsible for the various pigments that color the spores of the aspergilli (Bell & Wheeler, 1986; Kurtz & Champe, 1982). Interestingly, fungal secondary metabolism has been linked to membrane trafficking in recent years (Chanda et al., 2009a; Kistler & Broz, 2015; Rodrigues et al., 2008; Roze, Chanda, & Linz, 2011). In light of its localization throughout conidiophores and in secretory vesicles, it is possible that DnfA has a role in the trafficking of a component important for melanin production or deposition. The common role of P4-ATPases in secretion supports this position (Alder-Baerens et al., 2006; Poulsen et al., 2008).

In *Magnaporthe oryzae*, a major rice pathogen, two flippases were found to be essential for pathogenicity (Balhadère & Talbot, 2001; Gilbert, Thornton, Wakley, & Talbot, 2006). These flippases correspond to *dnfA* and *dnfC* in *A. nidulans*. Interestingly, *M. oryzae* is known to have two distinct secretion systems, although the link between these pathways and the flippases, or whether these produce different types of vesicles is unknown. *M. oryzae* also depends on melanin for production of a functional appressorium (Ebbole, 2007; Wilson & Talbot, 2009), the structure used to penetrate the host cell wall. One *M. oryzae* P4-ATPase mutant was deficient in appressorium formation and host penetration (Balhadère & Talbot, 2001), and in light of the present study the link between P4-ATPases and melanization should be explored further.

DnfA and DnfB are segregated in the Spitzenkörper and play complementary roles in hyphal growth of A. nidulans

The Spitzenkörper is a dynamic structure composed of many individual vesicles that can each exhibit independent trafficking. Moreover, these vesicles can be grouped into at least two classes. A smaller group of vesicles, termed microvesicles, are present in the center of the Spitzenkörper, while macrovesicles are larger and form a "Spitzenring" around the collection of microvesicles (Grove & Bracker, 1970; R. J. Howard, 1981; Löpez-Franco & Bracker, 1996; Verdín et al., 2009). These two classes find some analogy with budding yeast, wherein two separate secretory pathways, regulated by flippases, transport proteins to different locations (Harsay & Bretscher,

1995). Drs2p and Dnf3p are important in the production of vesicles containing invertase, for example (Alder-Baerens et al., 2006; Gall et al., 2002).

N. crassa chitin synthase Chs-1 is present on microvesicles in the center of the Spitzenkörper, while its 1,3 β-glucan synthase component Gs-1 is present on macrovesicles encircling Chs-1 (Verdín et al., 2009). Similarly, as shown here, *A. nidulans* GsaA forms a ring in the outer region of the Spitzenkörper. The separation of DnfA and DnfB is further evidence that this organelle is more than an artifactual collection of vesicles, and is rather a complex structure developed in some fungi, possibly to precisely regulate secretion and growth. It also suggests, along with the nearly essential role that these proteins play in hyphal growth, that they are responsible for producing complementary populations of secretory vesicles that are required for Spitzenkörper structure. Finally, supporting the idea that DnfA and DnfB are on different secretory vesicles, *dnfAΔ* mutants contain a much smaller Spitzenkörper as labeled by GFP-Lact-C2 than in the *dnfA*$^{+}$ parent strain. The Spitzenkörper that was left, moreover, associated with DnfB-mCherry, indicating that these vesicles may be specific to this flippase.

In contrast, DnfA and DnfB co-localize well in the cytosol, particularly when benomyl was applied. A previous study looked at *A. nidulans* subcellular organization (Torralba et al., 1998) after addition of benzimidazole-2-yl carbamate, the active component of benomyl. The authors found that microvesicles increased in concentration at the tip, while macrovesicles were seen to congregate around late Golgi. Similarly, DnfA and DnfB appeared to aggregate at both the Spitzenkörper and cytosolic structures

which were likely late Golgi equivalents, indicating that even though they are segregated in rapidly growing tips, they may follow similar routes on the way to the plasma membrane, and be closely associated during trafficking.

Finally, echoing the mutant phenotype data, DnfA was present earlier during germination, and later during conidiation. Interestingly, similar expression patterns were reported for DnfA and DnfB orthologs in germlings of *Aspergillus fumigatus* (Lamarre et al., 2008), and the DnfA ortholog is expressed in germlings of *M. oryzae* (Balhadère & Talbot, 2001). In all, the data collected here supports a model in which these proteins are responsible for the structure of the Spitzenkörper, but more work is required to understand the intricacies of their relationship.

Distribution and function of phosphatidylserine in A. nidulans

PS is ubiquitous in eukaryotes, but usually makes up less than 20% of the plasma membrane total phospholipids in fungi (Wassef, 1977). In the aspergilli, it is likely much less, between 0.3% (Chattopadhyay, Banerjee, Sen, & Chakrabarti, 1985) and 5% (Letoublon, Mayet, Frot-Coutaz, Nicolau, & Got, 1982) of the total for *Aspergillus niger,* for example. However, PS distribution is also actively regulated, and its asymmetry is similar in organisms separated by wide evolutionary timespans (Yeung et al., 2008). More recently, this asymmetry has been shown to be important for polarity in both budding and fission yeasts (Das et al., 2012; Fairn & Grinstein, 2010; Luo et al., 2009). The observations collected here suggest that PS is exposed at high levels on the outside of secretory vesicles *A. nidulans*, and that exposure occurs during or after secretory vesicle formation, as GFP-Lact-C2 showed little co-localization with late

Golgi. The low levels of PS in the plasma membrane may account for our inability to detect it there. This would be especially true if PS is enriched at a much higher level on secretory vesicles than the plasma membrane. Indeed, higher expression of the marker did not reveal any plasma membrane localization that was obscured at lower levels, and the GFP-Lact-C2-labeled Spitzenkörper resembled the accumulation of endosomes that occurs in *hookA* mutants when endosomal attachment to dynein for retrograde transport is impaired (Zhang et al., 2014), suggesting that the abnormal structure was a mass of secretory vesicles confined in the tip.

AN10701, the putative PS synthase, could not be deleted. PS could be essential on the outside of secretory vesicles, as filamentous fungi are dependent upon secretion presumably for utilizing energy sources in addition to growth. This brings up two tempting hypothesis. First, PS may have a role in the establishment of the endocytic collar, as it is required for polarization of endocytosis in budding yeast. Second, PS could have an unknown, essential function on the outside of secretory vesicles similar to its association with Cdc42p in yeast (Das et al., 2012; Fairn & Grinstein, 2010). Alternatively, it is possible that flipping PS is important for secretory vesicle budding from the late Golgi, as proposed in budding yeast, so PS concentration is simply a result of secretory vesicle budding. Interaction of apical proteins with PS-enriched vesicles will, in the future, shed light on how the tip maintains its dynamic organization, as well as the forces stabilizing the structure of the Spitzenkörper.

CHAPTER IV

DYNAMICS OF DNFA AND DNFB IN *Aspergillus nidulans* AND THEIR ROLES IN ENDOCYTOSIS AND SPITZENKORPER STABILITY*

Overview: DnfA and DnfB dynamics

Filamentous fungi exhibit rapid, polarized growth governed by the precise segregation of endocytosis and exocytosis at the site of cell expansion. Endocytosis is concentrated at a zone termed the endocytic collar, which surrounds the cell tip. Exocytosis, on the other hand, occurs specifically at the end of the cell. How the separation of these processes is established and maintained is still unclear, but one possible purpose for this organization is the ability of endocytosis to remove and recycle proteins that diffuse away from the site of growth. The phospholipid flippases DnfA and DnfB localize to sites of growth and endocytosis in the fungus *Aspergillus nidulans*, and may be involved in secretion. DnfA is endocytosed in part through an NPFxD motif, but whether DnfB is endocytosed or recycled is unknown.

Although both proteins are observed on the plasma membrane, the steady-state localization of both DnfA and DnfB is in the Spitzenkörper (**SPK**). The SPK is a

---

structure at the apex of growing cells that governs secretion in many filamentous fungi. Ultrastructural studies indicate that the SPK is an organized mass of secretory vesicles, with different types of vesicles present in outer and inner layers (Grove & Bracker, 1970; Löpez-Franco & Bracker, 1996).

This chapter addresses two questions: whether DnfB is also endocytosed and recycled, as seen for DnfA. Additionally, whether DnfA and DnfB have different dynamics within the SPK, and if they play distinct roles in the organization of the hyphal growth machinery, including the SPK and the endocytic collar.

Introduction: DnfA and DnfB dynamics

Filamentous fungi grow by concentrating cell expansion at a discrete region in the tips of their cells. These cells, called hyphae, can maintain a consistent shape and growth rate over large spatial and temporal scales. Coordinating the direction and rate of growth in the Ascomycete and Basidiomycete fungi is a specialized secretory structure, the SPK. The SPK is composed of post-Golgi secretory vesicles (**SV**) and endocytic vesicles that are continuously released for fusion with the plasma membrane (**PM**) (Pinar et al., 2015; Z. Schultzhaus et al., 2016; Z. S. Schultzhaus & Shaw, 2015; Verdín et al., 2009). A large proportion of secretory traffic produced in a mycelium, therefore, transits through the SPK. Beyond the basic ultrastructure, however, there is little insight into the forces regulating SPK dynamics and organization. Interestingly, a portion of SPK vesicles are derived from endocytic vesicles (Fischer-Parton et al., 2000; Z. S. Schultzhaus & Shaw, 2015; Shaw et al., 2011), and the vesicles within the SPK are

organized such that larger vesicles (macrovesicles) are present around the outside while smaller vesicles (microvesicles) are concentrated within the center. These different vesicles appear to have different cargo, with glucan synthases preferentially localizing to macrovesicles and chitin synthases enriched in microvesicles, for example (Girbardt, 1957; Grove & Bracker, 1970; R. J. Howard, 1981; Löpez-Franco & Bracker, 1996; Meritxell Riquelme et al., 2007; Sánchez-León et al., 2011; Z. Schultzhaus et al., 2015a).

Two proteins in *Aspergillus nidulans*, DnfA and DnfB, are segregated within the SPK. These proteins belong to a conserved group of phospholipid-translocating ATPases ("flippases"), which regulate the lipid organization of PM as well as intracellular organelles such as vacuoles and late Golgi. Their localization within the SPK suggested that the distribution of lipids on secretory vesicles could play a role in SPK structure, and provided a means to test the dynamics of different regions of the SPK (Baldridge & Graham, 2012; Z. Schultzhaus & Shaw, 2016; Z. Schultzhaus et al., 2015a).

The SPK, additionally, is at the intersection of endocytosis and exocytosis within hyphae. These are conserved processes that provide cells the chance to interact with their environment and regulate plasma membrane dynamics, among other things. Inhibiting endocytosis has many effects on filamentous fungi, including disrupting their ability to maintain polarity, an almost complete abolishment of growth, and causing aberrant cell shape (Araujo-Bazán et al., 2008; Hervás-Aguilar & Peñalva, 2010; M. Á. Peñalva, 2010; Z. S. Schultzhaus & Shaw, 2015; Shaw et al., 2011; Upadhyay & Shaw, 2008). The direct reason for these phenotypes has not been demonstrated. Most mutations or treatments that target endocytosis may also target the actin cytoskeleton, which has

several ancillary roles in growth and cell shape including intracellular membrane trafficking (Hervás-Aguilar & Peñalva, 2010; Pantazopoulou et al., 2014). Some hypotheses for the purpose of the endocytosis in growth and shape have been proposed, including the apical recycling model, which suggests that endocytosis acts to counteract to the passive diffusion of proteins from the site of growth. In this system, proteins that are necessary for certain processes at the cell tip are internalized at the endocytic collar as they are misplaced during growth. Additionally, some of these proteins could potentially be recycled back to the site of growth through a variety of endomembrane trafficking pathways (Caballero-Lima et al., 2013; Lee et al., 2008; Z. S. Schultzhaus & Shaw, 2015; Shaw et al., 2011).

To understand the function of endocytosis in fungi, as well as the results that come from mutations that block endocytosis, it is helpful to characterize proteins that are cargo of the endocytic collar. To this date, however, only a few proteins have been shown to be endocytosed in the tips of filamentous fungi (Pantazopoulou & Peñalva, 2011; Taheri-Talesh et al., 2008). One of these proteins is the *Aspergillus nidulans* phospholipid flippase DnfA (Z. Schultzhaus et al., 2015a). DnfA has an NPFxD motif, which is known to associate with the endocytic adaptor Sla1p in yeast (J. P. Howard et al., 2002; K. Liu et al., 2007; Piao et al., 2007). Upon mutation of this motif, DnfA relocalized from the hyphal tip to being present throughout the plasma membrane in an apolar manner, suggesting it is endocytosed in part through this motif. DnfA-GFP was, moreover, diffuse throughout the cytoplasm in a *vftD* deletion mutant. VftD is part of the Golgi Associated Retrograde Protein (**GARP**) complex, a four-subunit tethering

complex required for fusion of vesicles travelling from early and late endosomes to the late Golgi, and thus for endocytic recycling of proteins through the late Golgi(Conibear & Stevens, 2000; Z. Schultzhaus et al., 2015a). A *vftD* deletion confers a strong growth phenotype, which suggests that GARP function is abolished in this mutant, and, further, that endocytic recycling through the late Golgi could act to polarize tip components in *A. nidulans*. Here, we analyzed the dynamics of flippases DnfA and DnfB. First, we tested whether DnfB is cargo of endocytosis and endocytic recycling through genetic manipulation of these pathways. Next, we determined the of flow of both flippase proteins DnfA and DnfB through the SPK using Fluorescence Recovery after Photobleaching (**FRAP**), and examined the role of these flippases in the organization of the hyphal tip.

Experimental Procedures: DnfA and DnfB dynamics

Aspergillus culture conditions and genetic techniques

A. nidulans strains were cultured on minimal medium (**MM**) with supplements following standard protocols (Kaminskyj, 2001). DnfA-GFP, DnfB-GFP, and DnfB-mCherry, and *vftD*Δ strains were constructed previously (Z. Schultzhaus et al., 2015a). *gsaA*::*mCherry* or *fimA*::*mCherry* strains were obtained through insertion of the mCherry coding sequence immediately prior to the stop codon, and *niiA*::An*cdc50* and *niiA*::*fimA* were produced by insertion of the *niiA* promoter before the start codons of the relevant genes, (Z. Schultzhaus et al., 2015a). Expressing conditions used 40mM sodium nitrate as a nitrogen source, and repressing conditions used 40mM ammonium chloride as a

nitrogen source, as in previous studies (Hervás-Aguilar & Peñalva, 2010; Z. Schultzhaus & Shaw, 2016). Genetic manipulation was done using previously described protocols (Oakley et al., 2012). For each transformation, eight transformants were tested by PCR with primers flanking the transformation construct insertion site, as well as for expected fluorescence, growth, and development phenotypes.

Image capture and Analysis

Conidia were streaked onto a plate of solid MM with supplements and incubated for 16-20 hours in 30^{o}C, after which a block of agar containing the leading hyphae was excised and placed upside down on a 25mm x 60mm coverslip containing a 15µm drop of liquid MM (inverted microscope), or on a microscope slide and the cells were covered with 15µm of liquid minimal medium followed by a coverslip (upright microscope). All cells were then incubated at 30^{o}C for 30 minutes to facilitate attachment to coverslips.

FRAP for DnfA, DnfB were done on an Olympus FV1000 FluoView inverted laser scanning confocal microscope system (Olympus, Japan) as previously described (Lara-Rojas, Bartnicki-García, & Mouriño-Pérez, 2016). FRAP included capturing an image every 5s, and bleaching a circular region encompassing the Spitzenkörper for seven complete scans with full laser intensity. FRAP analysis was completed using the ImageJ FRAP Profiler plugin (from the Hardin lab http://worms.zoology.wisc.edu/research/4d/4d.html#frap) for image sequences in which cell growth was unperturbed and the cell tip did not leave the plane of focus during image capture. The StackReg ImageJ plugin was used to align growing hyphal tips for automated FRAP analysis.

Imaging of GsaA-mCherry and FimA-mCherry was completed on an Olympus BX-51 microscope equipped with a Hamamatsu Orca-ER CCD camera (Hamamatsu, Japan) driven by Slidebook 5.0 Software (Intelligent Imaging Innovations, Colorado, USA) as previously described (Shaw & Upadhyay, 2005).All figures and videos were processed for publication using ImageJ and Adobe Photoshop 5.0 (Adobe, California, USA).

Results and Discussion: DnfA and DnfB dynamics

The flippase DnfB is primarily localized to the hyphal tip and the plasma membrane under normal conditions (**Figure 4.1A**) (Z. Schultzhaus et al., 2015a). When endocytosis is blocked by downregulating the endocytic gene *fimA* (fimbrin)(Upadhyay & Shaw, 2008) with the nitrate-expressing, ammonium-repressible *niiA* promoter(Cove, 1966; Hervás-Aguilar & Peñalva, 2010; Punt et al., 1995), DnfB-mCherry depolarizes and moves from the tip (**Fig. 4.1C**) to being present throughout the plasma membrane (**Fig. 4.1D**). Interestingly, although DnfB trails off of the plasma membrane before DnfA in wild type cells (Z. Schultzhaus et al., 2015a), it does not possess an NPFxD motif, and its mechanism for being recognized by the endocytic machinery is not yet known.

DnfB is also present at the late Golgi in wild type (Z. Schultzhaus et al., 2015a). To see if it also traffics to the late Golgi after being endocytosed, we viewed DnfB-mCherry in a *vftD* deletion mutant. As seen in **Fig. 4.1B**, although DnfB-mCherry is still polarized, its apical accumulation is less organized, suggesting that the presence of DnfB-mCherry at the Spitzenkörper, and possibly Spitzenkörper structure, is dependent

upon traffic between endosomes and the late Golgi. Whether DnfB can be polarized through a secondary recycling pathway is unknown. The homolog in yeast, Drs2p, has been shown to act in concert with Rcy1p to support endocytic recycling (Hanamatsu, Fujimura-Kamada, Yamamoto, Furuta, & Tanaka, 2014), but the importance of the *A. nidulans* Rcy1p homolog, RcyA, in recycling is unclear (Herrero, Takeshita, & Fischer, 2014), and could be resolved in the future. What is clear is that one effect of abolished endocytosis is the likely loss of plasma membrane lipid asymmetry, the consequences of which is a currently unexplored topic in fungal cell biology.

As mentioned above, another feature of *A. nidulans* DnfA and DnfB is that they preferentially localize to different regions of the SPK and the PM (**Figure 4.2A**), with DnfA concentrated on the outside of the SPK and DnfB within the SPK core. This distribution suggests that these proteins may be present on different sets of vesicles (DnfA on macrovesicles, DnfB on microvesicles). If DnfA-GFP and DnfB-GFP are present on different vesicles, they may exhibit different FRAP recovery dynamics, as is the case for several SPK markers in *N. crassa* (Sánchez-León et al., 2015). To test this hypothesis, we performed FRAP on DnfA-GFP and DnfB-GFP in the SPK in growing hyphae (**see Experimental Procedures: dnfA and dnfB dynamics**) and determined the $t_{1/2}$. This quantity represents the time (s) at which one half of the final fluorescence intensity is recovered, and in this case it provides information on how rapidly new fluorophore traffic into the photobleached region. As shown in **Figure 4.2B**, DnfB-GFP has a significantly lower $t_{1/2}$ (15.81 +/- 1.17, N=14) compared to DnfA-GFP (30.78 +/-

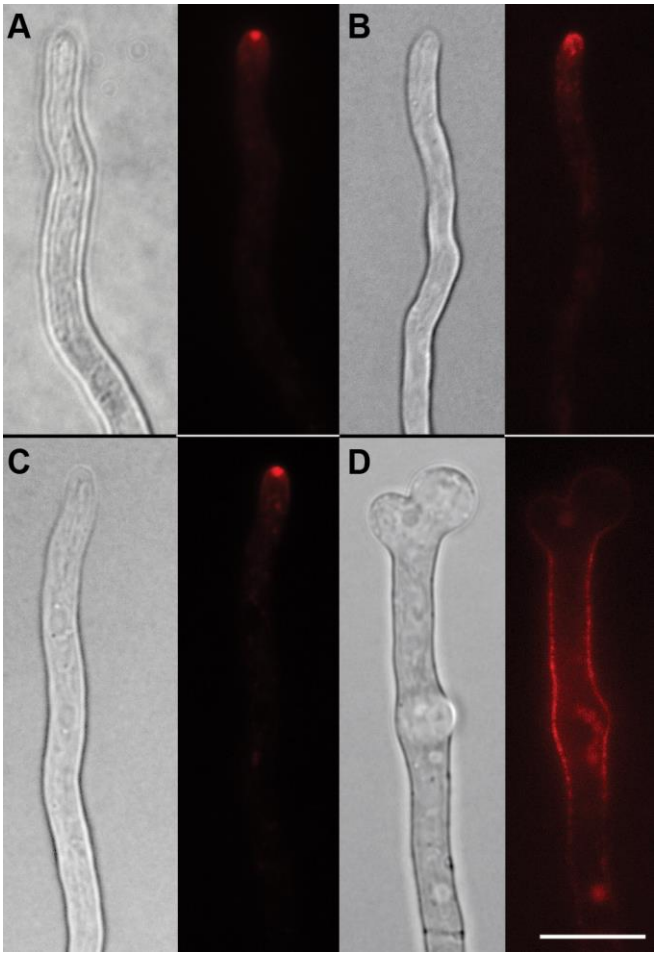

Figure 4.1. DnfB is endocytosed and possibly recycles through the late Golgi. DnfB-mCherry is present in the Spitzenkörper and the apical plasma membrane in wild type hyphae (**A**), while this organization is lost when *vftD* is deleted (**B**). When endocytosis is depleted through regulation of *fimA* by the ammonium-repressible *niiA* promoter, DnfB-mCherry relocalizes from the Spitzenkörper (**C, grown with NO_3**) to the plasma membrane (**D, grown with NH_4**). Scale bar = 5µm.

3.17, N=13). This differential rate can also be observed in **Movie 4.1** and **Figure 4.2C**, in which the concentrated SPK core labelled by DnfB-GFP is rapidly replenished when compared to the larger, more diffuse region labelled by DnfA-GFP. These quantities are similar to those calculated for some *N. crassa* proteins associated with macrovesicles (Fks-1, $t_{1/2}$ = 31.7s), and microvesicles (Ypt-1, $t_{1/2}$ = 15.5s) (Sánchez-León & Riquelme, 2015; Sánchez-León et al., 2015), but different than the *A. nidulans* Rab GTPase Ypt31/RabE, which was found to recover with a $t_{1/2}$ of ~10s (Pantazopoulou et al., 2014). This discrepancy could be the result of the characteristics of individual proteins and their association with vesicles (i.e. membrane bound or lacking in transmembrane domains), but more work is needed to assess the full spectrum of SPK protein dynamics.

Next, we looked at the role of flippases in SPK structure and dynamics during growth. In *A. nidulans,* the SPK generally maintains its position within the center of the hyphal tip, resulting in the production of straight hyphae, as seen in **Figure 4.2D** and **Movie 4.2** through labelling of the SPK with GsaA-mCherry, a subunit of *A. nidulans* 1, 3-β-glucan synthase. When the flippase *dnfA* is deleted, however, hyphae are wider and bulbous and exhibit a reduction in growth rate of ~70% (Z. Schultzhaus et al., 2015a). Accordingly, as shown in the lower four panels of **Figure 4.2D** (which comprise image sequences of two separate hyphae), the SPK moves laterally within the apical dome during growth, and occasionally diffuses and recovers. This effect could be explained if DnfA has a role in altering the lipid asymmetry of vesicles within the SPK, or the number of vesicles, with a resulting alteration to the interactions between molecular components (i.e. actin and vesicle-associated proteins) that contribute to SPK stability.

Deleting *dnfB* did not result in an observable change in SPK dynamics (not shown). This was expected, because although DnfB strongly labels the SPK, previous studies showed that a *dnfB* deletion alone did not radically effect hyphal growth or morphology (Z. Schultzhaus et al., 2015a). Additionally, although DnfB (Drs2 in yeast) was previously implicated in the production of a specialized set of clathrin-associated secretory vesicles in budding yeast (Gall et al., 2002), there is no evidence of a subset of clathrin-labelled secretory vesicles in *A. nidulans*, as clathrin is generally excluded from the hyphal tip (personal observations). Alternatively, DnfB could be involved in the trafficking of specific cargo from the late Golgi, rather than the production or alteration of secretory vesicles.

Finally, we considered the additive effects of depleting DnfA and DnfB on hyphal tip organization, through manipulation of the *A. nidulans cdc50* homolog (AN5100). Cdc50 proteins are involved in proper localization of phospholipid flippases represented in *A. nidulans* as DnfA, DnfB, and DnfC (Saito et al., 2004). An An*cdc50*Δ phenocopies a *dnfA* and *dnfB* double deletion mutant (Z. Schultzhaus et al., 2015a). We placed the native An*cdc50* promoter with the *niiA* promoter that we have used previously (Hervás-Aguilar & Peñalva, 2010; Punt et al., 1995; Z. Schultzhaus et al., 2015a), which exhibits strong repression in the presence of ammonium and expression in the presence of nitrate. This allowed us to effectively observe the secretory vesicle marker GsaA-mCherry and the endocytic marker FimA-mCherry when both DnfA and DnfB are depleted.

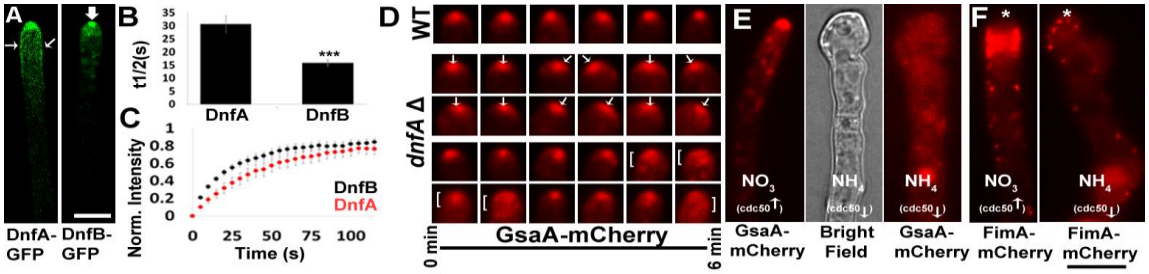

Figure 4.2 Spitzenkörper protein dynamics in *Aspergillus nidulans*. A Localization of flippases DnfA and DnfB within the Spitzenkörper of *A. nidulans*. **Thin Arrows** indicate plasma membrane localization of DnfA. **Thick Arrows** indicate the core of the Spitzenkörper as labeled by DnfB-GFP. **B.** $t_{1/2}$ of DnfA-GFP and DnfB-GFP fluorescence recovery profiles. The mean $t_{1/2}$ of DnfA-GFP and DnfB-GFP were found to be significantly different when compared using a Student's t-test, with a P-value of <0.001 (indicated by ***). **C.** Mean fluorescence recovery curves for DnfA-GFP (**Red**) and DnfB-GFP (**Black**). Bars on data points indicate +/- standard error. **D.** SPK dynamics as visualized by GsaA-mCherry in the apex of a wild type hypha (upper two panels) and a *dnfA* deletion mutant (lower four panels). Lower two groups of panels represent two separate image sequences of separate hyphae. Arrows represent lateral SPK movement, and brackets represent SPK dissipation. Time between images = ~60 seconds. **E.** GsaA-mCherry localization when An*cdc50* is expressed (NO_3 as nitrogen source, left panel) or repressed (NH_4 as nitrogen source, right two panels). **F.** FimA-mCherry localization when An*cdc50* is expressed (left panel) or repressed (right panel). Asterisks in **F** represent the apex of the hyphal tip.

Figure 4.2E shows GsaA-mCherry in An*cdc50* expressing conditions (with 40mM sodium nitrate as a nitrogen source) and in repressing conditions (with 40mM ammonium tartrate as a nitrogen source). When An*cdc50* is expressed, GsaA-mCherry labels the SPK. Repression of An*cdc50* results in extremely aberrant growth with the absence of a SPK. In these cells, GsaA-mCherry is not concentrated within the apex, but is diffuse within the cytoplasm, suggesting that, together, *dnfA* and *dnfB* share an essential role in *A. nidulans* secretion. Additionally, since the phospholipid character of the membrane may play a role in the localization of endocytosis, we examined the endocytic marker FimA-mCherry when An*cdc50* is repressed. Under inducing conditions, as in wild type, FimA-mCherry is strongly polarized. To quantify this, fluorescence intensity of a 2.5μm window was collected at the apex and compared to a similarly-sized region 10 μm behind this region. Under expressing conditions, this ratio was 3.52 +/- 0.08, while this value was reduced to 1.5 +/- 0.19 under repressing conditions (N=5 hyphae for both, $p<0.001$). The lifetimes of endocytic patches was not affected (not shown), which suggests that this difference results from a reduced ability to establish a normal zone of endocytosis when An*cdc50* is repressed and lipid asymmetry is disrupted.

In conclusion, flippases DnfA and DnfB have differential dynamics within the SPK, suggesting that they associate with different vesicles. Additionally, in the likely absence of flippase function, when An*cdc50* is depleted, secretion is highly disrupted, while the polarization of endocytosis is reduced, but not abolished. These results provide an insight into the origin and the maintenance of the SPK, as well as the role of flippases

in *A. nidulans*, but more experiments, in particular biochemical tests on the components of SPK-specific vesicles, and deeper quantitative analysis of flow of vesicles through the SPK, are necessary next steps to understand this organelle.

CHAPTER V

CONCLUSION

Much work has contributed to the current understanding of hyphal growth in fungi, and the studies included in this dissertation summarize and expand on one piece: the events happening at the plasma membrane. Although the strength of the cell wall is required for formation of the hyphoid shape, the cell wall is formed by enzymes that are deposited in the tip through targeted exocytosis and removed by endocytosis, and linear expansion occurs only through vesicle fusion, which precedes cell wall synthesis. The understanding of fungal growth is inseparable, then, from the understanding of two basic processes: endocytosis and exocytosis.

It is easy to understand why exocytosis is important for hyphal growth: it provides the new material for membrane and cell wall expansion. Why endocytosis is important for hyphal shape and growth is not as straightforward, and much of the work above was done to address this question.

First, I characterized a classical component of the endocytic pathway: clathrin (CHAPTER II). Clathrin acts early in endocytosis to promote and shape membrane budding, and it was essential for growth. Surprisingly, however, its essential role did not appear to be due to any function in regards to endocytosis. This was demonstrated by the fact that it did not localize strongly to the endocytic collar, and when a subunit of the clathrin coat, the clathrin heavy chain, was downregulated, endocytosis proceeded relatively normally. In contrast, clathrin localization on late Golgi was more informative.

Filamentous fungi have become useful models for studying the maturation of Golgi through the secretory pathway because individual stages of Golgi can be spatially resolved within the large cytosolic space of hyphae. Imaging clathrin at Golgi in *A. nidulans* revealed that clathrin arrives just prior to the dissipation of late Golgi into post-Golgi secretory vesicles, suggesting that events leading to the vesiculation of late Golgi in *A. nidulans* may be driven by clathrin. Because clathrin was not seen in the tip, where secretory vesicles are targeted, it was concluded that clathrin-coated vesicles from late Golgi traffic to different target, such as early endosomes. Together, these observations indicated that, although clathrin played an essential role in *A. nidulans*, endocytosis may be primarily clathrin-independent, something which should be studied further in other filamentous fungi using similar techniques. Revealing the components of a novel clathrin-independent endocytic pathway that is specific to filamentous fungi, considering the importance of endocytosis to fungal growth, would be an excellent advance towards drug design targeting fungal pathogens.

The rest of the work went towards characterizing proteins that require endocytosis for their polarized localization. Discovering proteins that follow such a route would provide a function for the endocytic collar. In fact, it would provide evidence to support the apical recycling model, a hypothesis previously proposed by our laboratory which states that the reason that the endocytic collar is important for hyphal growth is that it keeps landmark proteins involved in directing vesicle trafficking from diffusing away from the site of growth and therefore causing growth to be depolarized. I discovered two proteins that traffic through this pathway, the phospholipid flippases

DnfA and DnfB. It is not entirely surprising that these proteins rely on endocytosis for their localization: the yeast homologues Dnf1p and Drs2p, respectively, have similar properties and follow a similar route. However, a clear advantage that studies in filamentous fungi have over yeast, in this case, is the ability to image the dynamics of secretory vesicles at the SPK. These dynamics strikingly revealed that DnfA and DnfB are primarily associated with different secretory vesicle populations. Additionally, these different vesicles have different dynamics, with DnfB turning over more rapidly within the SPK than DnfA. These results bolster the hypothesis that the SPK is a non-homogeneous structure with a distinct role in hyphal growth and fungal secretion, and suggests that it may actively regulate the rate and targeting of membrane fusion by different sets of vesicles.

With these results, future directions should now be considered in order to further describe the role of endocytosis and flippases within filamentous fungi, as well as to test the apical recycling model. Some of these possible experiments are outlined below:

Clathrin and membrane trafficking

Whether clathrin has any role in the endocytic collar is still an open question. The ability to specifically target clathrin-mediated endocytosis has challenged cell biologists in many systems for years. A logical next experiment for our purposes would be to characterize mutants of the clathrin-mediated endocytosis adaptor complex AP-2, which should specifically act to attach clathrin coats to the endocytic machinery at the plasma membrane and only minimally affect clathrin function at other organelles such as late Golgi and endosomes. If mutants of these proteins have strong growth phenotypes,

particularly if they are depleted in endocytosis, or if these proteins localize to the endocytic collar, this would suggest that clathrin-mediated endocytosis does predominate in the collar. Care should be taken, however, to demonstrate that these proteins actually associate with *A. nidulans* clathrin, and not another, novel, coat protein.

Along with understanding whether clathrin is a component of the endocytic collar complex, understanding the "trigger" or the foundation for the endocytic collar, in terms of membrane lipid composition is another task that should be addressed. As discussed in Chapter III, phosphatidylserine is present at the plasma membrane, although this localization is not easy to image due to the large signal within the SPK. A hypothesis that should be tested is that phosphatidylserine, or another phospholipid regulated by flippases, is involved in endocytic initiation and/or dynamics. To test this hypothesis, it is necessary to view the distribution of phosphatidylcholine and phosphatidylethanolamine within growing or rapidly-fixed fungal cells, to see if these phospholipids are present within the endocytic collar. For this experiment, a comparative analysis would be useful to look at this distribution within other fungi, in order to determine if such distributions are as conserved as the endocytic collar. Next, more characterization of phosphatidylserine-deficient mutants should be done, with the phosphatidylserine synthase gene expressed at various low levels, followed by observation of endocytic patch dynamics and polarization of endocytosis. Finally, assays to determine the affinities of endocytic proteins for specific phospholipids, could provide a better idea of which phospholipids could be the signal for initiation of endocytosis.

The apical recycling model

The main focus of this dissertation was to test the apical recycling model. I discovered two new proteins that maintain their polarization seemingly through endocytic recycling. It is unclear, however, whether the polarized localization of these two proteins are required for normal hyphal growth, as blocking endocytosis of DnfA does not result in any distinct phenotype. To further identify proteins that may travel through a recycling pathway, two experiments could be done: First, it would be informative to examine the rest of the list of NPFxD proteins in *A. nidulans* to see if any of these also are polarized and recycled. Moreover, because this list is certainly not exhaustive for endocytosed proteins, a more ambitious experiment would be to characterize proteins that are "trapped" on the plasma membrane when endocytosis is disrupted. This could be accomplished using a knockdown of a gene involved in endocytosis or a temperature-sensitive version of an endocytic. Cells would then be fractionated after endocytosis is "turned off," and those that relocalize to the PM layer would be candidates for endocytic recycling. Finally, it is necessary to establish the existence or absence of a Golgi-independent recycling pathway in fungi. Tracking certain endocytic dyes such as FM4-64 as they traverse through the endocytic pathway back to the cell surface would assist in this task.

Phospholipid flippase function in filamentous fungi

Chapters II and IV clearly demonstrate that phospholipid flippases play important roles in filamentous fungi that should be further characterized. Because the

SPK is diminished and unstable in strains lacking DnfA, it is necessary to further characterize this effect through imaging the SPK in flippase mutants using transmission electron microscopy, which should demonstrate the localization of specific vesicle populations. Two additional, parallel experiments would complement this one: first, a characterization of the effect of deleting either *dnfA* or *dnfB* on the total secreted proteome would be useful in understanding the cargo of inner and outer SPK vesicles, and whether the sorting of this cargo is regulated by phospholipid asymmetry via DnfA or DnfB. Second, the effects of deleting either *dnfA* or *dnfB* on the events earlier in the secretory pathway, i.e. Golgi maturation, should be examined through analysis of late and early Golgi lifetimes and structure. Both DnfA and DnfB localize to the late Golgi in *A. nidulans*, and flippases are represented on Golgi membrane in many eukaryotes, but whether they have functions in Golgi maturation, or if Golgi maturation itself is linked to lipid asymmetry, is unknown in any organism.

Conclusion: endocytic recycling pathways in *A. nidulans*

The specific effects of phospholipid asymmetry on membrane budding, endocytosis, and cell growth are still unclear, and filamentous fungi are excellent for studying all of these processes. Following up on one or any of these proposed experiments is a logical strategy for uncovering the mechanisms underlying membrane dynamics in all eukaryotic cells, as well as the methods that nearly all fungi use in their colonization of the Earth.

REFERENCES

Abenza, J. F., Pantazopoulou, A., Rodríguez, J. M., Galindo, A., & Peñalva, M. A. (2009). Long-distance movement of *Aspergillus nidulans* early endosomes on microtubule tracks. *Traffic, 10*(1), 57-75.

Adamo, J. E., Moskow, J. J., Gladfelter, A. S., Viterbo, D., Lew, D. J., et al. (2001). Yeast Cdc42 functions at a late step in exocytosis, specifically during polarized growth of the emerging bud. *The Journal of Cell Biology, 155*(4), 581-592.

Albuquerque, P. C., Nakayasu, E. S., Rodrigues, M. L., Frases, S., Casadevall, A., et al. (2008). Vesicular transport in *Histoplasma capsulatum*: an effective mechanism for trans-cell wall transfer of proteins and lipids in ascomycetes. *Cellular Microbiology, 10*(8), 1695-1710.

Alder-Baerens, N., Lisman, Q., Luong, L., Pomorski, T., & Holthuis, J. C. (2006). Loss of P4 ATPases Drs2p and Dnf3p disrupts aminophospholipid transport and asymmetry in yeast post-Golgi secretory vesicles. *Molecular Biology of the Cell, 17*(4), 1632-1642.

Andersen, M. H., Berglund, L., Rasmussen, J. T., & Petersen, T. E. (1997). Bovine PAS-6/7 binds αvβ5 integrin and anionic phospholipids through two domains. *Biochemistry, 36*(18), 5441-5446.

Antonescu, C. N., Aguet, F., Danuser, G., & Schmid, S. L. (2011). Phosphatidylinositol-(4, 5)-bisphosphate regulates clathrin-coated pit initiation, stabilization, and size. *Molecular Biology of the Cell, 22*(14), 2588-2600.

Araujo-Palomares, C. L., Castro-Longoria, E., & Riquelme, M. (2007). Ontogeny of the Spitzenkörper in germlings of *Neurospora crassa*. *Fungal Genetics and Biology, 44*(6), 492-503.

Araujo-Bazán, L., Peñalva, M. A., & Espeso, E. A. (2008). Preferential localization of the endocytic internalization machinery to hyphal tips underlies polarization of the actin cytoskeleton in *Aspergillus nidulans*. *Molecular Microbiology, 67*(4), 891-905.

Aravanis, A., Pyle, J., & Tsien, R. (2003). Single synaptic vesicles fusing transiently and successively without loss of identity. *Nature, 423*(6940), 643-647.

Athanasopoulos, A., Boleti, H., Scazzocchio, C., & Sophianopoulou, V. (2013). Eisosome distribution and localization in the meiotic progeny of *Aspergillus nidulans*. *Fungal Genetics and Biology, 53*, 84-96.

Ayscough, K. R. (2000). Endocytosis and the development of cell polarity in yeast require a dynamic F-actin cytoskeleton. *Current Biology, 10*(24), 1587-1590.

Backer, J. M., & Dawidowicz, E. A. (1987). Reconstitution of a phospholipid flippase from rat liver microsomes. *Nature, 327*(6120), 341-343.

Baldridge, R. D., & Graham, T. R. (2012). Identification of residues defining phospholipid flippase substrate specificity of type IV P-type ATPases. *Proceedings of the National Academy of Sciences of the United States of America, 109*(6), E290-E298.

Balhadère, P. V., & Talbot, N. J. (2001). PDE1 encodes a P-type ATPase involved in appressorium-mediated plant infection by the rice blast fungus *Magnaporthe grisea*. *The Plant Cell Online, 13*(9), 1987-2004.

Banfield, D. K., Lewis, M. J., & Pelham, H. R. (1995). A SNARE-like protein required for traffic through the Golgi complex. *Nature, 375*(6534), 806-809.

Bartnicki-Garcia, S., Hergert, F., & Gierz, G. (1989). Computer simulation of fungal morphogenesis and the mathematical basis for hyphal (tip) growth. *Protoplasma, 153*(1-2), 46-57.

Becht, P., König, J., & Feldbrügge, M. (2006). The RNA-binding protein Rrm4 is essential for polarity in *Ustilago maydis* and shuttles along microtubules. *Journal of Cell Science, 119*(23), 4964-4973.

Bell, A. A., & Wheeler, M. H. (1986). Biosynthesis and functions of fungal melanins. *Annual review of phytopathology, 24*(1), 411-451.

Bendezu, F. O., Vincenzetti, V., & Martin, S. G. (2012). Fission yeast Sec3 and Exo70 are transported on actin cables and localize the exocyst complex to cell poles. *PloS One, 7*(6), e40248.

Berepiki, A., Lichius, A., Shoji, J.-Y., Tilsner, J., & Read, N. D. (2010). F-actin dynamics in *Neurospora crassa*. *Eukaryotic Cell, 9*(4), 547-557.

Boettner, D. R., D'Agostino, J. L., Torres, O. T., Daugherty-Clarke, K., Uygur, A., et al. (2009). The F-BAR protein Syp1 negatively regulates WASp-Arp2/3 complex activity during endocytic patch formation. *Current Biology, 19*(23), 1979-1987.

Bonifacino, J. S., & Glick, B. S. (2004). The mechanisms of vesicle budding and fusion. *Cell, 116*(2), 153-166.

Boucrot, E., Saffarian, S., Massol, R., Kirchhausen, T., & Ehrlich, M. (2006). Role of lipids and actin in the formation of clathrin-coated pits. *Experimental Cell Research, 312*(20), 4036-4048.

Bourett, T., & Howard, R. (1991). Ultrastructural immunolocalization of actin in a fungus. *Protoplasma, 163*(2-3), 199-202.

Bourett, T., James, S., & Howard, R. (2007). The endomembrane system of the fungal cell *Biology of the Fungal Cell* (pp. 1-47): Springer.

Bove, J., Vaillancourt, B., Kroeger, J., Hepler, P. K., Wiseman, P. W., et al. (2008). Magnitude and direction of vesicle dynamics in growing pollen tubes using spatiotemporal image correlation spectroscopy and fluorescence recovery after photobleaching. *Plant Physiology, 147*(4), 1646-1658.

Bowman, B. J., Draskovic, M., Freitag, M., & Bowman, E. J. (2009). Structure and distribution of organelles and cellular location of calcium transporters in *Neurospora crassa*. *Eukaryotic Cell, 8*(12), 1845-1855.

Brach, T., Godlee, C., Moeller-Hansen, I., Boeke, D., & Kaksonen, M. (2014). The initiation of clathrin-mediated endocytosis Is mechanistically highly flexible. *Current Biology, 24*(5), 548-554.

Bracker, C. E. (1967). Ultrastructure of Fungi. *Annual review of phytopathology, 5*(1), 343-372.

Brand, A. C., Morrison, E., Milne, S., Gonia, S., Gale, C. A., et al. (2014). Cdc42 GTPase dynamics control directional growth responses. *Proceedings of the National Academy of Sciences of the United States of America, 111*(2), 811-816.

Brodsky, F. M. (1988). Living with clathrin: its role in intracellular membrane traffic. *Science, 242*(4884), 1396-1402.

Brodsky, F. M., Chen, C.-Y., Knuehl, C., Towler, M. C., & Wakeham, D. E. (2001). Biological basket weaving: formation and function of clathrin-coated vesicles. *Annual review of cell and developmental biology, 17*(1), 517-568.

Brodsky, F. M., Hill, B. L., Acton, S. L., Näthke, I., Wong, D. H., et al. (1991). Clathrin light chains: arrays of protein motifs that regulate coated-vesicle dynamics. *Trends In Biochemical Sciences, 16*(6), 208-213.

Brunswick, H. (1924). Untersuchungen fiber die geschlechts-und kernverhaltnisse bie den hymeno-myceten gattung *Coprinus*. *Bot. Abh. K. Geobel, 5*.

Bryde, S., Hennrich, H., Verhulst, P. M., Devaux, P. F., Lenoir, G., et al. (2010). CDC50 proteins are critical components of the human class-1 P4-ATPase transport machinery. *Journal of Biological Chemistry, 285*(52), 40562-40572.

Bühler, N., Hagiwara, D., & Takeshita, N. (2015). Functional Analysis of Sterol Transporter Orthologues in the Filamentous Fungus *Aspergillus nidulans*. *Eukaryotic Cell, 14*(9), 908-921.

Caballero-Lima, D., Kaneva, I. N., Watton, S. P., Sudbery, P. E., & Craven, C. J. (2013). The spatial distribution of the exocyst and actin cortical patches is sufficient to organize hyphal tip growth. *Eukaryotic Cell, 12*(7), 998-1008.

Caballero-Lima, D., & Sudbery, P. E. (2014). In *Candida albicans*, phosphorylation of Exo84 by Cdk1-Hgc1 is necessary for efficient hyphal extension. *Molecular Biology of the Cell, 25*(7), 1097-1110.

Cao, H., Krueger, E. W., & McNiven, M. A. (2011). Hepatocytes internalize trophic receptors at large endocytic “Hot Spots”. *Hepatology, 54*(5), 1819-1829.

Carr, C. M., Grote, E., Munson, M., Hughson, F. M., & Novick, P. J. (1999). Sec1p binds to SNARE complexes and concentrates at sites of secretion. *The Journal of Cell Biology, 146*(2), 333-344.

Carroll, S. Y., Stimpson, H. E., Weinberg, J., Toret, C. P., Sun, Y., et al. (2012). Analysis of yeast endocytic site formation and maturation through a regulatory transition point. *Molecular Biology of the Cell, 23*(4), 657-668.

Casadevall, A., Nosanchuk, J. D., Williamson, P., & Rodrigues, M. L. (2009). Vesicular transport across the fungal cell wall. *Trends in Microbiology, 17*(4), 158-162.

Castillo-Lluva, S., Alvarez-Tabarés, I., Weber, I., Steinberg, G., & Pérez-Martín, J. (2007). Sustained cell polarity and virulence in the phytopathogenic fungus *Ustilago maydis* depends on an essential cyclin-dependent kinase from the Cdk5/Pho85 family. *Journal of Cell Science, 120*(9), 1584-1595.

Cerqueira, G. C., Arnaud, M. B., Inglis, D. O., Skrzypek, M. S., Binkley, G., et al. (2013). The *Aspergillus* Genome Database: multispecies curation and incorporation of RNA-Seq data to improve structural gene annotations. *Nucleic Acids Research*, gkt1029.

Chamberlain, L. H., Burgoyne, R. D., & Gould, G. W. (2001). SNARE proteins are highly enriched in lipid rafts in PC12 cells: implications for the spatial control of exocytosis. *Proceedings of the National Academy of Sciences of the United States of America, 98*(10), 5619-5624.

Chanda, A., Roze, L. V., Kang, S., Artymovich, K. A., Hicks, G. R., et al. (2009a). A key role for vesicles in fungal secondary metabolism. *Proceedings of the National Academy of Sciences, 106*(46), 19533-19538.

Chanda, A., Roze, L. V., Kang, S., Artymovich, K. A., Hicks, G. R., et al. (2009b). A key role for vesicles in fungal secondary metabolism. *Proceedings of the National Academy of Sciences of the United States of America, 106*(46), 19533-19538.

Chanda, A., Roze, L. V., & Linz, J. E. (2010). Aflatoxin export in *Aspergillus parasiticus*: a possible role for exocytosis. *Eukaryotic Cell*.

Chattopadhyay, P., Banerjee, S. K., Sen, K., & Chakrabarti, P. (1985). Lipid profiles of *Aspergillus niger* and its unsaturated fatty acid auxotroph, UFA2. *Canadian Journal of Microbiology, 31*(4), 352-355.

Chen, C. Y., Reese, M. L., Hwang, P. K., Ota, N., Agard, D., et al. (2002). Clathrin light and heavy chain interface: α-helix binding superhelix loops via critical tryptophans. *The EMBO Journal, 21*(22), 6072-6082.

Chen, Y. L., Montedonico, A. E., Kauffman, S., Dunlap, J. R., Menn, F. M., et al. (2010). Phosphatidylserine synthase and phosphatidylserine decarboxylase are essential for cell wall integrity and virulence in *Candida albicans*. *Molecular Microbiology, 75*(5), 1112-1132.

Cocucci, E., Aguet, F., Boulant, S., & Kirchhausen, T. (2012). The first five seconds in the life of a clathrin-coated pit. *Cell, 150*(3), 495-507.

Cole, L., Davies, D., Hyde, G., & Ashford, A. (2000). ER-Tracker dye and BODIPY-brefeldin A differentiate the endoplasmic reticulum and Golgi bodies from the tubular-vacuole system in living hyphae of *Pisolithus tinctorius*. *Journal of Microscopy, 197*(3), 239-248.

Conibear, E. (2010). Converging views of endocytosis in yeast and mammals. *Current Opinion in Cell Biology, 22*(4), 513-518.

Conibear, E., & Stevens, T. H. (2000). Vps52p, Vps53p, and Vps54p form a novel multisubunit complex required for protein sorting at the yeast late Golgi. *Molecular Biology of the Cell, 11*(1), 305-323.

Costaguta, G., Stefan, C., Bensen, E., Emr, S., & Payne, G. (2001). Yeast Gga coat proteins function with clathrin in Golgi to endosome transport. *Molecular Biology of the Cell, 12*(6), 1885-1896.

Cove, D. (1966). The induction and repression of nitrate reductase in the fungus *Aspergillus nidulans*. *Biochimica et Biophysica Acta, 113*(1), 51-56.

Curwin, A. J., von Blume, J., & Malhotra, V. (2012). Cofilin-mediated sorting and export of specific cargo from the Golgi apparatus in yeast. *Molecular Biology of the Cell, 23*(12), 2327-2338.

Daboussi, L., Costaguta, G., & Payne, G. S. (2012). Phosphoinositide-mediated clathrin adaptor progression at the trans-Golgi network. *Nature cell biology, 14*(3), 239-248.

Dargent, R., Touze, J.-M., Rami, J., & Montant, C. (1982). Cytochemical characterization of Golgi apparatus in some filamentous fungi. *Experimental Mycology, 6*(2), 101-114.

Das, A., Slaughter, B. D., Unruh, J. R., Bradford, W. D., Alexander, R., et al. (2012). Flippase-mediated phospholipid asymmetry promotes fast Cdc42 recycling in dynamic maintenance of cell polarity. *Nature cell biology, 14*(3), 304-310.

Delgado-Álvarez, D. L., Bartnicki-García, S., Seiler, S., & Mouriño-Pérez, R. R. (2014). Septum development in Neurospora crassa: the septal actomyosin tangle. *PLoS One, 9*(5), e96744.

Delgado-Álvarez, D. L., Callejas-Negrete, O. A., Gómez, N., Freitag, M., Roberson, R. W., et al. (2010). Visualization of F-actin localization and dynamics with live cell markers in *Neurospora crassa*. *Fungal Genetics and Biology, 47*(7), 573-586.

Dijksterhuis, J., & Molenaar, D. (2013). Vesicle trafficking via the Spitzenkörper during hyphal tip growth in *Rhizoctonia solani*. *Antonie Van Leeuwenhoek, 103*(4), 921-931.

Douglas, L. M., Martin, S. W., & Konopka, J. B. (2009). BAR domain proteins Rvs161 and Rvs167 contribute to *Candida albicans* endocytosis, morphogenesis, and virulence. *Infection and Immunity, 77*(9), 4150-4160.

Draper, R. K., Goda, Y., Brodsky, F. M., & Pfeffer, S. R. (1990). Antibodies to clathrin inhibit endocytosis but not recycling to the trans Golgi network in vitro. *Science, 248*(4962), 1539-1541.

Dutta, D., & Donaldson, J. G. (2012). Search for inhibitors of endocytosis: Intended specificity and unintended consequences. *Cellular logistics, 2*(4), 203-208.

Ebbole, D. J. (2007). *Magnaporthe* as a model for understanding host-pathogen interactions. *Annual review of phytopathology, 45*, 437-456.

Echauri-Espinosa, R. O., Callejas-Negrete, O. A., Roberson, R. W., Bartnicki-García, S., & Mouriño-Pérez, R. R. (2012). Coronin is a component of the endocytic collar of hyphae of *Neurospora crassa* and is necessary for normal growth and morphogenesis. *PLoS One, 7*(5), e38237.

Epp, E., Nazarova, E., Regan, H., Douglas, L. M., Konopka, J. B., et al. (2013). Clathrin-and Arp2/3-independent endocytosis in the fungal pathogen *Candida albicans*. *MBio, 4*(5), e00476-00413.

Epp, E., Walther, A., Lépine, G., Leon, Z., Mullick, A., et al. (2010). Forward genetics in *Candida albicans* that reveals the Arp2/3 complex is required for hyphal formation, but not endocytosis. *Molecular Microbiology, 75*(5), 1182-1198.

Fairn, G. D., & Grinstein, S. (2010). Phosphatidylserine polarization is required for proper Cdc42 localization and for development of cell polarity. *Nature cell biology, 13*, 1424-1430.

Fairn, G. D., Hermansson, M., Somerharju, P., & Grinstein, S. (2011). Phosphatidylserine is polarized and required for proper Cdc42 localization and for development of cell polarity. *Nature cell biology, 13*(12), 1424-1430.

Feldbrügge, M., Kämper, J., Steinberg, G., & Kahmann, R. (2004). Regulation of mating and pathogenic development in *Ustilago maydis*. *Current Opinion in Microbiology, 7*(6), 666-672.

Ferro-Novick, S., & Jahn, R. (1994). Vesicle fusion from yeast to man. *Nature, 370*(6486), 191-193.

Finger, F. P., & Novick, P. (1998). Spatial regulation of exocytosis: lessons from yeast. *The Journal of Cell Biology, 142*(3), 609-612.

Fischer-Parton, S., Parton, R., Hickey, P., Dijksterhuis, J., Atkinson, H., et al. (2000). Confocal microscopy of FM4-64 as a tool for analysing endocytosis and vesicle trafficking in living fungal hyphae. *Journal of Microscopy, 198*(3), 246-259.

Fu, C., Iyer, P., Herkal, A., Abdullah, J., Stout, A., et al. (2011). Identification and characterization of genes required for cell-to-cell fusion in *Neurospora crassa*. *Eukaryotic Cell, 10*(8), 1100-1109.

Fuchs, U., Hause, G., Schuchardt, I., & Steinberg, G. (2006). Endocytosis is essential for pathogenic development in the corn smut fungus *Ustilago maydis*. *The Plant Cell, 18*(8), 2066-2081.

Gall, W. E., Geething, N. C., Hua, Z., Ingram, M. F., Liu, K., et al. (2002). Drs2p-dependent formation of exocytic clathrin-coated vesicles in vivo. *Current Biology, 12*(18), 1623-1627.

Ge, W., Chew, T. G., Wachtler, V., Naqvi, S. N., & Balasubramanian, M. K. (2005). The novel fission yeast protein Pal1p interacts with Hip1-related Sla2p/End4p and is involved in cellular morphogenesis. *Molecular Biology of the Cell, 16*(9), 4124-4138.

Geitmann, A., & Dumais, J. (2009). Not-so-tip-growth. *Plant Signaling & Behavior, 4*(2), 136-138.

Geli, M. I., & Riezman, H. (1996). Role of type I myosins in receptor-mediated endocytosis in yeast. *Science, 272*(5261), 533-535.

Gierz, G., & Bartnicki-Garcia, S. (2001). A three-dimensional model of fungal morphogenesis based on the vesicle supply center concept. *Journal of Theoretical Biology, 208*(2), 151-164.

Gilbert, M. J., Thornton, C. R., Wakley, G. E., & Talbot, N. J. (2006). A P-type ATPase required for rice blast disease and induction of host resistance. *Nature, 440*(7083), 535-539.

Giraldo, M. C., Dagdas, Y. F., Gupta, Y. K., Mentlak, T. A., Yi, M., et al. (2013). Two distinct secretion systems facilitate tissue invasion by the rice blast fungus *Magnaporthe oryzae*. *Nature Communications, 4*, doi:10.1038/ncomms2996.

Girbardt, M. (1957). Der Spitzenkörper von *Polystictus versicolor* (L.). *Planta, 50*(1), 47-59.

Goldman, G. H., & Osmani, S. A. (2007). *The Aspergilli: genomics, medical aspects, biotechnology, and research methods*: CRC press.

Götte, M., & Fischer von Mollard, G. (1998). A new beat for the SNARE drum. *Trends in Cell Biology, 8*(6), 215-218.

Granseth, B., Odermatt, B., Royle, S. J., & Lagnado, L. (2006). Clathrin-mediated endocytosis is the dominant mechanism of vesicle retrieval at hippocampal synapses. *Neuron, 51*(6), 773-786.

Grant, B. D., & Donaldson, J. G. (2009). Pathways and mechanisms of endocytic recycling. *Nature Reviews: Molecular Cell Biology, 10*(9), 597-608.

Griffiths, G., & Simons, K. (1986). The trans Golgi network: sorting at the exit site of the Golgi complex. *Science, 234*(4775), 438-443.

Grove, S. N., & Bracker, C. E. (1970). Protoplasmic organization of hyphal tips among fungi: Vesicles and Spitzenkörper. *Journal of bacteriology, 104*(2), 989.

Guest, G. M., Lin, X., & Momany, M. (2004). *Aspergillus nidulans* RhoA is involved in polar growth, branching, and cell wall synthesis. *Fungal Genetics and Biology, 41*(1), 13-22.

Guo, W., Grant, A., & Novick, P. (1999). Exo84p is an exocyst protein essential for secretion. *Journal of Biological Chemistry, 274*(33), 23558-23564.

Guo, W., Roth, D., Walch-Solimena, C., & Novick, P. (1999). The exocyst is an effector for Sec4p, targeting secretory vesicles to sites of exocytosis. *The EMBO journal, 18*(4), 1071-1080.

Guo, W., Sacher, M., Barrowman, J., Ferro-Novick, S., & Novick, P. (2000). Protein complexes in transport vesicle targeting. *Trends in Cell Biology, 10*(6), 251-255.

Guo, W., Tamanoi, F., & Novick, P. (2001). Spatial regulation of the exocyst complex by Rho1 GTPase. *Nature Cell Biology, 3*(4), 353-360.

Gupta, Y. K., Dagdas, Y. F., Martinez-Rocha, A.-L., Kershaw, M. J., Littlejohn, G. R., et al. (2015). Septin-dependent assembly of the exocyst is essential for plant infection by *Magnaporthe oryzae*. *The Plant Cell, 27*(11), 3277-3289.

Haarer, B., Corbett, A., Kweon, Y., Petzold, A., Silver, P., et al. (1996). SEC3 mutations are synthetically lethal with profilin mutations and cause defects in diploid-specific bud-site selection. *Genetics, 144*(2), 495.

Hanamatsu, H., Fujimura-Kamada, K., Yamamoto, T., Furuta, N., & Tanaka, K. (2014). Interaction of the phospholipid flippase Drs2p with the F-box protein Rcy1p plays an important role in early endosome to trans-Golgi network vesicle transport in yeast. *Journal of biochemistry, 155*(1), 51-62.

Harris, S. D. (2013). Golgi organization and the apical extension of fungal hyphae: an essential relationship. *Molecular Microbiology, 89*(2), 212-215.

Harris, S. D., Hamer, L., Sharpless, K. E., & Hamer, J. E. (1997). The *Aspergillus nidulans sepA* gene encodes an FH1/2 protein involved in cytokinesis and the maintenance of cellular polarity. *The EMBO Journal, 16*(12), 3474-3483.

Harsay, E., & Bretscher, A. (1995). Parallel secretory pathways to the cell surface in yeast. *The Journal of Cell Biology, 131*(2), 297-310.

Hayakawa, Y., Ishikawa, E., Shoji, J. y., Nakano, H., & Kitamoto, K. (2011). Septum-directed secretion in the filamentous fungus *Aspergillus oryzae*. *Molecular microbiology, 81*(1), 40-55.

He, B., & Guo, W. (2009). The exocyst complex in polarized exocytosis. *Current Opinion in Cell Biology, 21*(4), 537-542.

He, B., Xi, F., Zhang, X., Zhang, J., & Guo, W. (2007). Exo70 interacts with phospholipids and mediates the targeting of the exocyst to the plasma membrane. *The EMBO journal, 26*(18), 4053-4065.

Helling, D., Possart, A., Cottier, S., Klahre, U., & Kost, B. (2006). Pollen tube tip growth depends on plasma membrane polarization mediated by tobacco PLC3 activity and endocytic membrane recycling. *The Plant Cell, 18*(12), 3519-3534.

Herrero-Garcia, E., Garzia, A., Cordobés, S., Espeso, E. A., & Ugalde, U. (2011). 8-Carbon oxylipins inhibit germination and growth, and stimulate aerial conidiation in *Aspergillus nidulans*. *Fungal Biology, 115*(4), 393-400.

Herrero, S., Takeshita, N., & Fischer, R. (2014). F-Box Protein RcyA Controls Turnover of the Kinesin-7 Motor KipA in *Aspergillus nidulans*. *Eukaryotic Cell, 13*(8), 1085-1094.

Hervás-Aguilar, A., & Peñalva, M. A. (2010). Endocytic machinery protein SlaB is dispensable for polarity establishment but necessary for polarity maintenance in hyphal tip cells of *Aspergillus nidulans*. *Eukaryotic Cell, 9*(10), 1504-1518.

Higuchi, Y., Shoji, J.-y., Arioka, M., & Kitamoto, K. (2009). Endocytosis is crucial for cell polarity and apical membrane recycling in the filamentous fungus *Aspergillus oryzae*. *Eukaryotic cell, 8*(1), 37-46.

Hinners, I., & Tooze, S. A. (2003). Changing directions: clathrin-mediated transport between the Golgi and endosomes. *Journal of Cell Science, 116*(5), 763-771.

Hoch, H., & Howard, R. (1980). Ultrastructure of freeze-substituted hyphae of the basidiomycete *Laetisaria arvalis*. *Protoplasma, 103*(3), 281-297.

Hoch, H. C., Staples, R. C., Whitehead, B., Comeau, J., & Wolf, E. D. (1987). Signaling for growth orientation and cell differentiation by surface topography in *Uromyces*. *Science, 235*(4796), 1659-1662.

Hoffmann, J., & Mendgen, K. (1998). Endocytosis and Membrane Turnover in the Germ Tube of *Uromyces fabae*. *Fungal Genetics and Biology, 24*(1), 77-85.

Hohmann-Marriott, M. F., Uchida, M., Van De Meene, A. M., Garret, M., Hjelm, B. E., et al. (2006). Application of electron tomography to fungal ultrastructure studies. *New Phytologist, 172*(2), 208-220.

Horio, T., & Oakley, B. R. (2005). The role of microtubules in rapid hyphal tip growth of *Aspergillus nidulans*. *Molecular Biology of the Cell, 16*(2), 918-926.

Howard, J. P., Hutton, J. L., Olson, J. M., & Payne, G. S. (2002). Sla1p serves as the targeting signal recognition factor for NPFX (1, 2) D-mediated endocytosis. *The Journal of Cell Biology, 157*(2), 315-326.

Howard, R. J. (1981). Ultrastructural analysis of hyphal tip cell growth in fungi: Spitzenkörper, cytoskeleton and endomembranes after freeze-substitution. *Journal of Cell Science, 48*(1), 89-103.

Howell, A. S., Jin, M., Wu, C.-F., Zyla, T. R., Elston, T. C., et al. (2012). Negative feedback enhances robustness in the yeast polarity establishment circuit. *Cell, 149*(2), 322-333.

Hua, Z., Fatheddin, P., & Graham, T. R. (2002). An essential subfamily of Drs2p-related P-type ATPases is required for protein trafficking between Golgi complex and endosomal/vacuolar system. *Molecular Biology of the Cell, 13*(9), 3162-3177.

Jahn, R., & Südhof, T. C. (1999). Membrane fusion and exocytosis. *Annual Review of Biochemistry, 68*(1), 863-911.

Jones, L. A., & Sudbery, P. E. (2010). Spitzenkörper, exocyst, and polarisome components in *Candida albicans* hyphae show different patterns of localization and have distinct dynamic properties. *Eukaryotic Cell, 9*(10), 1455-1465.

Jorde, S., Walther, A., & Wendland, J. (2011). The *Ashbya gossypii* fimbrin SAC6 is required for fast polarized hyphal tip growth and endocytosis. *Microbiological research, 166*(3), 137-145.

Jose, M., Tollis, S., Nair, D., Sibarita, J.-B., & McCusker, D. (2013). Robust polarity establishment occurs via an endocytosis-based cortical corralling mechanism. *The Journal of Cell Biology, 200*(4), 407-418.

Kaksonen, M., Toret, C. P., & Drubin, D. G. (2005). A modular design for the clathrin- and actin-mediated endocytosis machinery. *Cell, 123*(2), 305-320.

Kaminskyj, S. (2001). Fundamentals of growth, storage, genetics and microscopy of *Aspergillus nidulans*. *Fungal Genetics Newsletter*, 25-31.

Ketelaar, T., Galway, M., Mulder, B., & Emons, A. (2008). Rates of exocytosis and endocytosis in *Arabidopsis* root hairs and pollen tubes. *Journal of Microscopy, 231*(2), 265-273.

Khatri, M., & Rajam, M. (2007). Targeting polyamines of *Aspergillus nidulans* by siRNA specific to fungal ornithine decarboxylase gene. *Medical Mycology, 45*(3), 211-220.

Kim, D.-U., Hayles, J., Kim, D., Wood, V., Park, H.-O., et al. (2010). Analysis of a genome-wide set of gene deletions in the fission yeast *Schizosaccharomyces pombe*. *Nature biotechnology, 28*(6), 617-623.

Kim, J. J., Lipatova, Z., Majumdar, U., & Segev, N. (2016). Regulation of golgi cisternal progression by Ypt/Rab GTPases. *Developmental cell, 36*(4), 440-452.

Kim, K., Galletta, B. J., Schmidt, K. O., Chang, F. S., Blumer, K. J., et al. (2006). Actin-based motility during endocytosis in budding yeast. *Molecular Biology of the Cell, 17*(3), 1354-1363.

Kirchhausen, T. (2000). Clathrin. *Annual Review of Biochemistry, 69*(1), 699-727.

Kirchhausen, T., Owen, D., & Harrison, S. C. (2014). Molecular structure, function, and dynamics of clathrin-mediated membrane traffic. *Cold Spring Harbor perspectives in biology, 6*(5), a016725.

Kishimoto, T., Sun, Y., Buser, C., Liu, J., Michelot, A., et al. (2011). Determinants of endocytic membrane geometry, stability, and scission. *Proceedings of the National Academy of Sciences of the United States of America, 108*(44), E979-E988.

Kistler, H., & Broz, K. (2015). Cellular compartmentalization of secondary metabolism. *Frontiers in Microbiology, 6*, 68.

Köhli, M., Galati, V., Boudier, K., Roberson, R. W., & Philippsen, P. (2008). Growth-speed-correlated localization of exocyst and polarisome components in growth zones of *Ashbya gossypii* hyphal tips. *Journal of Cell Science, 121*(23), 3878-3889.

Kübler, E., & Riezman, H. (1993). Actin and fimbrin are required for the internalization step of endocytosis in yeast. *The EMBO Journal, 12*(7), 2855.

Kukulski, W., Andrea Picco, Tanja Specht, John AG Briggs, and Marko Kaksonen. (2016). Clathrin modulates vesicle scission, but not invagination shape, in yeast endocytosis. *eLife*. doi: eLife 2016;10.7554/eLife.16036

Kukulski, W., Schorb, M., Kaksonen, M., & Briggs, J. A. (2012). Plasma membrane reshaping during endocytosis is revealed by time-resolved electron tomography. *Cell, 150*(3), 508-520.

Kukulski, W., Schorb, M., Welsch, S., Picco, A., Kaksonen, M., et al. (2011). Correlated fluorescence and 3D electron microscopy with high sensitivity and spatial precision. *The Journal of Cell Biology, 192*(1), 111-119.

Kurtz, M. B., & Champe, S. P. (1982). Purification and characterization of the conidial laccase of *Aspergillus nidulans*. *Journal of bacteriology, 151*(3), 1338-1345.

Kwon, M. J., Arentshorst, M., Fiedler, M., de Groen, F. L., Punt, P. J., et al. (2014). Molecular genetic analysis of vesicular transport in *Aspergillus niger* reveals partial conservation of the molecular mechanism of exocytosis in fungi. *Microbiology, 160*(Pt 2), 316-329.

Lamarre, C., Sokol, S., Debeaupuis, J.-P., Henry, C., Lacroix, C., et al. (2008). Transcriptomic analysis of the exit from dormancy of *Aspergillus fumigatus* conidia. *BMC genomics, 9*(1), 417.

Lara-Rojas, F., Bartnicki-García, S., & Mouriño-Pérez, R. R. (2016). Localization and role of MYO-1, an endocytic protein in hyphae of *Neurospora crassa*. *Fungal Genetics and Biology, 88*, 24-34.

Lauvrak, S. U., Torgersen, M. L., & Sandvig, K. (2004). Efficient endosome-to-Golgi transport of Shiga toxin is dependent on dynamin and clathrin. *Journal of Cell Science, 117*(11), 2321-2331.

Le Borgne, R., & Hoflack, B. (1997). Mannose 6-phosphate receptors regulate the formation of clathrin-coated vesicles in the TGN. *The Journal of Cell Biology, 137*(2), 335-345.

Lee, S. C., Schmidtke, S. N., Dangott, L. J., & Shaw, B. D. (2008). *Aspergillus nidulans* ArfB plays a role in endocytosis and polarized growth. *Eukaryotic Cell, 7*(8), 1278-1288.

Lee, S. C., & Shaw, B. D. (2008). Localization and function of ADP ribosylation factor A in *Aspergillus nidulans*. *FEMS Microbiology Letters, 283*(2), 216-222.

Lemmon, S. K., & Jones, E. W. (1987). Clathrin requirement for normal growth of yeast. *Science, 238*(4826), 504-509.

Letoublon, R., Mayet, B., Frot-Coutaz, J., Nicolau, C., & Got, R. (1982). Subcellular distribution of phospholipids and of polyprenyl phosphate in *Aspergillus niger van Tieghem*. *Biochimica et Biophysica, 711*(3), 509-514.

Levine, T. P., & Munro, S. (2002). Targeting of Golgi-specific pleckstrin homology domains involves both PtdIns 4-kinase-dependent and-independent components. *Current Biology, 12*(9), 695-704.

Li, C.-R., Lee, R. T.-H., Wang, Y.-M., Zheng, X.-D., & Wang, Y. (2007). Candida albicans hyphal morphogenesis occurs in Sec3p-independent and Sec3p-dependent phases separated by septin ring formation. *Journal of cell science, 120*(11), 1898-1907.

Lichius, A., Yáñez-Gutiérrez, M. E., Read, N. D., & Castro-Longoria, E. (2012). Comparative live-cell imaging analyses of SPA-2, BUD-6 and BNI-1 in

Neurospora crassa reveal novel features of the filamentous fungal polarisome. *PLoS One, 7*(1), e30372.

Liu, H.-L., De Souza, C. P., Osmani, A. H., & Osmani, S. A. (2009). The three fungal transmembrane nuclear pore complex proteins of *Aspergillus nidulans* are dispensable in the presence of an intact An-Nup84-120 complex. *Molecular Biology of the Cell, 20*(2), 616-630.

Liu, K., Hua, Z., Nepute, J. A., & Graham, T. R. (2007). Yeast P4-ATPases Drs2p and Dnf1p are essential cargos of the NPFXD/Sla1p endocytic pathway. *Molecular Biology of the Cell, 18*(2), 487-500.

Liu, K., Surendhran, K., Nothwehr, S. F., & Graham, T. R. (2008). P4-ATPase requirement for AP-1/clathrin function in protein transport from the trans-Golgi network and early endosomes. *Molecular Biology of the Cell, 19*(8), 3526-3535.

Löpez-Franco, R., & Bracker, C. E. (1996). Diversity and dynamics of the Spitzenkörper in growing hyphal tips of higher fungi. *Protoplasma, 195*(1-4), 90-111.

Lucena-Agell, D., Galindo, A., Arst, H. N., & Peñalva, M. A. (2015). *Aspergillus nidulans* ambient pH signaling does not require endocytosis. *Eukaryotic Cell, 14*(6), 545-553.

Luo, J., Matsuo, Y., Gulis, G., Hinz, H., Patton-Vogt, J., et al. (2009). Phosphatidylethanolamine is required for normal cell morphology and cytokinesis in the fission yeast *Schizosaccharomyces pombe*. *Eukaryotic Cell, 8*(5), 790-799.

Mahadev, R. K., Di Pietro, S. M., Olson, J. M., Piao, H. L., Payne, G. S., et al. (2007). Structure of Sla1p homology domain 1 and interaction with the NPFxD endocytic internalization motif. *The EMBO Journal, 26*(7), 1963-1971.

Mähs, A., Ischebeck, T., Heilig, Y., Stenzel, I., Hempel, F., et al. (2012). The essential phosphoinositide kinase MSS-4 Is required for polar hyphal morphogenesis, localizing to sites of growth and cell fusion in *Neurospora crassa*. *PLoS One, 7*(12), e51454.

Markina-Iñarrairaegui, A., Pantazopoulou, A., Espeso, E. A., & Peñalva, M. A. (2013). The *Aspergillus nidulans* peripheral ER: disorganization by ER stress and persistence during mitosis. *PloS One, 8*(6), e67154.

Matsuo, K., Higuchi, Y., Kikuma, T., Arioka, M., & Kitamoto, K. (2013). Functional analysis of Abp1p-interacting proteins involved in endocytosis of the MCC component in *Aspergillus oryzae*. *Fungal Genetics and Biology, 56*, 125-134.

Mayor, S., Parton, R. G., & Donaldson, J. G. (2014). Clathrin-independent pathways of endocytosis. *Cold Spring Harbor perspectives in biology, 6*(6), a016758.

McDonald, T., Brown, D., Keller, N. P., & Hammond, T. M. (2005). RNA silencing of mycotoxin production in *Aspergillus* and *Fusarium* species. *Molecular Plant-Microbe Interactions, 18*(6), 539-545.

McGoldrick, C. A., Gruver, C., & May, G. S. (1995). *myoA* of *Aspergillus nidulans* encodes an essential myosin I required for secretion and polarized growth. *The Journal of Cell Biology, 128*(4), 577-587.

McMahon, H. T., & Mills, I. G. (2004). COP and clathrin-coated vesicle budding: different pathways, common approaches. *Current Opinion in Cell Biology, 16*(4), 379-391.

Meinecke, M., Boucrot, E., Camdere, G., Hon, W.-C., Mittal, R., et al. (2013). Cooperative recruitment of dynamin and BIN/amphiphysin/Rvs (BAR) domain-containing proteins leads to GTP-dependent membrane scission. *Journal of Biological Chemistry, 288*(9), 6651-6661.

Mioka, T., Fujimura-Kamada, K., & Tanaka, K. (2014). Asymmetric distribution of phosphatidylserine is generated in the absence of phospholipid flippases in *Saccharomyces cerevisiae*. *MicrobiologyOpen, 3*(5), 803-821.

Moebius, N., Üzüm, Z., Dijksterhuis, J., Lackner, G., & Hertweck, C. (2014). Active invasion of bacteria into living fungal cells. *eLife, 3*, e03007.

Mooney, J. L., & Yager, L. N. (1990). Light is required for conidiation in *Aspergillus nidulans*. *Genes and Development, 4*(9), 1473-1482.

Mouriño-Pérez, R. R. (2013). Septum development in filamentous ascomycetes. *Fungal Biology Reviews, 27*(1), 1-9.

Mueller, O., Kahmann, R., Aguilar, G., Trejo-Aguilar, B., Wu, A., et al. (2008). The secretome of the maize pathogen *Ustilago maydis*. *Fungal Genetics and Biology, 45*, S63-S70.

Mulholland, J., Konopka, J., Singer-Kruger, B., Zerial, M., & Botstein, D. (1999). Visualization of receptor-mediated endocytosis in yeast. *Molecular Biology of the Cell, 10*(3), 799-817.

Mulholland, J., Preuss, D., Moon, A., Wong, A., Drubin, D., et al. (1994). Ultrastructure of the yeast actin cytoskeleton and its association with the plasma membrane. *The Journal of Cell Biology, 125*(2), 381-391.

Muñoz, A., Marcos, J. F., & Read, N. D. (2012). Concentration-dependent mechanisms of cell penetration and killing by the de novo designed antifungal hexapeptide PAF26. *Molecular Microbiology, 85*(1), 89-106.

Nakayashiki, H., Hanada, S., Quoc, N. B., Kadotani, N., Tosa, Y., et al. (2005). RNA silencing as a tool for exploring gene function in ascomycete fungi. *Fungal Genetics and Biology, 42*(4), 275-283.

Nayak, T., Szewczyk, E., Oakley, C. E., Osmani, A., Ukil, L., et al. (2006). A versatile and efficient gene-targeting system for *Aspergillus nidulans*. *Genetics, 172*(3), 1557-1566.

Newpher, T. M., Smith, R. P., Lemmon, V., & Lemmon, S. K. (2005). In vivo dynamics of clathrin and its adaptor-dependent recruitment to the actin-based endocytic machinery in yeast. *Developmental cell, 9*(1), 87-98.

Novick, P., Ferro, S., & Schekman, R. (1981). Order of events in the yeast secretory pathway. *Cell, 25*(2), 461-469.

Nunes, C. C., & Dean, R. A. (2012). Host-induced gene silencing: a tool for understanding fungal host interaction and for developing novel disease control strategies. *Molecular Plant Pathology, 13*(5), 519-529.

Oakley, C. E., Edgerton-Morgan, H., & Oakley, B. R. (2012). Tools for manipulation of secondary metabolism pathways: rapid promoter replacements and gene deletions in *Aspergillus nidulans Fungal Secondary Metabolism* (Vol. 944, pp. 143-161): Springer.

Olmo, V. N., & Grote, E. (2010). Prm1 targeting to contact sites enhances fusion during mating in *Saccharomyces cerevisiae*. *Eukaryotic Cell, 9*(10), 1538-1548.

Onelli, E., & Moscatelli, A. (2013). Endocytic pathways and recycling in growing pollen tubes. *Plants, 2*(2), 211-229.

Osherov, N., Mathew, J., & May, G. S. (2000). Polarity-defective mutants of *Aspergillus nidulans*. *Fungal Genetics and Biology, 31*(3), 181-188.

Osmani, A. H., Oakley, B. R., & Osmani, S. A. (2006). Identification and analysis of essential *Aspergillus nidulans* genes using the heterokaryon rescue technique. *Nature Protocols, 1*(5), 2517-2526.

Ovečka, M., Illés, P., Lichtscheidl, I., Derksen, J., & Šamaj, J. (2012). Endocytosis and vesicular recycling in root hairs and pollen tubes *Endocytosis in Plants* (pp. 81-106): Springer.

Pantazopoulou, A. (2016). The Golgi apparatus: insights from filamentous fungi. *Mycologia, 108*(3), 603-622.

Pantazopoulou, A., & Peñalva, M. A. (2009). Organization and dynamics of the *Aspergillus nidulans* Golgi during apical extension and mitosis. *Molecular Biology of the Cell, 20*(20), 4335-4347.

Pantazopoulou, A., & Peñalva, M. A. (2011). Characterization of *Aspergillus nidulans* RabC/Rab6. *Traffic, 12*(4), 386-406.

Pantazopoulou, A., Pinar, M., Xiang, X., & Peñalva, M. A. (2014). Maturation of late Golgi cisternae into RabE/RAB11 exocytic post-Golgi carriers visualized in vivo. *Molecular Biology of the Cell, 25*(16), 2428-2443.

Parton, R. G., & Richards, A. A. (2003). Lipid rafts and caveolae as portals for endocytosis: new insights and common mechanisms. *Traffic, 4*(11), 724-738.

Pearse, B. (1976). Clathrin: a unique protein associated with intracellular transfer of membrane by coated vesicles. *Proceedings of the National Academy of Sciences of the United States of America, 73*(4), 1255-1259.

Pearson, C. L., Xu, K., Sharpless, K. E., & Harris, S. D. (2004). MesA, a novel fungal protein required for the stabilization of polarity axes in *Aspergillus nidulans*. *Molecular Biology of the Cell, 15*(8), 3658-3672.

Peñalva, M. A. (2005). Tracing the endocytic pathway of *Aspergillus nidulans* with FM4-64. *Fungal Genetics and Biology, 42*(12), 963-975.

Peñalva, M. Á. (2010). Endocytosis in filamentous fungi: Cinderella gets her reward. *Current Opinion in Microbiology, 13*(6), 684-692.

Peters, C., Baars, T. L., Bühler, S., & Mayer, A. (2004). Mutual control of membrane fission and fusion proteins. *Cell, 119*(5), 667-678.

Piao, H. L., Machado, I. M., & Payne, G. S. (2007). NPFXD-mediated endocytosis is required for polarity and function of a yeast cell wall stress sensor. *Molecular Biology of the Cell, 18*(1), 57-65.

Pinar, M., Arst, H. N., Pantazopoulou, A., Tagua, V. G., de los Ríos, V., et al. (2015). TRAPPII regulates exocytic Golgi exit by mediating nucleotide exchange on the Ypt31 ortholog RabERAB11. *Proceedings of the National Academy of Sciences of the United States of America, 112*(14), 4346-4351.

Pinar, M., Pantazopoulou, A., Arst, H. N., & Peñalva, M. A. (2013). Acute inactivation of the *Aspergillus nidulans* Golgi membrane fusion machinery: correlation of apical extension arrest and tip swelling with cisternal disorganization. *Molecular Microbiology, 89*(2), 228-248.

Pomorski, T., Lombardi, R., Riezman, H., Devaux, P. F., van Meer, G., et al. (2003). Drs2p-related P-type ATPases Dnf1p and Dnf2p are required for phospholipid

translocation across the yeast plasma membrane and serve a role in endocytosis. *Molecular Biology of the Cell, 14*(3), 1240-1254.

Poulsen, L. R., López-Marqués, R. L., McDowell, S. C., Okkeri, J., Licht, D., et al. (2008). The *Arabidopsis* P4-ATPase ALA3 localizes to the Golgi and requires a β-subunit to function in lipid translocation and secretory vesicle formation. *The Plant Cell Online, 20*(3), 658-676.

Prosser, D. C., Drivas, T. G., Maldonado-Báez, L., & Wendland, B. (2011). Existence of a novel clathrin-independent endocytic pathway in yeast that depends on Rho1 and formin. *The Journal of Cell Biology, 195*(4), 657-671.

Puertollano, R., Van Der Wel, N. N., Greene, L. E., Eisenberg, E., Peters, P. J., et al. (2003). Morphology and dynamics of clathrin/GGA1-coated carriers budding from the trans-Golgi network. *Molecular Biology of the Cell, 14*(4), 1545-1557.

Punt, P. J., Strauss, J., Smit, R., Kinghorn, J. R., Van den Hondel, C., et al. (1995). The intergenic region between the divergently transcribed *niiA* and *niaD* genes of *Aspergillus nidulans* contains multiple NirA binding sites which act bidirectionally. *Molecular and Cellular Biology, 15*(10), 5688-5699.

Qiu, R., Zhang, J., & Xiang, X. (2013). Identification of a novel site in the tail of dynein heavy chain important for dynein function in vivo. *Journal of Biological Chemistry, 288*(4), 2271-2280.

Raiborg, C., Bache, K. G., Gillooly, D. J., Madshus, I. H., Stang, E., et al. (2002). Hrs sorts ubiquitinated proteins into clathrin-coated microdomains of early endosomes. *Nature cell biology, 4*(5), 394-398.

Raiborg, C., Bache, K. G., Mehlum, A., Stang, E., & Stenmark, H. (2001). Hrs recruits clathrin to early endosomes. *The EMBO Journal, 20*(17), 5008-5021.

Rasband, W. (1997). ImageJ. US National Institutes of Health, Bethesda, MD.

Read, N. D. (2011). Exocytosis and growth do not occur only at hyphal tips. *Molecular microbiology, 81*(1), 4-7.

Read, N. D., & Kalkman, E. R. (2003). Does endocytosis occur in fungal hyphae? *Fungal Genetics and Biology, 39*(3), 199-203.

Rice, P., Longden, I., & Bleasby, A. (2000). EMBOSS: The European molecular biology open software suite. *Trends in Genetics, 16*(6), 276-277.

Riddell, R. W. (1950). Permanent stained mycological preparations obtained by slide culture. *Mycologia*, 265-270.

Riquelme, M. (2013). Tip growth in filamentous fungi: A road trip to the apex. *Annual Review of Microbiology, 67*, 587-609.

Riquelme, M., Bartnicki-García, S., González-Prieto, J. M., Sánchez-León, E., Verdín-Ramos, J. A., et al. (2007). Spitzenkörper localization and intracellular traffic of green fluorescent protein-labeled CHS-3 and CHS-6 chitin synthases in living hyphae of *Neurospora crassa*. *Eukaryotic Cell, 6*(10), 1853-1864.

Riquelme, M., Bredeweg, E. L., Callejas-Negrete, O., Roberson, R. W., Ludwig, S., et al. (2014). The *Neurospora crassa* exocyst complex tethers Spitzenkörper vesicles to the apical plasma membrane during polarized growth. *Molecular Biology of the Cell, 25*(8), 1312-1326.

Riquelme, M., Roberson, R., & Sánchez-León, E. (2016). 3 Hyphal Tip Growth in Filamentous Fungi *Growth, Differentiation and Sexuality* (pp. 47-66): Springer.

Riquelme, M., & Sánchez-León, E. (2014). The Spitzenkörper: a choreographer of fungal growth and morphogenesis. *Current Opinion in Microbiology, 20*, 27-33.

Roberson, R. W. (1992). The actin cytoskeleton in hyphal cells of *Sclerotium rolfsii*. *Mycologia*, 41-51.

Robinson, M. S. (1994). The role of clathrin, adaptors and dynamin in endocytosis. *Current Opinion in Cell Biology, 6*(4), 538-544.

Robinson, M. S. (2015). Forty Years of Clathrin-coated Vesicles. *Traffic, 16*(12), 1210-1238.

Rodrigues, M. L., Nakayasu, E. S., Oliveira, D. L., Nimrichter, L., Nosanchuk, J. D., et al. (2008). Extracellular vesicles produced by *Cryptococcus neoformans* contain protein components associated with virulence. *Eukaryotic Cell, 7*(1), 58-67.

Rodrigues, M. L., Nimrichter, L., Oliveira, D. L., Frases, S., Miranda, K., et al. (2007). Vesicular polysaccharide export in *Cryptococcus neoformans* is a eukaryotic solution to the problem of fungal trans-cell wall transport. *Eukaryotic Cell, 6*(1), 48-59.

Röhrig, J., Kastner, C., & Fischer, R. (2013). Light inhibits spore germination through phytochrome in *Aspergillus nidulans*. *Current Genetics, 59*(1-2), 55-62.

Rothman, J. E., & Orci, L. (1990). Movement of proteins through the Golgi stack: a molecular dissection of vesicular transport. *The FASEB journal, 4*(5), 1460-1468.

Roze, L. V., Chanda, A., & Linz, J. E. (2011). Compartmentalization and molecular traffic in secondary metabolism: a new understanding of established cellular processes. *Fungal Genetics and Biology, 48*(1), 35-48.

Saffarian, S., Cocucci, E., & Kirchhausen, T. (2009). Distinct dynamics of endocytic clathrin-coated pits and coated plaques. *PLoS Biology, 7*(9), e1000191.

Saito, K., Fujimura-Kamada, K., Furuta, N., Kato, U., Umeda, M., et al. (2004). Cdc50p, a protein required for polarized growth, associates with the Drs2p P-type ATPase implicated in phospholipid translocation in *Saccharomyces cerevisiae*. *Molecular Biology of the Cell, 15*(7), 3418-3432.

Salamero, J., Sztul, E. S., & Howell, K. E. (1990). Exocytic transport vesicles generated in vitro from the trans-Golgi network carry secretory and plasma membrane proteins. *Proceedings of the National Academy of Sciences of the United States of America, 87*(19), 7717-7721.

Salaün, C., James, D. J., & Chamberlain, L. H. (2004). Lipid rafts and the regulation of exocytosis. *Traffic, 5*(4), 255-264.

Saleh, M.-C., van Rij, R. P., Hekele, A., Gillis, A., Foley, E., et al. (2006). The endocytic pathway mediates cell entry of dsRNA to induce RNAi silencing. *Nature Cell Biology, 8*(8), 793-802.

Sánchez-Ferrero, J. C., & Peñalva, M. A. (2007). Endocytosis. *The Aspergilli: Genomics, Medical Aspects, Biotechnology, and Research Methods*, 177 - 197.

Sánchez-León, E., & Riquelme, M. (2015). Live imaging of β-1, 3-glucan synthase FKS-1 in *Neurospora crassa* hyphae. *Fungal Genetics and Biology, 82*, 104-107.

Sánchez-León, E., Verdín, J., Freitag, M., Roberson, R. W., Bartnicki-Garcia, S., et al. (2011). Traffic of chitin synthase 1 (CHS-1) to the Spitzenkörper and developing septa in hyphae of *Neurospora crassa*: Actin dependence and evidence of distinct microvesicle populations. *Eukaryotic Cell, 10*(5), 683-695.

Sánchez-León, E., Bowman, B., Seidel, C., Fischer, R., Novick, P., et al. (2015). The Rab GTPase YPT-1 associates with Golgi cisternae and Spitzenkörper microvesicles in *Neurospora crassa*. *Molecular Microbiology, 26*.

Schekman, R., & Orci, L. (1996). Coat proteins and vesicle budding. *Science, 271*(5255), 1526-1533.

Schindelin, J., Arganda-Carreras, I., Frise, E., Kaynig, V., Longair, M., et al. (2012). Fiji: an open-source platform for biological-image analysis. *Nature Methods, 9*(7), 676-682.

Schultzhaus, Z., Quintanilla, L., Hilton, A., & Shaw, B. D. (2016). Live Cell Imaging of Actin Dynamics in the Filamentous Fungus *Aspergillus nidulans*. *Microscopy and Microanalysis*, 1-11.

Schultzhaus, Z., & Shaw, B. D. (2016). The flippase DnfB is cargo of fimbrin-associated endocytosis in Aspergillus nidulans, and likely recycles through the late Golgi. *Communicative & Integrative Biology, 9*(2), e1141843.

Schultzhaus, Z., Yan, H., & Shaw, B. (2015a). *Aspergillus nidulans* flippase DnfA is cargo of the endocytic collar, and plays complementary roles in growth and

phosphatidylserine asymmetry with another flippase, DnfB. *Molecular Microbiology, 97*(1), 18-32.

Schultzhaus, Z., Yan, H., & Shaw, B. (2015b). Aspergillus nidulans flippase DnfA is cargo of the endocytic collar, and plays complementary roles in growth and phosphatidylserine asymmetry with another flippase, DnfB. *Molecular microbiology*.

Schultzhaus, Z. S., & Shaw, B. D. (2015). Endocytosis and exocytosis in hyphal growth. *Fungal Biology Reviews, 29*(2), 43-53.

Seger, S., Rischatsch, R., & Philippsen, P. (2011). Formation and stability of eisosomes in the filamentous fungus Ashbya gossypii. *Journal of Cell Science, 124*(10), 1629-1634.

Sharpless, K. E., & Harris, S. D. (2002). Functional characterization and localization of the *Aspergillus nidulans* formin *sepA*. *Molecular Biology of the Cell, 13*(2), 469-479.

Shaw, B. D., Chung, D.-W., Wang, C.-L., Quintanilla, L. A., & Upadhyay, S. (2011). A role for endocytic recycling in hyphal growth. *Fungal Biology, 115*(6), 541-546.

Shaw, B. D., Momany, C., & Momany, M. (2002). *Aspergillus nidulans swoF* encodes an N-myristoyl transferase. *Eukaryotic Cell, 1*(2), 241-248.

Shaw, B. D., & Upadhyay, S. (2005). *Aspergillus nidulans swoK* encodes an RNA binding protein that is important for cell polarity. *Fungal Genetics and Biology, 42*(10), 862-872.

Siniossoglou, S., & Pelham, H. R. (2001). An effector of Ypt6p binds the SNARE Tlg1p and mediates selective fusion of vesicles with late Golgi membranes. *The EMBO Journal, 20*(21), 5991-5998.

Smaczynska-de Rooij, I. I., Allwood, E. G., Aghamohammadzadeh, S., Hettema, E. H., Goldberg, M. W., et al. (2010). A role for the dynamin-like protein Vps1 during endocytosis in yeast. *Journal of Cell Science, 123*(20), 3496-3506.

Söllner, T., Bennett, M. K., Whiteheart, S. W., Scheller, R. H., & Rothman, J. E. (1993). A protein assembly-disassembly pathway in vitro that may correspond to sequential steps of synaptic vesicle docking, activation, and fusion. *Cell, 75*(3), 409-418.

Steinberg, G. (2007a). Hyphal growth: a tale of motors, lipids, and the Spitzenkörper. *Eukaryotic Cell, 6*(3), 351-360.

Steinberg, G. (2007b). On the move: endosomes in fungal growth and pathogenicity. *Nature Reviews Microbiology, 5*(4), 309-316.

Stephenson, K. S., Gow, N. A., Davidson, F. A., & Gadd, G. M. (2014). Regulation of vectorial supply of vesicles to the hyphal tip determines thigmotropism in *Neurospora crassa*. *Fungal Biology, 118*(3), 287-294.

Stimpson, H. E., Toret, C. P., Cheng, A. T., Pauly, B. S., & Drubin, D. G. (2009). Early-arriving Syp1p and Ede1p function in endocytic site placement and formation in budding yeast. *Molecular Biology of the Cell, 20*(22), 4640-4651.

Stradalova, V., Blazikova, M., Grossmann, G., Opekarová, M., Tanner, W., et al. (2012). Distribution of cortical endoplasmic reticulum determines positioning of endocytic events in yeast plasma membrane. *PloS One, 7*(4), e35132.

Sudbery, P. (2011). Fluorescent proteins illuminate the structure and function of the hyphal tip apparatus. *Fungal Genetics and Biology, 48*(9), 849-857.

Sun, Y., Carroll, S., Kaksonen, M., Toshima, J. Y., & Drubin, D. G. (2007). PtdIns (4, 5) P_2 turnover is required for multiple stages during clathrin-and actin-dependent endocytic internalization. *The Journal of Cell Biology, 177*(2), 355-367.

Sun, Y., & Drubin, D. G. (2012). The functions of anionic phospholipids during clathrin-mediated endocytosis site initiation and vesicle formation. *Journal of Cell Science, 125*(24), 6157-6165.

Surma, M. A., Klose, C., Klemm, R. W., Ejsing, C. S., & Simons, K. (2011). Generic sorting of raft lipids into secretory vesicles in yeast. *Traffic, 12*(9), 1139-1147.

Taheri-Talesh, N., Horio, T., Araujo-Bazán, L., Dou, X., Espeso, E. A., et al. (2008). The tip growth apparatus of *Aspergillus nidulans*. *Molecular Biology of the Cell, 19*(4), 1439-1449.

Takagi, K., Iwamoto, K., Kobayashi, S., Horiuchi, H., Fukuda, R., et al. (2012). Involvement of Golgi-associated retrograde protein complex in the recycling of the putative Dnf aminophospholipid flippases in yeast. *Biochemical and Biophysical Research Communications, 417*(1), 490-494.

Takagi, T., Ishijima, S. A., Ochi, H., & Osumi, M. (2003). Ultrastructure and behavior of actin cytoskeleton during cell wall formation in the fission yeast *Schizosaccharomyces pombe*. *Journal of electron microscopy, 52*(2), 161-174.

Takeda, M., Yamagami, K., & Tanaka, K. (2014). Role of phosphatidylserine in phospholipid flippase-mediated vesicle transport in *Saccharomyces cerevisiae*. *Eukaryotic Cell, 13*(3), 363-375.

Takeshita, N., Diallinas, G., & Fischer, R. (2012). The role of flotillin FloA and stomatin StoA in the maintenance of apical sterol-rich membrane domains and polarity in the filamentous fungus *Aspergillus nidulans*. *Molecular Microbiology, 83*(6), 1136-1152.

Takeshita, N., Higashitsuji, Y., Konzack, S., & Fischer, R. (2008). Apical sterol-rich membranes are essential for localizing cell end markers that determine growth directionality in the filamentous fungus *Aspergillus nidulans*. *Molecular Biology of the Cell, 19*(1), 339-351.

Tan, P. K., Howard, J. P., & Payne, G. S. (1996). The sequence NPFXD defines a new class of endocytosis signal in *Saccharomyces cerevisiae*. *The Journal of Cell Biology, 135*(6), 1789-1800.

Tarutani, Y., Ohsumi, K., Arioka, M., Nakajima, H., & Kitamoto, K. (2001). Cloning and characterization of *Aspergillus nidulans vpsA* gene which is involved in vacuolar biogenesis. *Gene, 268*(1), 23-30.

TerBush, D. R., Maurice, T., Roth, D., & Novick, P. (1996). The Exocyst is a multiprotein complex required for exocytosis in *Saccharomyces cerevisiae*. *The EMBO journal, 15*(23), 6483.

That, T., Hoang-Van, K., Turian, G., & Hoch, H. (1987). Isolation and characterization of coated vesicles from filamentous fungi. *European journal of cell biology, 43*(2), 189-194.

Torralba, S., Raudaskoski, M., & Pedregosa, A. (1998). Effects of methyl benzimidazoIe-2-yl carbamate on microtubule and actin cytoskeleton in *Aspergillus nidulans*. *Protoplasma, 202*(1-2), 54-64.

Treitschke, S., Doehlemann, G., Schuster, M., & Steinberg, G. (2010). The myosin motor domain of fungal chitin synthase V is dispensable for vesicle motility but required for virulence of the maize pathogen *Ustilago maydis*. *The Plant Cell, 22*(7), 2476-2494.

Tuo, S., Nakashima, K., & Pringle, J. R. (2013). Role of endocytosis in localization and maintenance of the spatial markers for bud-site selection in yeast. *PLoS One, 8*(9), e72123.

Upadhyay, S., & Shaw, B. D. (2008). The role of actin, fimbrin and endocytosis in growth of hyphae in *Aspergillus nidulans*. *Molecular Microbiology, 68*(3), 690-705.

Valdez-Taubas, J., & Pelham, H. R. (2003). Slow diffusion of proteins in the yeast plasma membrane allows polarity to be maintained by endocytic cycling. *Current Biology, 13*(18), 1636-1640.

Valkonen, M., Kalkman, E. R., Saloheimo, M., Penttilä, M., Read, N. D., et al. (2007). Spatially segregated SNARE protein interactions in living fungal cells. *Journal of Biological Chemistry, 282*(31), 22775-22785.

van der Bliek, A. M., & Meyerowrtz, E. M. (1991). Dynamin-like protein encoded by the *Drosophila* shibire gene associated with vesicular traffic. *Nature, 351*(6325), 411-414.

Vercauteren, D., Vandenbroucke, R. E., Jones, A. T., Rejman, J., Demeester, J., et al. (2010). The use of inhibitors to study endocytic pathways of gene carriers: optimization and pitfalls. *Molecular Therapy, 18*(3), 561-569.

Verdín, J., Bartnicki-Garcia, S., & Riquelme, M. (2009). Functional stratification of the Spitzenkörper of *Neurospora crassa*. *Molecular Microbiology, 74*(5), 1044-1053.

Vernay, A., Schaub, S., Guillas, I., Bassilana, M., & Arkowitz, R. A. (2012). A steep phosphoinositide bis-phosphate gradient forms during fungal filamentous growth. *The Journal of Cell Biology, 198*(4), 711-730.

Viotti, C., Bubeck, J., Stierhof, Y.-D., Krebs, M., Langhans, M., et al. (2010). Endocytic and secretory traffic in Arabidopsis merge in the trans-Golgi network/early endosome, an independent and highly dynamic organelle. *The Plant Cell, 22*(4), 1344-1357.

Vlanti, A., & Diallinas, G. (2008). The *Aspergillus nidulans* FcyB cytosine-purine scavenger is highly expressed during germination and in reproductive compartments and is downregulated by endocytosis. *Molecular microbiology, 68*(4), 959-977.

Wakeham, D. E., Abi-Rached, L., Towler, M. C., Wilbur, J. D., Parham, P., et al. (2005). Clathrin heavy and light chain isoforms originated by independent mechanisms of gene duplication during chordate evolution. *Proceedings of the National Academy of Sciences of the United States of America, 102*(20), 7209-7214.

Wang, C.-L., & Shaw, B. D. (2016). F-actin localization dynamics during appressorium formation in *Colletotrichum graminicola*. *Mycologia, 108*(3), 506-514. doi: 10.3852/15-068

Wang, D., Sletto, J., Tenay, B., & Kim, K. (2011). Yeast dynamin implicated in endocytic scission and the disassembly of endocytic components. *Communicative & Integrative Biology, 4*(2), 178-181.

Wassef, M. K. (1977). Fungal Lipids. *Advances in Lipid Research, 15*, 159-232.

Wedlich-Söldner, R., Bölker, M., Kahmann, R., & Steinberg, G. (2000). A putative endosomal t-SNARE links exo-and endocytosis in the phytopathogenic fungus Ustilago maydis. *The EMBO Journal, 19*(9), 1974-1986.

Weinberg, J., & Drubin, D. G. (2012). Clathrin-mediated endocytosis in budding yeast. *Trends in cell biology, 22*(1), 1-13.

Weinberg, J. S., & Drubin, D. G. (2014). Regulation of clathrin-mediated endocytosis by dynamic ubiquitination and deubiquitination. *Current Biology, 24*(9), 951-959.

Weise, R., Kreft, M., Zorec, R., Homann, U., & Thiel, G. (2000). Transient and permanent fusion of vesicles in *Zea mays* coleoptile protoplasts measured in the cell-attached configuration. *The Journal of Membrane Biology, 174*(1), 15-20.

Wessels, J. (1986). Cell wall synthesis in apical hyphal growth. *International Review of Cytology, 104*(1), 37-79.

Wilson, R. A., & Talbot, N. J. (2009). Under pressure: investigating the biology of plant infection by *Magnaporthe oryzae*. *Nature Reviews Microbiology, 7*(3), 185-195.

Xu, D., Jiang, B., Ketela, T., Lemieux, S., Veillette, K., et al. (2007). Genome-wide fitness test and mechanism-of-action studies of inhibitory compounds in *Candida albicans*. *PLoS Pathogens, 3*(6), e92.

Yamashita, R. A., & May, G. S. (1998). Constitutive Activation of Endocytosis by Mutation of *myoA*, the Myosin I Gene of *Aspergillus nidulans*. *Journal of Biological Chemistry, 273*(23), 14644-14648.

Yamashita, R. A., Osherov, N., & May, G. S. (2000). Localization of wild type and mutant class I myosin proteins in *Aspergillus nidulans* using GFP-fusion proteins. *Cell Motility and the Cytoskeleton, 45*(2), 163-172.

Yang, L., Ukil, L., Osmani, A., Nahm, F., Davies, J., et al. (2004). Rapid production of gene replacement constructs and generation of a green fluorescent protein-tagged centromeric marker in *Aspergillus nidulans*. *Eukaryotic Cell, 3*(5), 1359-1362.

Yeung, T., Gilbert, G. E., Shi, J., Silvius, J., Kapus, A., et al. (2008). Membrane phosphatidylserine regulates surface charge and protein localization. *Science, 319*(5860), 210-213.

Youn, J.-Y., Friesen, H., Kishimoto, T., Henne, W. M., Kurat, C. F., et al. (2010). Dissecting BAR domain function in the yeast Amphiphysins Rvs161 and Rvs167 during endocytosis. *Molecular Biology of the Cell, 21*(17), 3054-3069.

Zhang, J., Qiu, R., Arst, H. N., Peñalva, M. A., & Xiang, X. (2014). HookA is a novel dynein–early endosome linker critical for cargo movement in vivo. *The Journal of Cell Biology, 204*(6), 1009-1026.

Zheng, Z., Gao, T., Zhang, Y., Hou, Y., Wang, J., et al. (2014). FgFim, a key protein regulating resistance to the fungicide JS399-19, asexual and sexual development, stress responses and virulence in Fusarium graminearum. *Molecular plant pathology, 15*(5), 488-499.

Zhu, Y., Drake, M. T., & Kornfeld, S. (1999). ADP-ribosylation factor 1 dependent clathrin-coat assembly on synthetic liposomes. *Proceedings of the National Academy of Sciences of the United States of America, 96*(9), 5013-5018.

Zick, M., & Wickner, W. T. (2014). A distinct tethering step is vital for vacuole membrane fusion. *eLife, 3*.

APPENDIX

Strain Name	**Genotype**	**Description**	**Source**
TN02A7	*pyrG89;* Δ*nkuA*::*argB; pyroA4; riboB2; veA1*	Δ*nkuA* deletion (wild type recipient for ClaH-GFP, ClaL-GFP, Δ*claL*)	(Nayak et al., 2006)
NKUNU	*pyrG89;* Δ*nkuA*::*argB; pabaA1; pyroA4; veA1*	nku80 deletion (wild type recipient for FimA-mCherry)	(Z. Schultzhaus et al., 2015a)
ZS100	*pyrG89; claH::gfp::pyrG*$^{A.fum}$*;* Δ*nkuA*::*argB; pyroA4; riboB2; veA1*	ClaH-GFP	This Study
ZS101	*(pyrG89?);* *claH::gfp::pyrG*$^{A.fum}$*;* *veA1;* (Δ*nkuA*::*argB?); (pabaA1?); (pyroA4?)*	ClaH-GFP (without riboflavin auxotrophy)	This Study
ZS102	*pyrG89; claL::gfp::pyrG*$^{A.fum}$*;* Δ*nkuA*::*argB; pyroA4; riboB2; veA1*	ClaL-GFP	This Study
ZS103	*pyrG89;* Δ*nkuA*::*argB; pyroA4; riboB2;* Δ*claL::riboB*$^{A.fum}$*; veA1*	Δ*claL*	This Study
ZS104	*pyrG89; claL::gfp::pyrG*$^{A.fum}$*;* Δ*nkuA*::*argB; pyroA4; claH::mcherry::pyroA*$^{A.\ fum}$*; riboB2; veA1*	ClaL-GFP, ClaH-mCherry	This Study
MAD2243	*wA4; argB2; pyroA4[pyroA*-gpdAmini::mrfp::PHOSBP]; veA1 (niiA4?)*	mRFP-PH^{OSBP} (late Golgi marker)	(Pantazopoulou & Peñalva, 2009)
ZS105	*wA4;(pyrG?)* *claH::gfp::pyrG*$^{A.fum}$*; (argB2?);* *(*Δ*nkuA*::*argB?)* *pyroA4[pyroA*gpdAmini::mrfp ::PHOSBP]; veA1; (niiA4?)*	ClaH-GFP x mRFP-PH^{OSBP}	This Study
L01028	*pyrG89; metG1; choA1; chaA1; gfp::tubA::pyrG*	GFP-TubA	(Horio & Oakley, 2005)

ZS106	*(pyrG89?); gfp::tubA::pyrG; (pyroA4?); claH::mCherry::PyroA$^{A.\ fum}$; metG1; choA1; chaA1; veA1; (nkuA::argB?)*	ClaH-mCherry, GFP-TubA	This Study
ASUFGA77	*fimA::*GFP*::argB; methG1; biA1; argB2; veA1*	FimA-GFP	(Upadhyay & Shaw, 2008)
ZS107	*pyrG89; ΔnkuA::argB; pabaA1; pyroA4; fimA::mcherry::pyroA$^{A.fum}$; veA1*	FimA-mCherry	This Study
ZS108	*(pyrG89?); claH::gfp::pyrG$^{A.fum}$; (ΔnkuA::argB?); (pyroA4?); fimA::mcherry::pyroA$^{A.fum}$; veA1*	FimA-mCherry, ClaH-GFP	This Study
RQ54	*argB2::[argB*-alcAp::mCherry-RabA]; ΔnkuA::argB; pyrG89; pyroA4; wA2*	mCherry-RabA	(Abenza et al., 2009; Qiu, Zhang, & Xiang, 2013)
ZS109	*argB2::[argB*-alcAp::mCherry-RabA]; ΔnkuA::argB?; pyrG89?, claH::GFP::pyrG^{Afum}*	ClaH-GFP, mCherry-RabA	This Study
ZS110	*pyrG89; pyrG::niiA::claH; pyroA4?; fimA::mcherry::pyroA^{Afum}*	*niiA::claH*, FimA-mCherry	This Study
ZS111	*pyrG89?; ΔnkuA::argB?; claH::GFP::pyrG^{Afum}*	ClaH-GFP, *fimA*Δ	This Study

Supplemental Table ST2.1. *Aspergillus nidulans* strains used in this study.

Primer Name	Primer Sequence
Clathrin Heavy Chain Deletion	
claH^F	CTGTAATATGAAACTGGTCAGCCA
claH^RRibo	GGCGGTAGGTGTCCTTTTTCATTTACAAGGGCCGCAGTAC
claHvFRibo	ATTGGGAAAACTAGAGACCCCGGCTCGCCTTGTCTTTTTGAG
claHvR	TTCTTGGTCGTTGCTCACC
claHnested^F	TTGAGCGAGGTTCATTGCA
claHnestedvR	CGTTTCTTTTTCTCTTTGGTCC
Clathrin Light Chain Deletion	
claL^F	GAATTGGAGGCTCGAAGATAT
claL^RRibo	GGCGGTAGGTGTCCTTTTTCAATGAGAGTTTTATGATTACCACCA
claLvFRibo	ATTGGGAAAACTAGAGACCCCGTTTACTTTTCTGCTGATTCCCTAA
claLvR	CTCTCTCGGTCCTGATGGG
claLnested^F	GCTGAATATCGTTGGATGCA
claLnestedvR	GTTTGCAGGGAGGTATAAGCT
Clathrin Heavy Chain GFP Fusion	
claHF	GTTCACCGAACTGGGTATTG
claHRGFP	AGCGCCTGCACCAGCTCCGAAAGGACGGAACCCCG
claHvFPyrG	ATCAGTGCCTCCTCTCAGACAGGCTCGCCTTGTCTTTTTGAGG
claHnestedF	CTGGTCTCGTATCAACATTCCC
Clathrin Light Chain GFP Fusion	
claLF	TCGTGGCAGAATCCCCGGTCT
claLRGFP	AGCGCCTGCACCAGCTCCAACCCCGCTAGCGCCAGGCG
claLvFPyrG	ATCAGTGCCTCCTCTCAGACAGTTTACTTTTCTGCTGATTCCCTAA
claLnestedF	CATCATTTCTCGCTTACCGACC
Clathrin Heavy Chain mCherry Fusion	
claHRmCherry	CCAGCGCCTGCACCAGCTCCGAAAGGACGGAACCCCG
claHvFPyroA	GGTGTTCTGTGCATTTGTCCTTCGCTCGCCTTGTCTTTTTGAGG
Fimbrin mCherry Fusion	
fimAF	CGACAACCGCTCCAAACC

fimARmCherry	CCAGCGCCTGCACCAGCTCCCATTTTTTCGTACGTAGCCA TTAGAGAG
fimAvFPyroA	GGTGTTCTGTGCATTTGTCCTTCTGCAGCCTGTGAACTATT AGGGG
fimAvR	TCTCCTCGCTATTGCCGC
fimAnestedF	GCGGAGAAATTGAACTGTCGC
fimAnestedvR	TTTTCTTCCGTTTGTTGTCA
niiA*::*claH	
niiAclaH^F	ATAAAACTGTAATATGAAACTGGTCAG
ClaH^R(pyrGF)	GAAGAGGGTGAAGAGCATTG GTA CGA CCT AAC CAC CCA
(niiAR)ClaHF	TGCTCATCACCGCGCCCGCCATC ATGGCTCCTCTTCCCATCAA
ClaHORFR	ACA GAC AAT ACT TGA CCC TTG CG
ClaHnORFR	AGA TCG TAG AGG TGA ATG AAA C
ClaHn^F	GCCGAGTTACTAGCTTCTACC

Supplemental Table ST2.2 Primers used in this study

Name	**Relevant Construct**	**Source**
pFNO3	*GFP*::*pyrG*^{Afum}	(Yang et al., 2004)
p1863	*pyrG*^{Afum}::*niiA*	(Hervás-Aguilar & Peñalva, 2010)
pHL85	*mCherry*::*pyroA*^{Afum}	(H.-L. Liu et al., 2009)

Supplemental Table ST2.3 Primers used in this study

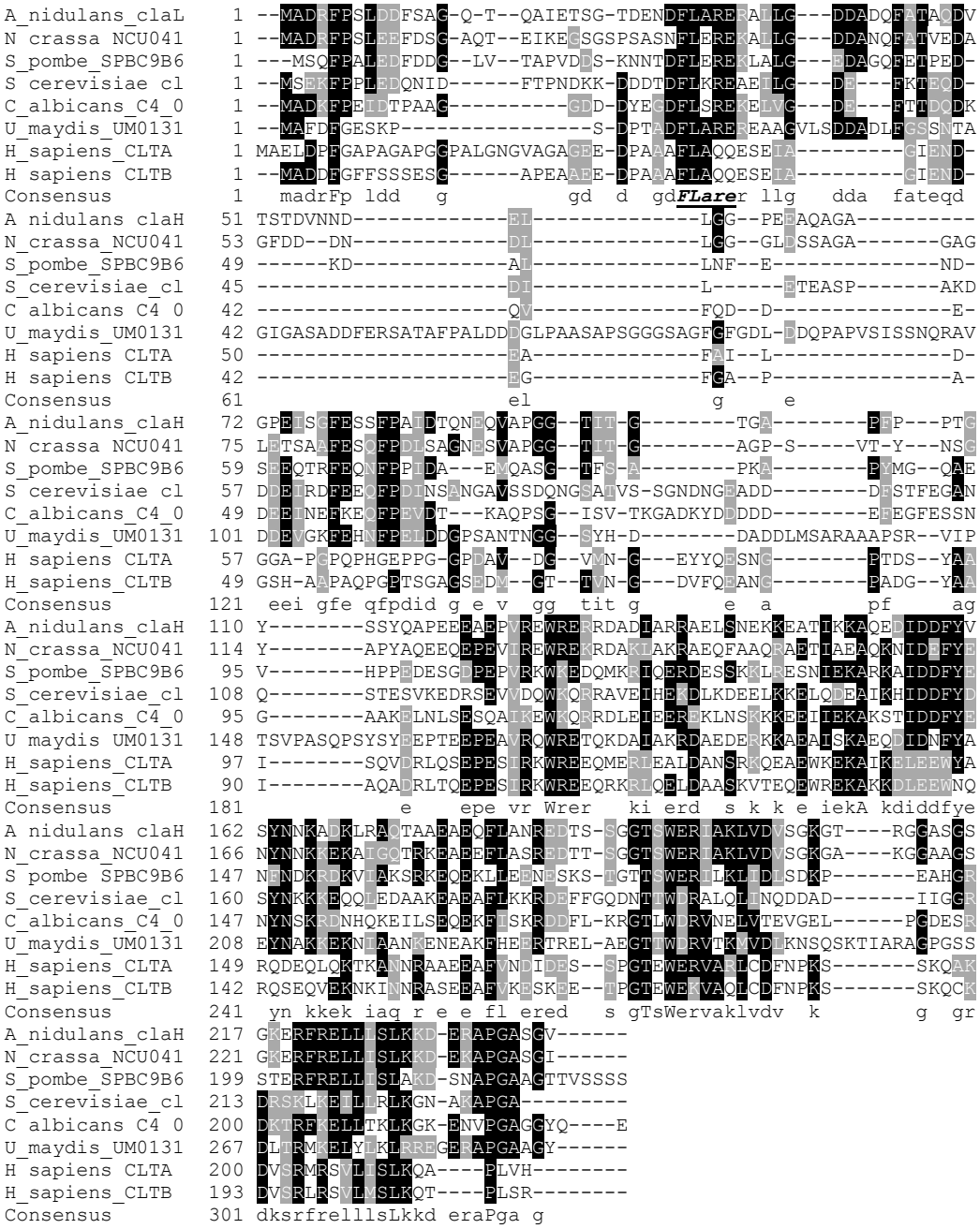

Supplemental Figure SF2.1 Sequence alignment of representative fungal and human clathrin light chain orthologs demonstrating sequence conservation at the C-terminal region, along with the conserved FLxRE motif (bolded and italicized) near the N-terminus. Alignment generated by M-coffee (http://tcoffee.crg.cat/apps/tcoffee/do:mcoffee), shading and consensus generated by Boxshade (http://www.ch.embnet.org/software/BOX_form.html).

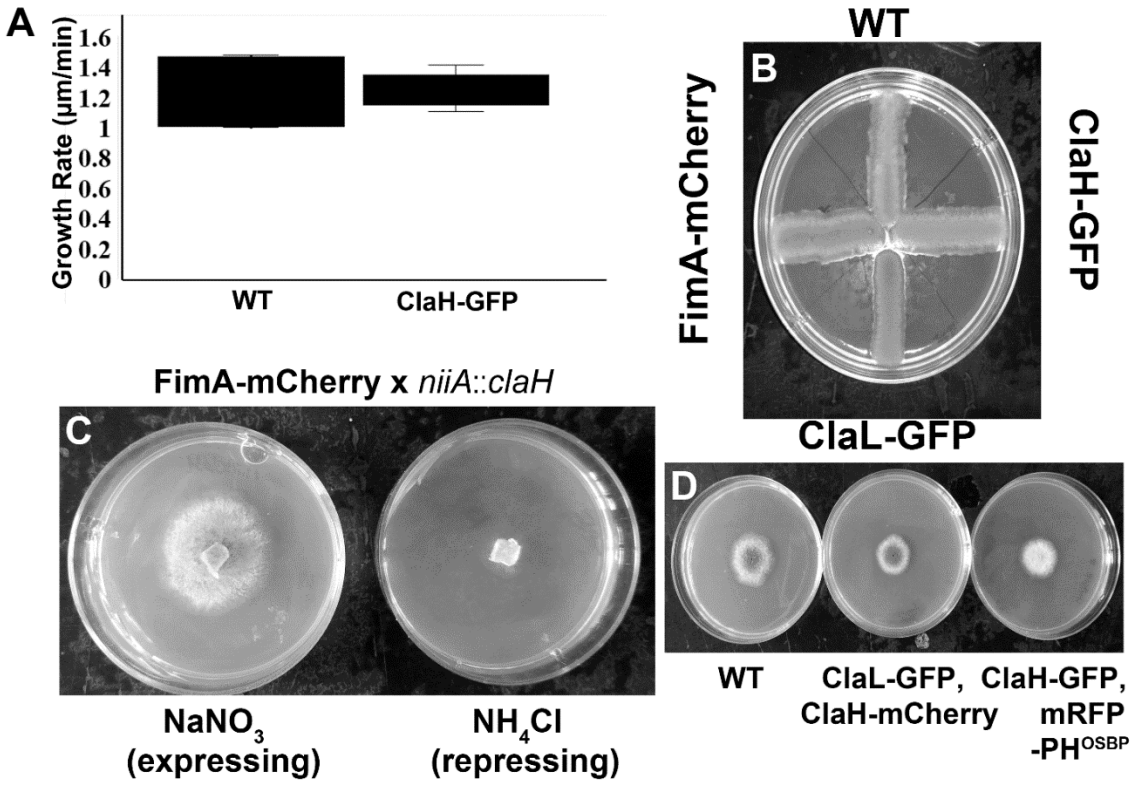

Supplemental Figure SF2.2 A. ClaH-GFP does not significantly affect hyphal growth rate. The growth rate of individual, leading hyphae was measured by taking a time lapse videos over four minutes and measuring the distance grown by the hyphal tip in this time period. **B.** Radial growth of colonies was not affected by the addition of ClaH-GFP, ClaL-GFP, or FimA-mCherry. **C.** Growth of *claH*::*niiA* under expressing conditions (left), and the minimal growth seen under repressing conditions (right). **D.** Coexpression of ClaH with ClaL and TGN marker mRFP-PH^{OSBP} had minimal effects on colony morphology and radial growth.

Movie 2.1 ClaH-GFP/clathrin in growing, leading edge hyphae. **time** = hh:mm:ss, **scale bar** = 5µm.

Movie 2.2 ClaH-GFP/clathrin and mRFP-PH^{OSBP}/late Golgi dynamics. **Arrows** = individual late Golgi progressing through both mRFP-PH^{OSBP} maximum localization followed by ClaH-GFP maximum localization. **time** = hh:mm:ss, **scale bar** = 5µm.

Movie 2.3 Individual ClaH-GFP/clathrin and mRFP-PH^{OSBP}/late Golgi structure (**arrow**) dissipating near the hyphal tip. **time** = hh:mm:ss, **scale bar** = 5µm

Movie 2.4 ClaH-GFP/clathrin (left) and FimA-mCherry/fimbrin (center) individually (presented in inverted greyscale) and together (right) at the endocytic collar. Insets = 2x zoom of the endocytic collar. Arrows indicate the location of FimA:mCherry patch. **time** = hh:mm:ss, **scale bar** = 5µm

Movie 2.5 Conidium expressing ClaH-GFP/clathrin and FimA-mCherry/fimbrin. Images taken every four seconds, arrows indicate endocytic patches that complete lifetimes during image capture, arrowhead indicates independently moving ClaH-GFP/clathrin puncta, **time** = hh:mm:ss, **scale bar** = 5µm.
Movie 2.6 ClaH-GFP puncta dynamics movement at the endocytic collar (**arrows**) of two individual hyphae. Video presented in greyscale, **time** = hh:mm:ss, **scale bar** = 5µm.
Movie 2.7 FimA-GFP/fimbrin time lapse throughout a large area of a leading hypha. Insets = 2x zoom. Arrows indicate patches fusing (**lower right arrows**) or elongating and maintaining at the plasma membrane over several patch lifetimes (**upper left arrow**), **time** = hh:mm:ss, **scale bar** = 5µm.
Movie 2.8 FimA-mCherry patch dynamics with *niiA*::*claH* induced (**upper video**) and repressed (**lower video**). Video presented in inverted greyscale. **Arrows** indicate concentrations of FimA-mCherry near hyphal tips. **time =** hh:mm:ss, s**cale bar** = 5µm.
Movie 2.9 ClaH-GFP dynamics in a *fimA* deletion mutant. Video presented in inverted greyscale. **Arrows** indicate the endocytic collar in hyphae, **time** = hh:mm:ss, **scale bar** = 5µm.
Movie 2.10 Long distance, bidirectional, saltatory movement of ClaH-GFP/clathrin puncta (**arrows**), Video presented in inverted greyscale. **time** = hh:mm:ss.msmsms, **scale bar** = 5µm.
Movie 2.11 Effects of Cycochalasin A (**upper video and kymograph**) and benomyl (**lower video and kymograph**) on ClaH-GFP trafficking. Video and kymographs presented in inverted greyscale. **Arrows** in kymograph indicate trafficking events. **time** = hh:mm:ss, **scale bar** = 5µm.

Gene	Yeast Homologue	TMD?[a]	Predicted function[b]
AN6459	None	No	UDP-N-acetylmuramate dehydrogenase, FAD-binding
AN2669	**rsb1**	**7**	**Stress response**
AN7552	**None**	**9**	**Type IV transmembrane protein**
AN5302	**None**	**11**	**CrzA-induced protein**
AN1268	None	No	None
AN1130	hos4	No	None
AN12318	None	No	None
AN8621	**tpo1**	**12**	**Transmembrane transport**
AN12305	**lsb5**	**No**	**Cortex/spindle pole body localization**
AN8890	None	5	Carbohydrate binding and catabolism
AN2492	**pal1**	**No**	**None**
AN1557	None	7	None
AN10792	irc20	No	Zinc ion binding
AN1060	rph1	No	DNA and zinc ion binding
myoA/AN1558	**myo5**	**No**	**Myosin I**
AN2429	None	No	None
pkiC/AN3381	fas1	No	Fatty acid synthesis
AN6228	syh1	No	mRNA export from nucleus
AN3108	upc2	No	Sequence-specific DNA binding RNA polymerase II transcription factor, zinc ion binding
AN10656	pyc2	No	ATP binding, biotin carboxylase, metal ion binding
AN6850	None	No	None
AN0777	None	No	Intracellular protein transport
AN0594	**tao3**	**No**	**Actin filament reorganization, cell morphogenesis,**
AN1950	**flc1**	**7**	**FAD transmembrane transporter activity, Ca2+ channel activity**
AN4945	**None**	**1**	**None**
AN10090	**None**	**1**	**None**
sldA/AN3946	**bub1**	**No**	**Spindle assembly checkpoint protein kinase**
AN6164	ubp15	No	Ubiquitin thiolesterase, ubiquitin-dependent catabolism

AN6341	**crn1**	**No**	**Coronin, actin patch assembly**
AN10296	frd1	No	Fumarate reductase (NADH), atoxia response
AN8672	**dnf1**	**10**	**Phospholipid-translocating ATPase activity**
bxlB/AN8401	None	No	alpha-L-arabinofuranosidase, beta-1,4-xylosidase
AN12031	None	No	None
AN3739	gbp2	No	Cytosol, nucleus localization
AN10451	trm8	1	tRNA (guanine-N7-)-methyltransferase
AN4106	**YIL166C**	**9**	**Transmembrane transport**
AN7616	None	No	None
AN1909	YBR062C	No	Zinc ion binding activity
sepK/AN2459[c]	**cyr1**	**No**	**Septation initiation network**
chsA/AN7032[c]	**chs2**	**7**	**Class II chitin synthase**
exgD/AN7533[c]	**exg1**	**1**	**Exo-beta-(1,3)-glucanase**
AN0697[c]	**syp1**	**No**	**Actin cortical patch assembly, septin cytoskeleton organization**
AN0698[c]	**None**	**1**	**None**

[a] Indicates the presence of predicted transmembrane domain(s)

[b] Function of yeast protein homolog or, where possible, predicted role of *A. nidulans* protein

[c] Proteins with DPFxD rather than NPFxD

Supplemental Table ST3.1: Proteins in *A. nidulans* with one or more NPFxD motifs, and select proteins with one or more DPFxD motifs

		Saccharomyces cerevisiae						
		Dnf1p(2p)[a]	**Drs2p**	**Dnf3p**	**Neo1p**	**Cdc50p**	Lem3p	Crf1p
Aspergillus nidulans	**DnfA /AN8 672**	51(49)/67(65)[b]	39/56	35/53	28/48	-	-	-
	DnfB /AN6 112	37(37)/56(56)	62/78	34/55	31/49	-	-	-
	DnfC /AN2 011	36(34)/53(54)	33/52	42/59	33/54	-	-	-
	DnfD /AN6 614	27(27)/44(43)	26/43	30/50	54/69	-	-	-
	AN51 00	-	-	-	-	47/66	39/58	46/63

[a] Dnf1p and Dnf2p are paralogues, information for Dnf2p is given in parentheses
[b] For each protein comparison, identity/similarity are provided

Supplemental Table ST3.2. P4-ATPases in *A. nidulans* and Comparison with probable Yeast homologs

Name	Genotype	Source
TNO2A7	*pyrG89; ΔnkuA::argB; pyroA4; riboB2*	FGSC
NKUNU	*pyrG89; ΔnkuA::argB; pabaA1; pyroA4;*	This Study
A773	*pyrG89; wA3; pyroA4*	FGSC
MAD2130	*pyrG89?; synA::gfp::pyrG; ' pyroA4*	(Abenza et al., 2009)
ZSS20	*pyrG89?; ΔnkuA::argB; vps54::riboB; DnfA-GFP::pyrG; pabaA1; pyroA4; riboB2?;*	This Study
MAD2243	*wA4; argB2; pyroA4[pyroA*-gpdAmini::mrfp::PHOSBP]; (niiA4?)*	(Pantazopoulou & Peñalva, 2009)
ZSS1	*pyrG89; ΔnkuA::argB gsaA::gfp::pyrG; pabaA1; pyroA4*	This Study
ZSS2	*pyrG89; ΔnkuA::argB DnfB-GFP::pyrG; pabaA1; pyroA4*	This Study
ZSS3	*pyrG89; ΔnkuA::argB DnfA-GFP::pyrG; pabaA1; pyroA4*	This Study
ZSS4	*pyrG89; ΔnkuA::argB DnfA-GFP::pyrG; pabaA1; pyroA4; DnfB-mCherry::pyroA*	This Study
ZSS5	*pyrG89; ΔnkuA::argB; pyroA4; riboB2; ΔdnfA::riboB*	This Study
ZSS6	*pyrG89; ΔdnfB::pyrG*; *ΔnkuA::argB; pyroA4; riboB2; ΔdnfA::riboB*	This Study
ZSS7	*pyrG89; ΔnkuA::argB; pyroA4; riboB2; ΔdnfB::riboB*	This Study
ZSS8	*pyrG89; ΔnkuA::argB; gsaA::gfp::pyrG; pabaA1; pyroA4; DnfB-mCherry::pyroA*	This Study
ZSS9	*pyrG89; ΔnkuA::argB synA::gfp::pyrG; pabaA1; pyroA4; DnfB-mCherry::pyroA*	This Study
ZSS10	*pyrG89; pyrG::pniiA::gfp::lact-c2; pabaA1; pyroA4; DnfB-mCherry::pyroA*	This Study
ZSS11	*pyrG89?; DnfB-GFP::pyrG; wA4; argB2; pyroA4; pyroA::gpdAmini::mrfp::PHOSBP; niiA4?*	This Study
ZSS12	*pyrG89?; DnfA-GFP::pyrG; wA4; argB2; pyroA4; pyroA::gpdAmini::mrfp::PHOSBP; niiA4?*	This Study
ZSS13	*pyrG89?; synA::gfp::pyrG; ' pyroA4; riboB2?; ΔdnfA::riboB*	This Study
ZSS14	*pyrG89; pyrG::pniiA::GFP-LactC2; wA3; pyroA4*	This Study
ZSS15	*pyrG89?; pyrG::pniiA::GFP-LactC2; Δnku?; wA3; pyroA4; riboB2?; ΔdnfA::riboB*	This Study
ZSS16	*pyrG89?; pyrG::pniiA::GFP-LactC2; wA3; ΔnkuA?; pyroA4; riboB2?; ΔdnfB::riboB*	This Study

ZSS17	*pyrG89; dnfA^{AAFxD}::gfp::pyrG; ΔnkuA::argB; pabaA1; pyroA4*	This Study
ZSS18	*pyrG89; ΔnkuA::argB; pyroA4; DnfB-mCherry; riboB2; ΔdnfA::riboB*	This Study
ZSS19	*pyrG89; pyrG::GFP-Lact-C2; ΔnkuA::argB; pyroA4; DnfB-mCherry; riboB2; ΔdnfA::riboB*	This Study
ZSS20	*pyrG89; dnfA::pyrG; ΔnkuA::argB; pyroA4; riboB2; ΔdnfA::riboB*	This Study
ZSS21	*pyrG89; dnfB::pyrG; ΔnkuA::argB; pyroA4; riboB2; ΔdnfB::riboB*	This Study

Supplemental Table ST3.3: Strains created or used for this study

Plasmid Name	Source
pFNO3	**(Yang et al., 2004)**
p1863	**(Hervás-Aguilar & Peñalva, 2010)**
pLact-C2-GFP-416	**(Yeung et al., 2008)**
Primer Name	**Sequence (3' - 5')**
DnfA-GFP	
DnfAF	GCAGATTACGCCATAGGG
DnfAR	TGCGCCTGCACCAGCTCCGTTCGATTTGAGCGGGC
DnfAvF	ATCAGTGCCTCCTCTCAGACAGTCCTCCATCATTTTGCGAC
DnfAvR	CGAAAATCAATTATAGTAACAACCC
DnfAnF	CCCTGGCATACTTTTCAAA
DnfAnR	GGTTGTTGCGATAGACG
GsaA::GFP	
GsaAF	GGTTCCGGAGATTCAAATG
GsaAR	AGCGCCYGCACCAGCTCCGATAGCGACATTCTTCATCTC
GsaAvF	ATCAGTGCCTCCTCTCAGACAG GCTACGGTCGTATGTCTG
GsaAvR	GGTATTCGGACTGGGATTA
GsaAnF	ACGATAACCTCTGTGAAGG
GsaAnR	GATATTGTCTGCTATGCGG
DnfA Deletion	
DnfA^F	CAATAATGCCAATGCCCGC
DnfA^R	GGCGGTAGGTGTCCTTTTTCCCTGGTTTAAGACTCGTTCG
DnfAvF	ATTGGGAAAACTAGAGACCCCGTCCTCCATCATTTTGCGAC
DnfAvR	GTAACAACCCAAGAACAGGG
DnfAnF	CCTGTGGTATGTATCAATGG
DnfA^{AAFxD}::GFP	
DnfA^{AAFxD} F	CGATTCTGGTTACGAGGCATGCTGCTTTTTCAGATGATC
DnfA^{AAFxD} R	GATCATCTGAAAAAGCAGCATGCCTCGTACCAGAATCG
GFP-Lact-C2	
LactR	GGGACCTAGACTTCAGGTT
LactnR	CTAACAGCCCAGCAGCTCCACTCG
PyrGnF	ACGGCTATGTGTACTC

NiiAR	GATGGCGGGCGCGGTGATGAGCA
NiiAR GFPF	TGCTCATCACCGCGCCCGCCATCATGGTGAGCAAGGGCGAGG
PyrGF	CAATGCTCTTCACCCTCTTC
***An*Cho1p Deletion**	
Cho^F	ACCCATTGGCAAGATCGA
Cho^R	GGCGGTAGGTGTCCTTTTTCACAAGGGAAAGCTAGAAAAGAG
ChovF	ATTGGGAAAACTAGAGACCCCATAGCATAAGCACATGACGA
ChovR	GTTCTACGGGGCTGACTT
Chon^F	CTTCACCATCAAGCCCC
ChonR	GGACAGAATAAATTAAGTCCTGC
DnfB Deletion	
DnfB^F	CCTGAACATCACTCATAAGCC
DnfB^R	GGCGGTAGGTGTCCTTTTTCAGGGCTAACACCGTCAAT
DnfBvF	ATTGGGAAAACTAGAGACCCC GTTCAAGTGCATTCGGTACTGCATCT
DnfBvR	GCTACTATCATTCTTGAAGCG
DnfBn^F	CTTGCTATTCTGGATGCGAC
DnfBnR	CCGAGTGAGTGACTTACC
DnfB-GFP	
DnfBF	ATTGTCTCAAGCTAATGTTCCC
DnfBR	AGCGCCYGCACCAGCTCCAACCAAATTTCGCGAGCT
DnfBvF	ATCAGTGCCTCCTCTCAGACAGTATTTTTGTTTTCTTTTTGTTCAAGTGC
DnfBnF	GTGAAGTTATCTACGAATCATGG
DnfB-mCherry	
DnfB mCherryR	CCAGCGCCTGCACCAGCTCCAACCAAATTTCGCGAGCT
DnfBvF mCherryR	GGGTGTTCTGTGCATTTGTCCTTCTATTTTTGTTTTCTTTTTGTTCAAGTGC
mCherryF	GGAGCTGGTGCAGGCG
PyroR	GAAGGACAAATGCACAGAACACCC
DnfA Complement	
DnfA^R ORFDnfAF	TGGAGGCTATCTGAAGCCATCCTGGTTTAAGACTCGTTCG

DnfAORFF	ATGGCTTCAGATAGCCTCCA
DnfAORFR PyrGF	GAAGAGGGTGAAGAGCATTGCAGTTCGATTTGAGCGGG
RiboBnR	GCCGACGTCTCGCCGATATC
PyrGR RiboBF	ATCAGTGCCTCCTCTCAGACAGGAAAAAGGACACCTACCGCC
PyrGR	CTGAGAGGAGGCACTGAT
***An*Vps54 Deletion**	
Vps54^F	GGAGATATTCGTTGCATTCAG
Vps54^R	GGCGGTAGGTGTCCTTTTTCCTCGCCGTCAAACTGGC
Vps54vF	ATTGGGAAAACTAGAGACCCCGTAATCATCACCATGTGTGCG
Vps54vR	CTGACCAGAGTCGAGTCC
Vps54nF	GGGTTGGAAGCACGATATCTC
Vps54nR	AGCGCTTCTAGAACCAGCG
DnfB-PyrG Deletion	
DnfB^R PyrGF	GAAGAGGGTGAAGAGCATTGAGGGCTAACACCGTCAAT
DnfBvF PyrGR	CGCATCAGTGCCTCCTCTCAGGTTCAAGTGCATTCGGTACTGCATCT
DnfB Complement	
DnfB^R C	AGGGCTAACACCGTCAAT
DnfBORFF	ATTGACGGTGTTAGCCCT
DnfBORFR PyrGF	GAAGAGGGTGAAGAGCATTGTCAAACCAAATTTCGCGAGC
DnfA-PyrG Deletion	
DnfA^R PyrGF	GAAGAGGGTGAAGAGCATTGCCTGGTTTAAGACTCGTTCG
DnfAvF PyrGR	ATCAGTGCCTCCTCTCAGACAGTCCTCCATCATTTTGCGAC
PyrG^F	CTATATAAGTATCTTTCCCCCTTCAAC
PyrGn^F	CTCAAGCATTCAGATCCACATAA
Targeted Lact-C2	
PyrG^R PyrGORFF	ATTGTTTGAGGCGACCGGTGATGGCGGTTCTCCAA

Lact-C2vR PyrGvF	GACAACCTGAAGTCTAGGTCCCGTGTGAGTGGAAATGTG TAAC
PyrGvR	TTCTAGAGACAATCACTGGACA
PyrGnvR	CATGTGTTTCCTAAAGAGAAGC
PyrG::GFP	
PFNO3 PyrGF	GGAGCTGGTGCAGGCGCT
PFNO3 GFP R	CTGTCTGAGAGGAGGCACTGAT
***A. fumigatus* RiboB**	
RiboBF	GAAAAAGGACACCTACCGCC
RiboBR	CGGGGTCTCTAGTTTTCCCAAT

Supplemental Table ST3.4: Plasmids and primers used in this study

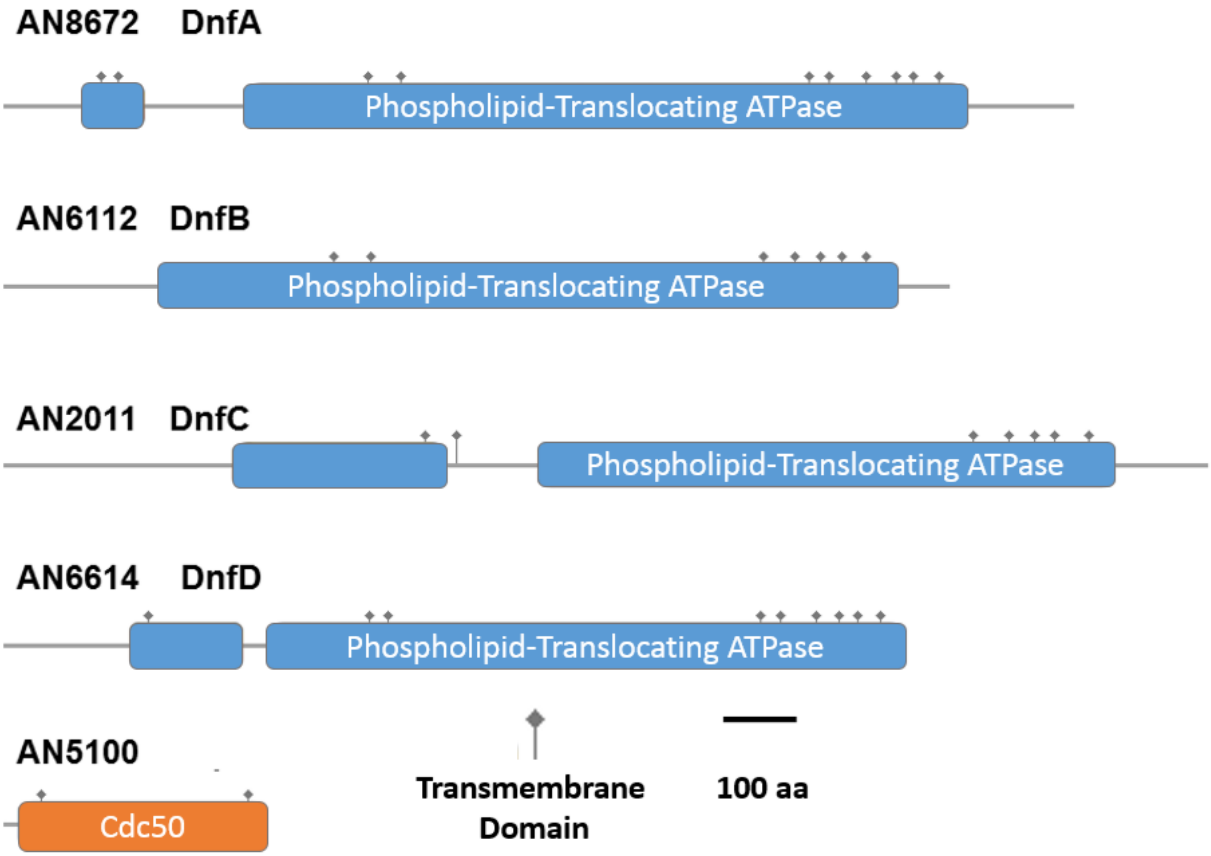

Supplemental Figure SF3.1: Protein schemes of the four predicted P4-ATPases of *A. nidulans.* Secondary structure maps for the aminophospholipid flippases DnfA, DnfB, DnfC, and DnfD from *A. nidulans*. The Cdc50p ortholog AN5100, is also provided. Important conserved domains are marked, as are transmembrane domains. Proteins are scaled relative to each other, transmembrane domains are drawn to scale, and a 100 amino acid scale bar is provided.

A.

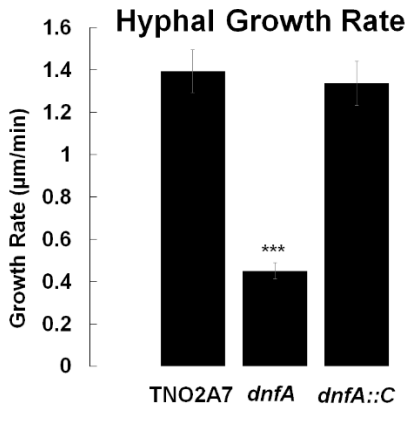
Hyphal Growth Rate
Growth Rate (µm/min)
1.6
1.4
1.2
1
0.8
0.6
0.4
0.2
0
***
TNO2A7
dnfA
dnfA::C

B.

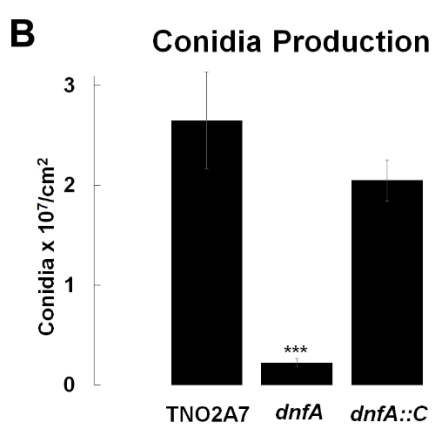
B
Conidia Production
Conidia x 10⁷/cm²
3
2
1
0
***
TNO2A7
dnfA
dnfA::C

C.

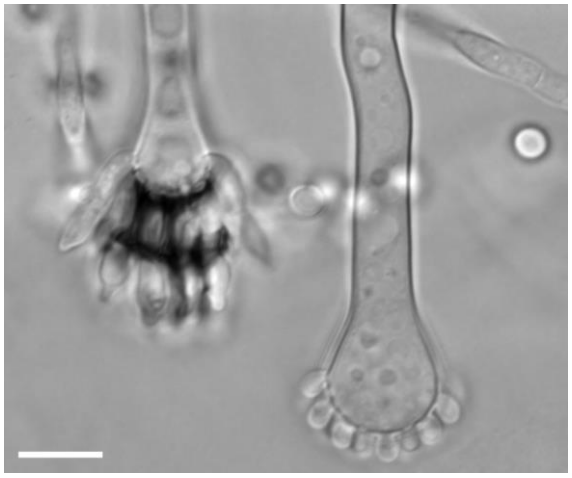

D.

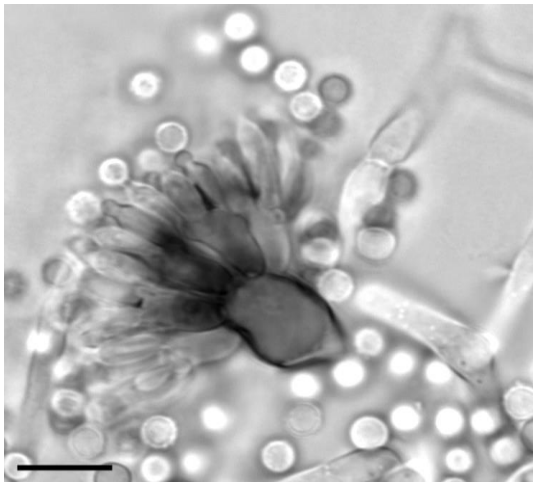

E.

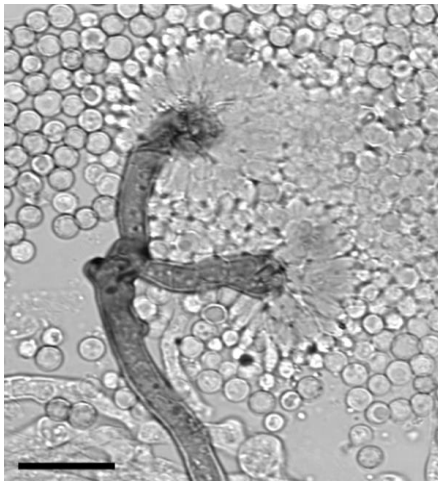

F.

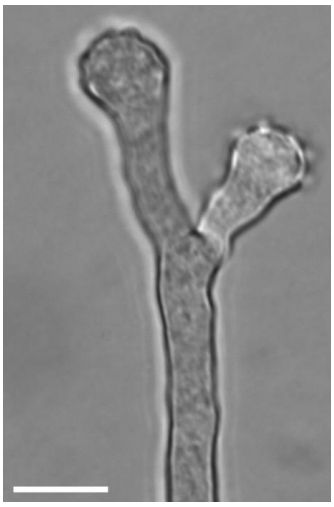

Supplemental Figure SF3.2: Quantitative growth and conidiation phenotypes and conidiophore structure of *dnfAΔ* mutants. A. Growth rate of individual hyphal tips of TNO2A7 (*dnfA*$^{+}$), *dnfAΔ* mutant, and the complemented strain (*dnfA::C*). **B.** Conidia production of each strain, as measured by the number of conidia collected from a 1cm in diameter plug from the center of a 7 day old colony. Bars indicate the standard error, N=10 for all strains, *** = $p < 0.001$. **C, D.** Wild type conidiophores showing the characteristic swollen vesicles and the three layers of cells including metullae, phialides, and conidia at the end (scale bars = 5μm). **E, F.** In *dnfAΔ* mutants, conidiophores possess all cell types eventually, but are irregularly branched such that two or more conidiophores are made from one compartment (scale bars = 10μm).

A.

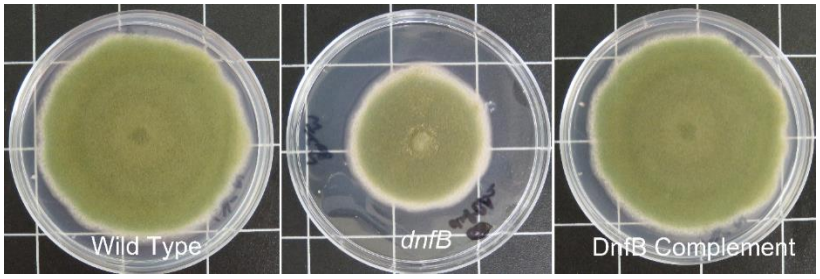
Wild Type
dnfB
DnfB Complement

B.

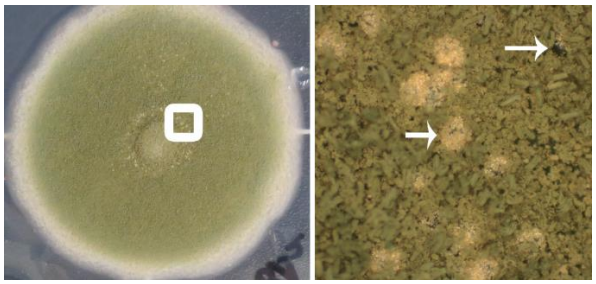

C.

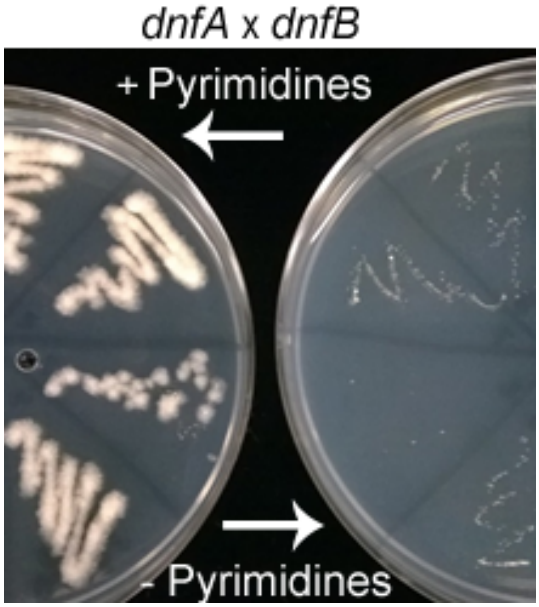
dnfA x dnfB
+ Pyrimidines
- Pyrimidines

D.


dnfA dnfB

E.

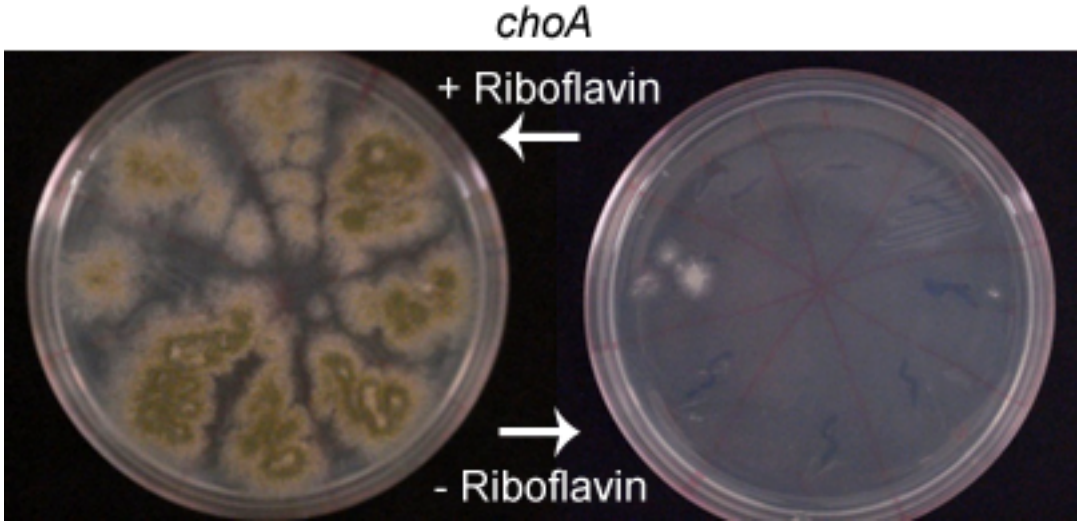

Supplemental Figure SF3.3. Phenotypes of *choAΔ* and *dnfAΔ dnfBΔ* mutants. *dnfB* deletion resulted in a slight growth reduction (**A**), as well as a premature induction of sexual spore production (**B**), with cleistothecia being produced after seven days (**arrows, left panel**) on minimal media at 30°C. **C.** Deleting *dnfB* in *dnfA* mutants resulted in mutants with extremely limited growth, as shown here when primary transformants were plated on selective (- Pyrimidines) and non-selective (+ Pyrimidines) plates. **D.** *dnfA dnfB* double deletion colonies were dense and misshapen (scale bars = 5μm). **E.** *choA* deletion was attempted, but primary transformants were unable to be propagated on selective plates (- Riboflavin).

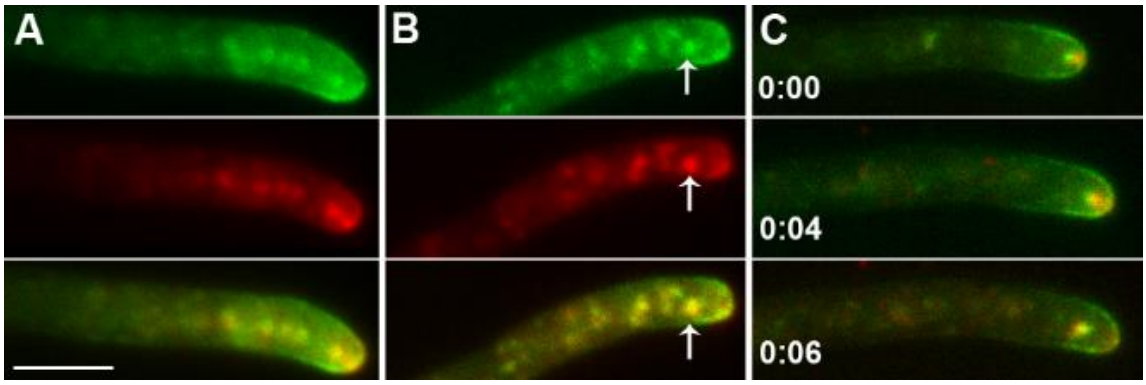

Supplemental Figure SF3.4. DnfA and DnfB and Disruption of Microtubule Trafficking by Benomyl. A. DnfA-GFP (**top panel**), DnfB-mCherry (**center panel**), colocalize in an elongate structure derived from the Spitzenkörper (**bottom panel**) upon application of benomyl. **B.** DnfA-GFP (**top panel**), DnfB-mCherry (**center panel**) also aggregate (**bottom panel**) in cytosolic structures (**arrows**) together and **C.** are associated with each other such that they are able to retract as one unit when the Spitzenkörper is disrupted by benomyl treatment. Scale bars = 5 µm.

A.

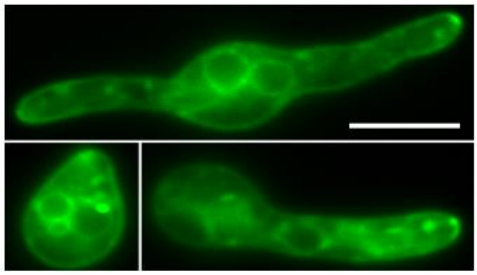

B.

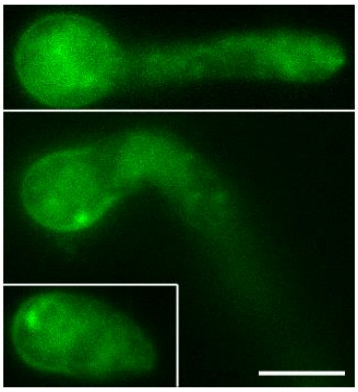

C.

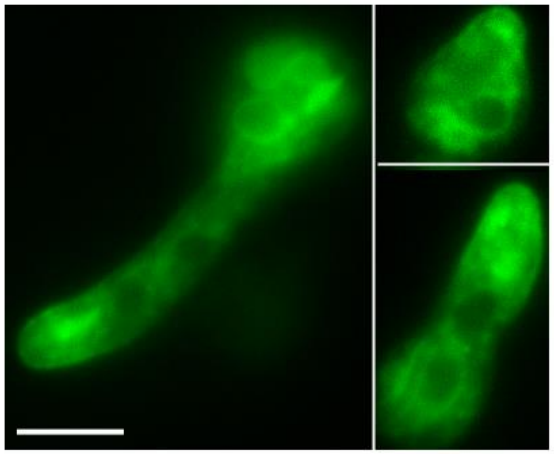

Supplemental Figure SF3.5. GFP-Lact-C2 in *dnfA*$^{+}$*dnfB*$^{+}$ (wild type), and *dnfAΔ* and *dnfBΔ* mutants. In *dnfA*$^{+}$*dnfB*$^{+}$, GFP-Lact-C2 labeled the plasma membrane indiscriminately (**A**), although often an accumulation could be seen just below the germling tip. This localization was lost in *dnfAΔ* mutants (**B**), which did not exhibit plasma membrane labelling in the germ tubes. *dnfBΔ*, however, did not greatly affect GFP-Lact-C2 labelling, although more marker appeared to accumulate in the cytoplasm (**C**). Scale bars = 5µm.

Movie 3.1: DnfA-GFP and DnfB-mCherry (500ms between each frame).
Movie 3.2: GFP-Lact-C2 traffic into and out of the Spitzenkörper (time in hh:mm:ss.sss).
Movie 3.3: GFP-Lact-C2 diminished Spitzenkörper and diffuse cytoplasmic localization in *dnfAΔ* (time in hh.mm.ss).
Movie 3.4: GFP-Lact-C2 plasma membrane labelling, and intracellular trafficking in *dnfBΔ* (250ms between each frame).
Movie 3.5: GFP-Lact-C2 and DnfB-mCherry (500ms between each frame).

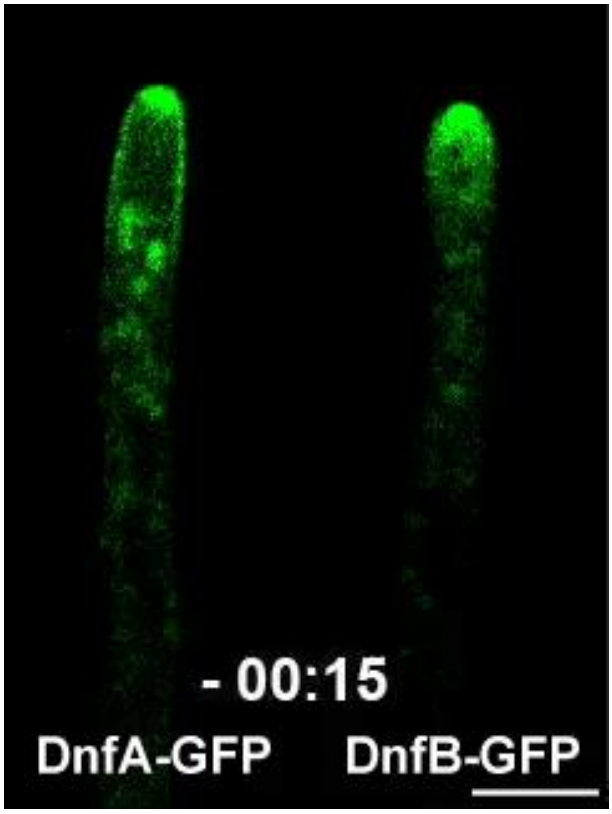

Movie 4.1 (still): Representative FRAP videos of DnfA-GFP and DnfB-GFP. This video shows a representative image sequence of DnfA-GFP fluorescence recovery in the left panel. DnfB-GFP recovery after photobleaching with similar microscope settings is shown in the right panel. In this comparison of the image sequences, DnfB-GFP can be seen recovering more quickly than DnfA-GFP. DnfA-GFP which is also more diffuse in the apex, while the DnfB-GFP-labeled Spitzenkörper is highly concentrated and recovers relatively rapidly. Scale bar = 5µm, time in mm:ss.

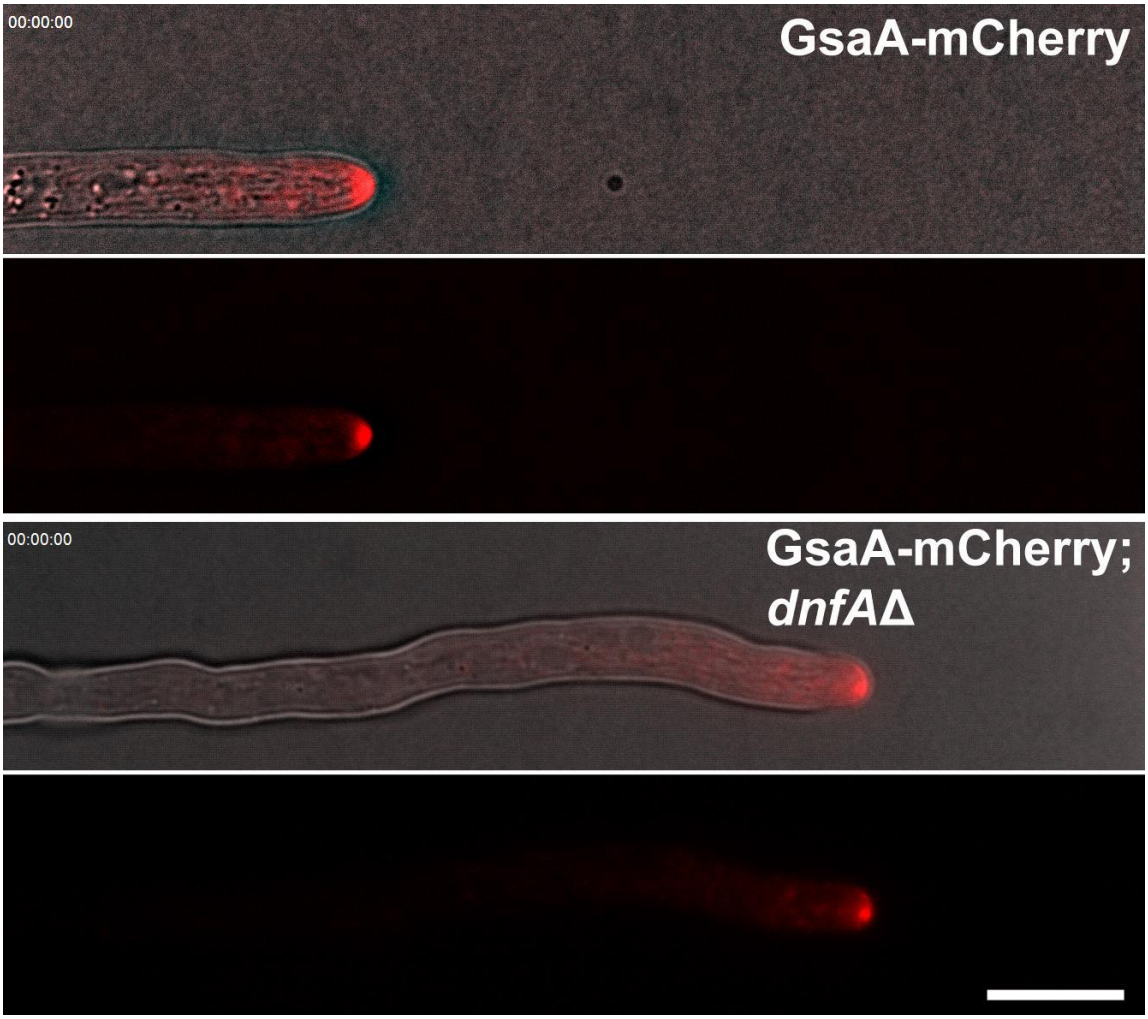

Movie 4.2 (still): Spitzenkörper dynamics in *dnfA*Δ. In this video, the Spitzenkörper is marked by GsaA-mCherry. The upper panel shows a rapidly growing wild type hyphal cell with an SPK remaining a consistent size, brightness, and location during growth. Lower panels show GsaA-mCherry localization in a *dnfA* deletion mutant. In this mutant, hyphae exhibit markedly slower growth than in wild type, which corresponds to a somewhat smaller and more diffuse SPK, which can be seen changing in size and moving laterally within the apex during growth. Scale bar = 10µm, time in hh:mm:ss.